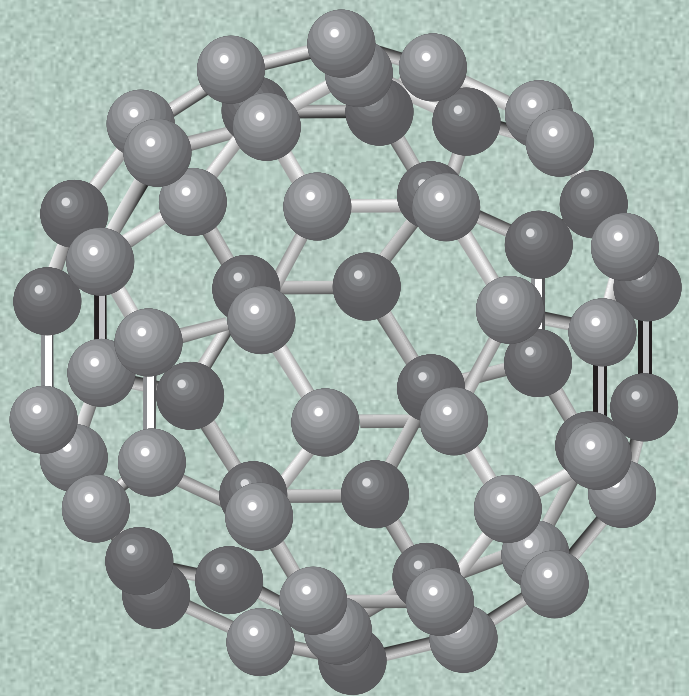


AUTOMOTIVE PROPULSION MATERIALS

2001
ANNUAL
PROGRESS
REPORT



U.S. Department of Energy
Energy Efficiency and Renewable Energy
Office of Transportation Technologies

A C K N O W L E D G E M E N T

We would like to express our sincere appreciation to Argonne National Laboratory, Computer Systems Management, Inc., and Oak Ridge National Laboratory, for their artistic and technical contributions in preparing and publishing this report.

In addition, we would like to thank all our program participants for their contributions to the programs and all the authors who prepared the project abstracts that comprise this report.

**U.S. Department of Energy
Office of Advanced Automotive Technologies
1000 Independence Avenue S.W.
Washington, DC 20585-0121**

FY 2001

Progress Report for Propulsion Materials

Energy Efficiency and Renewable Energy
Office of Transportation Technologies
Office of Advanced Automotive Technologies
Energy Conversion Team

Steven Chalk Energy Conversion Team Leader

October 2001

CONTENTS

INTRODUCTION.....	1
2. POWER ELECTRONICS.....	9
A. Low-Cost, High-Energy-Product Permanent Magnets	9
B. Development of Improved Powder for Bonded Permanent Magnets	14
C. Carbon Foam for Electronics Cooling	18
D. dc Bus Capacitors for PNGV Power Electronics.....	25
E. Mechanical Reliability of Electronic Ceramics and Electronic Ceramic Devices.....	31
3. FUEL CELLS	35
A. Carbon Composite Bipolar Plates	35
B. Cost-Effective Surface Modification for Metallic Bipolar Plates.....	39
C. Low-Friction Coatings and Materials for Fuel Cell Air Compressors.....	43
D. Microstructural Characterization of PEM Fuel Cells	47
E. Nano-Particulate Porous Oxide Electrolyte Membranes as PEMs	53
F. Metallized Bacterial Cellulose Membranes in Fuel Cells.....	57
G. Carbon Foam for Radiators for Fuel Cells.....	62
4. ADVANCED COMBUSTION	66
A. Microwave-Regenerated Diesel Exhaust Particulate Filter Durability Testing	66
B. Rapid Surface Modifications of Aluminum Automotive Components for Weight Reduction.....	70
C. Material Support for Nonthermal Plasma Diesel Engine Exhaust Emission Control.....	74
APPENDIX A: ACRONYMS AND ABBREVIATIONS.....	77

1. INTRODUCTION

Automotive Propulsion Materials R&D: Enabling Technologies to Meet Technology Program Goals



**Patrick B. Davis
Program Manager**



**Nancy Garland
Program Manager**

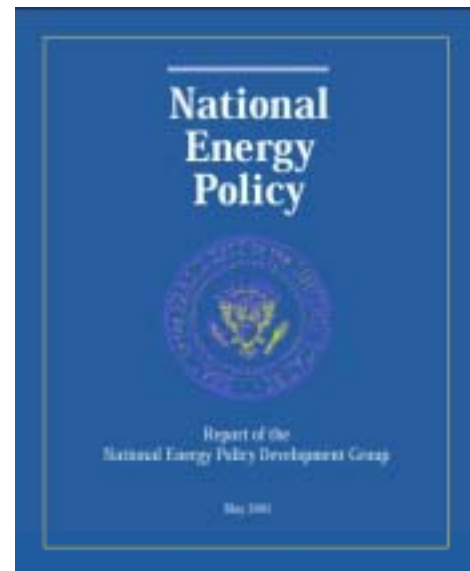
On behalf of the Department of Energy's (DOE's) Office of Transportation Technologies (OTT), I am pleased to introduce the FY 2001 Annual Progress Report for the Automotive Propulsion Materials Research and Development Program. I am also pleased to introduce you to Nancy Garland, who is taking over management of this important program starting in FY 2002. Nancy brings with her years of bench research experience at the Naval Research Laboratory and several years of program management experience here at DOE with our Fuel Cells for Transportation Program. This change in program management will allow me to take on an expanded role in other Office of Advanced Automotive Technologies (OAAT) activities. I wish to stress that no fundamental

changes in the activities of the Automotive Propulsion Materials Program are planned. Together with DOE national laboratories and in partnership with private industry and universities across the United States, the program will continue to engage in high-risk research and development (R&D) that provides enabling materials technology for fuel-efficient and environmentally friendly light-duty vehicles.

This introduction summarizes the objectives and progress of the program in FY 2001 and highlights the technical barriers remaining and the future direction of the program. The reader is also referred to the FY 2001 Annual Progress Reports on *Combustion and Emission Control for Advanced CIDI Engines* and *Fuel Cells for Transportation* for additional information on OTT's R&D activities supporting the development of propulsion materials technology.

In May of 2001, the President's National Energy Policy Development Group published the National Energy Policy (NEP). This comprehensive energy policy specifically addresses the development of energy-efficient vehicle technologies, including hybrid systems, advanced emission control technologies, fuel cells, and hydrogen-based systems. The NEP is a strong indicator of the continuing federal support for advanced automotive technologies in the transportation sector and the materials work that supports these technologies.

The Automotive Propulsion Materials Research and Development Program supports the Partnership for a New Generation of Vehicles (PNGV). Through many of its technology research programs, OAAT has supported PNGV since its inception. The PNGV leadership is now re-evaluating the partnership goals to identify changes that will maximize the potential national petroleum-savings



**Report of the National Energy Policy
Development Group**

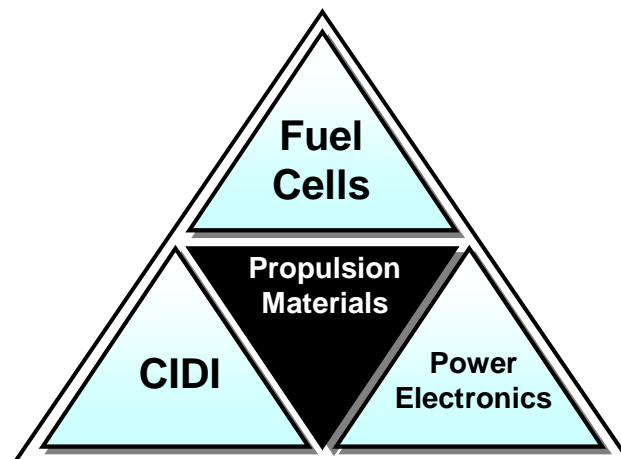
benefits of the emerging PNGV technologies. When these PNGV goal changes have been defined, the OAAT will adjust the focus of its technology research programs accordingly.

The Automotive Propulsion Materials Program is an integral partner with the programs for Vehicle Power Electronics and Electric Machines, Combustion and Emissions Control for Advanced CIDI Engines, and Vehicle Fuel Cell Power Systems R&D. Projects within the Automotive Propulsion Materials Program address materials concerns that directly impact the critical technical barriers in each of these programs—barriers such as thermal management, emissions reduction, and reduced manufacturing costs. The program engages only the barriers that involve basic, high-risk materials issues.

Enabling Technologies

The Automotive Propulsion Materials Program focuses effort on enabling materials technologies—technologies that are critical in removing barriers to the power electronics, fuel cell, and compression-ignition, direct-injection (CIDI) engine combustion and emissions control research programs.

Thermal management remains a cross-cutting materials issue, affecting both the power electronics and fuel cell programs. The components necessary for the high-fuel-economy, low-emission PNGV vehicles require power electronics to be smaller and lighter in weight and to operate at higher temperatures. These requirements are being addressed by developing electronic materials (i.e., low-cost dc buss capacitors) that operate at higher temperatures and by improving the capability to dissipate heat generated in these devices. Fuel cell systems also require improved heat dissipation because the lower operating temperature of the fuel cell system (80°C) provides a smaller temperature differential between the fuel cell system and ambient conditions. The Propulsion Materials Program has been addressing both heat dissipation issues through the development of advanced carbon foam technology.



The Propulsion Materials Program focuses on three applications.

The Program has supported the development of two innovative membranes for polymer electrolyte membrane (PEM) fuel cells. The first is a high-surface-area microporous inorganic porous oxide (TiO_2 and Al_2O_3) membrane, and the second is an innovative metallized bacterial cellulose membrane. Both types of membranes promise to be capable of operating at temperatures above 100°C to minimize platinum requirements, to improve waste heat dissipation, and to involve minimal water management problems and less CO poisoning.

CIDI engine and aftertreatment system development will greatly benefit from the Program through research in advanced wear coatings and the development of improved particulate filters for diesel engines. Cost-effective surface treatments are being developed to reduce wear of lightweight aluminum and titanium components, such as engine blocks, fuel pumps, and compressor housings. Wear of components, particularly piston rings and cylinder liners, can lead to increased emissions, lower efficiency, and lower durability. In addition, current CIDI engine technology faces the difficult balance of engine efficiency versus tailpipe emissions. The Propulsion Materials Program is working to maximize efficiency while reducing emissions through the development of advanced particulate filters and is collaborating with Pacific Northwest National Laboratory (PNNL) in the development of a nonthermal plasma aftertreatment device to reduce NO_x emissions from diesel engines.

Collaboration and Cooperation

As with other programs under PNGV, collaboration and cooperation across organizations is a critical part of the Automotive Propulsion Materials Program. Across the materials projects, scientists at the national laboratories are collaborating with manufacturers to identify and refine the characteristics necessary for meeting performance requirements. Component manufacturers and scientists from the national laboratories and from contractors are also working together to identify the technological barriers to manufacturing optimal materials to meet component requirements.

There is also cooperation among national laboratories to take advantage of the expertise of each facility. Oak Ridge and Argonne National Laboratories (ORNL and ANL), for example, are collaborating in the development of higher-strength NdFeB permanent magnets that will enable significant reductions in the size, weight, and cost of electric motors used in hybrid vehicles. In another project, Sandia National Laboratories (SNL) is fabricating smaller, higher-temperature dc buss capacitors; and ORNL is developing techniques to characterize the ~5-micron-thick polymer films developed by SNL and correlate their mechanical properties with their dielectric behavior.

Laboratory/Contractor-Industry Collaboration

Laboratory		Industrial Partner	
Argonne National Laboratory	✓	Ability Engineering Technology, Inc.	✓ Daimler-Chrysler Corporation
	✓	Atlas Cylinders, Inc.	✓ Ford Motor Company
	✓	Bronson and Bratton, Inc.	✓ Lucas-Varity
	✓	Cryomagnetics, Inc.	✓ MagnaQuench UG
	✓	CRUMAX	✓ Purdue University
Oak Ridge National Laboratory	✓	AVX	✓ Industrial Ceramic Solutions
	✓	Bronson and Bratton, Inc.	✓ Kemet
	✓	Conoco Corporation	✓ MagnaQuench UG
	✓	Cryomagnetics, Inc.	✓ Modine
	✓	CRUMAX	✓ National Security Agency
	✓	Daimler-Chrysler Corporation	✓ Poco Graphite
	✓	Delphi	✓ Plug Power, LLC
	✓	Dow Chemical Company	✓ Rensselaer Polytechnic Inst.
	✓	Ford Motor Company	✓ SatCon
	✓	General Motors	✓ University of Wisconsin
Sandia National Laboratory	✓	AVX	✓ Murata
	✓	Daimler-Chrysler Corporation	✓ Pennsylvania State University
	✓	Ford Motor Company	✓ TAM
	✓	General Motors	✓ Tokay
	✓	Degussa	✓ TPC Ligne Puissance
	✓	Ferro	✓ TPL, Inc.
	✓	Kemet	✓ TRS Ceramics
	✓	Materials Research Associates	

In addition to national laboratory and large industry participation, the FY 2001 Automotive Propulsion Materials Program included important R&D conducted by a small business. Industrial Ceramic Solutions, LLC (ICS), located in Oak Ridge, Tennessee, is developing a ceramic filter to reduce particulate emissions from diesel engines. As in the collaborative efforts of national laboratories with industry, researchers at ICS are working closely with representatives from DaimlerChrysler, Ford, General Motors, and ORNL to develop a filter that will meet PNGV emissions targets.

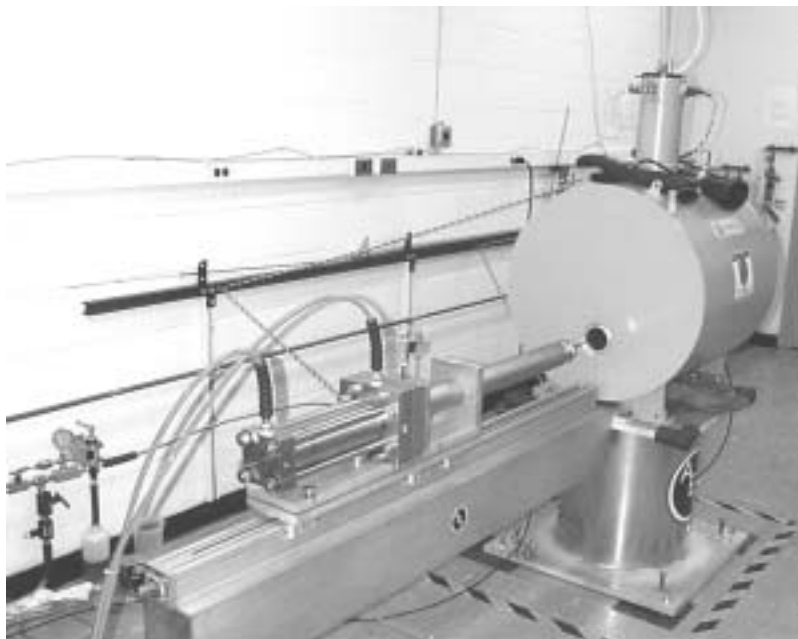
Accomplishments

FY 2001 featured notable accomplishments in all three materials program areas. While the remainder of the report provides summaries on all of the Automotive Propulsion Materials projects, this section provides a highlight of some of the major accomplishments during FY 2001. Materials development in support of power electronics, for example, featured the fabrication of NdFeB permanent magnets that are ~20% stronger than commercial magnets. Fuel-cell-related materials activities demonstrated carbon composite bipolar plates that are low-cost, weigh about half as much as graphite materials, and have equal or better electrical properties. Finally, materials research in the support of combustion engine and aftertreatment technologies led to the demonstration of microwave-regenerated exhaust particulate filters in diesel-powered vehicles.

Power Electronics

The cost, weight, and volume of existing electric motors are too large to meet the PNGV performance targets for hybrid vehicles. One approach to reducing weight and volume in an electric motor is to increase the magnetic capability, or “energy product” of the permanent magnets used in the motors. Higher energy products will not only reduce the weight of the permanent magnet, but also reduce (by a similar fraction) the weight in the balance of a motor producing the same torque. These weight reductions potentially translate into cost savings. Today’s highest-performance permanent magnets are made of NdFeB powders that are first aligned in a magnetic field, compacted in the field, and then sintered to yield a fine-grained highly-oriented magnet. The production of sintered NdFeB magnets is a mature technology, but it is limited in industry by the maximum orientation fields (<2 Tesla) of conventional electromagnets. To overcome this limitation, ANL has utilized low-temperature superconducting magnet technology to achieve enhanced alignment of the NdFeB powders during compact pressing operations.

In this phase of this project, NdFeB powders supplied by an industrial partner have been aligned and uniaxially pressed in the bore of a 9-T superconducting magnet at ANL and then returned to the partner for sintering and measurement. Results for batch-mode processing of cylindrical permanent magnets indicate that improvements of 10–25% are possible, and it was confirmed that the higher aligning fields led to enhanced orientation texture in the sintered magnets.

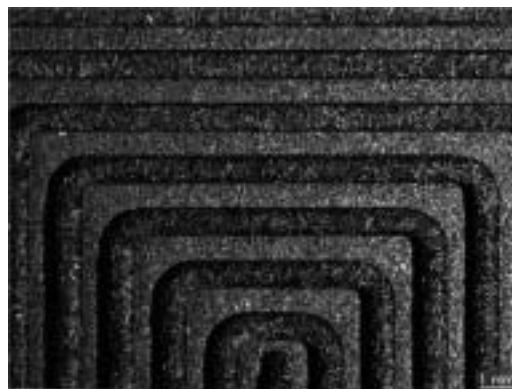


The 9-Tesla superconducting magnet system at Argonne.

One reason manufacturers do not presently use superconducting solenoids for die-pressing magnets is that they cannot be cycled quickly, and it was believed that the magnet would need to be switched off before the pressed compact could be removed and a new powder sample inserted. However, the best permanent magnets pressed at ANL to date were achieved with the magnet always on, so a reciprocating feed system should yield a production rate competitive with that of present methods.

Fuel Cells R&D

The challenges for PEM fuel cell technology for automobiles lie in reducing the cost and weight of the fuel cell stack, an impediment to which is the cost and weight of the bipolar plate. The bipolar plate is the electrode plate that separates individual cells in a stack. A stack is formed when multiple cells are aligned one after another so as to work in series, with the bipolar plate providing an electrode current collector for the cells on either side. The reference material for the bipolar plate is high-density graphite with machined flow channels. Both material and machining costs for graphite, however, are prohibitive for many fuel cell applications. This situation has led to substantial development efforts to replace graphite. The requirements for a bipolar plate are stringent, including low-cost materials and processing, low weight, thinness ($<3\text{mm}$), sufficient mechanical integrity, high surface and bulk electronic conductivity, low permeability (boundary between fuel and oxidant), and high corrosion resistance (in the moist atmosphere of the cell).



Carbon composite bipolar plate.

The bipolar plate approach developed at ORNL appears to have successfully met the challenge for an effective bipolar plate. The technology uses a low-cost, water-based carbon fiber slurry-molding process to produce a porous, carbon-fiber preform. The molded carbon-fiber component has impressed flow-field channels for diffusing fuel or air to the electrolyte surface. The bipolar plate is made hermetic through chemical vapor infiltration with carbon, that is, by pyrolyzing methane at high temperatures so that it deposits a coating of graphitic carbon. The infiltrated carbon also serves to make the component highly conductive. The result is a component with about half the weight of the graphite reference material and equal or better electrical and corrosion resistant properties.

The technology for producing the carbon composite bipolar plate has been licensed to Porvair Fuel Cell Technology, which is currently scaling the plate and building pilot facilities for commercial production. Porvair has also won a DOE award to support its scale-up efforts under the solicitation for Research and Development and Analysis for Energy-Efficient Technologies in Transportation and Building Applications.

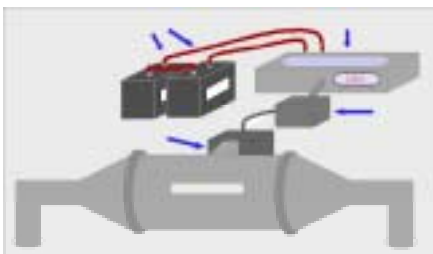
Advanced Combustion Engine and Emissions R&D

A major PNGV goal is to develop a vehicle with outstanding fuel economy that meets stringent emissions standards. Balancing high fuel economy with low emissions is a challenge that is being addressed through the materials activities in support of the R&D program for Combustion and Emission Control for Advanced CIDI Engines. Specifically, work conducted at ICS has led to the development and demonstration of an advanced exhaust filter system capable of capturing more than 95% of the carbon particulates from diesel engine exhaust. ICS has developed a new, patented technology known as the “Microwave-Cleaned Particulate Filter System” that is capable of removing and destroying fine particulate pollution from diesel exhaust streams. The system features a ceramic-fiber filter that can be automatically cleaned through the use of microwave power.

During FY 2001, results from a stationary diesel 1.9-liter test cell demonstrated an average particulate removal efficiency of 97%, over a spectrum of normal engine operating conditions. The microwave filter was installed on a Ford F-250 7.3-liter diesel pickup, with full exhaust backpressure and temperature data acquisition, for a 6000-mile road test. Preliminary results have proved that the filter could survive the full loading of 1000 ft^3 per minute of exhaust flow without mechanical failure. The microwave filter system has also been installed on a 1.9-liter diesel Volkswagen for a 7000-mile controlled test track evaluation, with periodic Federal Test Protocol cycle emission testing. Data from these on-road tests will be used to improve



On-road controlled test-track vehicle.



Schematic diagram of the Volkswagen microwave filter.

the performance of the microwave-regenerated particulate filter, verify system durability, and precisely quantify the fuel penalty resulting from filter operation.

Positive results from these tests should lead to product development partnerships with exhaust system suppliers, engine builders, or vehicle manufactures. These strategic partnerships can move this technology to integration into a total commercial diesel exhaust emissions control system for pick-up trucks, sport utility vehicles, and large trucks.

Future Direction

The Automotive Propulsion Materials Program will continue to work closely with PNGV partners and industry to understand propulsion materials-related requirements. Building upon the recent advances in materials technologies, many of this year's projects will be moved out of the laboratory and over to industry for testing. For example, Porvair has licensed the carbon composite bipolar plate technology and is scaling up the process for commercial production. Strategic partnerships will be established in 2002 with exhaust system, engine, or vehicle manufacturers to move the microwave particulate filter system from vehicle testing toward commercialization. The scale-up and commercialization of carbon foam at POCO Graphite for thermal

management applications is ahead of schedule and will continue with the focus on cost reduction. Other projects will continue to refine manufacturing requirements and necessary characteristics to meet the challenges of the PNGV program.

Awards and Achievements

Carbon Foam Thermal Management Consortium (ORNL)

- ✓ Federal Laboratory Technology Transfer Award—2001
- ✓ Three patents granted

Near-Frictionless Coatings (ANL)

- ✓ ASM International Fellow Award—2001: Ali Erdemir
- ✓ Distinguished Engineering Award (Georgia Institute of Technology)

Industrial Ceramic Solutions

- ✓ Most Promising Investment Opportunity in Tennessee (Tennessee Technology Development Corporation)

Electronic Ceramic Capacitors

- ✓ Outstanding Achievement Award—2001 (International Symposium on Integrated Ferroelectrics)

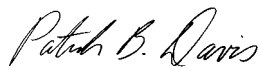
A promising new activity in the Automotive Propulsion Materials Program for FY 2001 was the collaboration with the National Security Agency to develop passive, evaporatively cooled heat sinks. These carbon foam heat sinks would be submerged in an organic liquid that would evaporate as heat is dissipated from the electronics and condense in another region of the device. These systems should be able to dissipate three to four times more heat than conventional systems, without the need for systems to circulate air or water coolants.

As advanced automotive technology developments uncover new challenges, the Automotive Propulsion Materials Program will continue to provide breakthrough technology solutions through collaboration with industry, PNGV partners, national laboratories, and small businesses.

Project Abstracts

The remainder of this report communicates the progress achieved during FY 2001 under the Automotive Propulsion Materials Program. It consists of 15 abstracts of national laboratory projects—five that address power electronics, three that address combustion and emission technologies, and seven that address fuel cells. The abstracts provide an overview of the critical work being conducted in order to improve these systems, reduce overall cost, and maintain component performance. In addition, these abstracts provide insight into the challenges and opportunities associated with advanced materials for high-efficiency automobiles.

Patrick B. Davis

A handwritten signature in black ink that reads "Patrick B. Davis". The signature is written in a cursive style with a large, stylized 'P' and 'D'.

Program Manager
Energy Conversion Team
Office of Advanced Automotive Technologies
Office of Transportation Technologies

2. POWER ELECTRONICS

A. Low-Cost, High-Energy-Product Permanent Magnets

Tom M. Mulcahy and John R. Hull
Argonne National Laboratory

Andrew E. Payzant
Oak Ridge National Laboratory

DOE Program Manager: Patrick Davis
ORNL Technical Advisor: David Stinton

Contractor: Argonne National Laboratory, Argonne, Illinois
Prime Contract No.: W-31-109-Eng-38

Objectives

- Develop a low-cost process to fabricate an anisotropic NdFeB permanent magnet (PM) with up to a 25% increase in energy product, which is a measure of the torque that a motor can produce for a given magnet mass. The higher-performance magnets will replace ones made by traditional powder metallurgy processing and enable significant size and weight reductions in traction motors for hybrid vehicles.
- Use high fields of superconducting solenoids to improve magnetic grain alignment while pressing compacts for sintering, thus producing higher-performance magnets.

OAAT R&D Plan: Section 3.5: Task 3; Barriers B, C, D

Approach

- Develop a batch-mode press that enables alignment of the magnetic domains of NdFeB powders in the higher-strength magnetic fields created by a superconducting solenoid.
- Characterize, compare, and correlate engineering and microscopic magnetic properties of magnets processed under varying conditions, including some in current production.
- Use a reciprocating feed to automate the insertion of loose and compacted magnet powder into and its removal from the steady magnetic field of a superconducting solenoid.

Accomplishments

- Achieved energy products that were within 10% of the theoretical maximum by optimizing batch-mode alignment/pressing of cylindrical axial-die-pressed PMs in a 9-Tesla (T) superconducting solenoid. The magnetic properties are comparable to the more expensive magnets made by the transverse-die pressing technique.
- Achieved energy product improvements of 15% for thin near-final-shape magnets, production of which is the current cost-saving thrust in the PM industry.
- Proved the crucial step in enabling automation feasible. For the first time, powder-filled dies were inserted into and pressed compacts were removed from an active (always on) superconducting solenoid. Most important, these magnets were the best made.

- Characterized the microscopic texture (alignment) of PMs made in the Argonne axial-die press facility and correlated the alignment with macroscopic magnetic properties.

Future Direction

- Demonstrate the feasibility of competitive factory operation by fabricating and operating a reciprocating press in continuous-mode operation.
- For cost-effective near-final-shape magnets, completely identify the improvements that can be gained in engineering and microscopic magnet properties by alignment and pressing of powder in the higher magnetic fields of the 9-T superconducting solenoid.
- Provide design rules for the fabrication of PMs, including knowledge related to scale-up to larger magnets at commercial rates of production.

Introduction

More than 250 NdFeB compacts were pressed this year in Argonne's batch-mode axial-die press facility. The facility includes a 9-T superconducting solenoid, which can produce alignment fields that significantly exceed those of the 2-T electromagnets in common industrial use. (The Argonne facility was completed in the fourth quarter of 2000.)

Production-grade magnet powder was obtained from Magnequench UG. The 3- to 5-micron, single-crystal grains of powder were aligned in the same direction and compacted at Argonne. Then anisotropic compacts, with their grains mechanically locked in place, were returned to Magnequench UG for sintering, annealing, machining, and measurement of engineering magnetic properties. Finally, selected PMs were sent to Oak Ridge National Laboratory (ORNL) for measurement of microscopic properties and texture (the alignment of the crystals' easy magnetic axes). The better the alignment, the greater is the energy product.

Industry considers an improvement of 2–3% in the magnetic properties of today's PMs as significant. The properties of current PMs can be brought to within 5–25% of their theoretical maximums. The strength of the magnet greatly depends on the method by which the compact is aligned and pressed. Large blocks can be made by cold-isostatic pressing that are within 5% of their theoretical maximum, but then the blocks must be sliced, diced, and ground to final shape. Machining operations add significantly to the cost of magnets. Magnets that are axial-die pressed and sintered to near-final shape have magnetic properties farthest from their theoretical maximums, but they are the least expensive to make. The current industry goal is

to make better near-final-shape magnets by axial-die pressing.

Even cheaper isotropic magnets can be made if the grain alignment step is eliminated. But they have, at most, one-fourth the energy product of orientated, anisotropic magnets. If lower-energy products are acceptable, then hot-formed or bonded isotropic magnets are a more cost-effective alternative.

Results

The first PMs made in the fourth quarter of 2000 had properties that were far from optimal. Thus a significant effort was made, in cooperation with our industrial partner, to optimize processing at Argonne. Different press loads, press rates, lubricants, and powder-fill techniques were studied. Argonne learned that a lower fill density than can be achieved by gravity pouring is necessary to produce the best magnetic properties.

The results of the fill-density optimization study for cylindrical compacts with a length-to-diameter ratio $L/D \sim 1$ are shown in Figure 1, where the maximum energy product, BH_{max} , is given for various die-fill densities. The alignment fields were applied only immediately before and during the pressing of the compacts. When the fill density was reduced to ~20% below the fill-density levels for gravity pouring, the energy product improved by ~20% for a 4-T alignment field. In essence, "head room" must be left in the die cavity during powder filling. When the alignment field is turned on, the powder redistributes and the entire cavity is filled

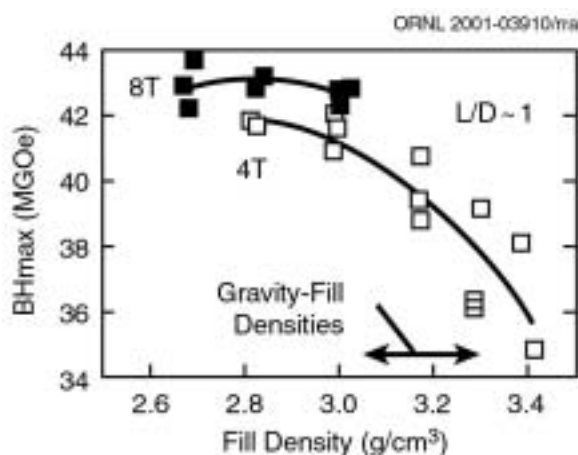


Figure 1. Energy product maximized by reducing fill density.

for pressing. The same optimal fill density was found for compacts aligned at 8 T.

The compacts aligned at 8 T were made as part of a study to correlate energy-product improvements with increases in the alignment field, again for compacts with $L/D \sim 1$. Results are summarized in Figure 2. The maximum energy product BH_{max} was increased by $\sim 12\%$ by tripling the maximum 2-T alignment field of electromagnets. The increase was the same for the first magnets made and for magnets made after the processing was optimized, but the optimized magnets had 30% higher energy products.

It was initially believed that the superconducting magnet would need to be de-energized between cycles to allow for sample insertion in zero field. Unexpectedly, the best magnets (solid symbols)

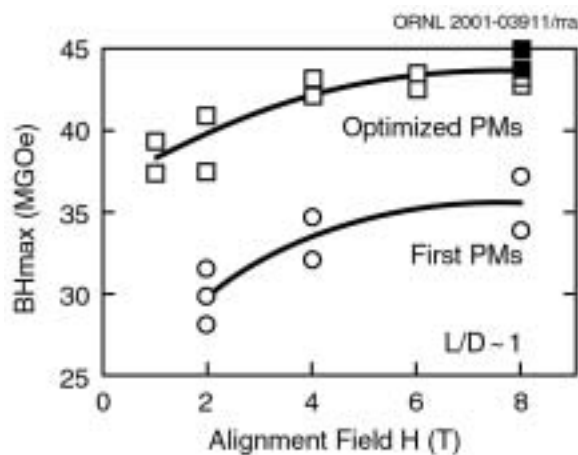


Figure 2. BH_{max} was increased 12% by tripling alignment field. Best magnets (solid square) made for reciprocating press conditions.

were made when the alignment field was always on. This condition simulates the severe field gradients that loose powder in the die would experience during insertion into an operating superconducting solenoid by a reciprocating press. Most important, these maximum energy products are comparable to those of more expensive magnets made by the transverse-die pressing technique. About 92% of the theoretical maximum was achieved. Thus what was expected by industry to be a show-stopper in using superconducting solenoids turned out to be a potentially significant cost-savings feature.

The need to leave head room in powder-filled-die cavities was not a feature originally included in the design of the Argonne axial-die press facility. To maintain head room, split-ring plastic constraints were attached to each punch, as shown in Figure 3, where the right punch is positioned in the die and the left punch will be inserted after the powder fill. The friction on each ring was calibrated to hold during handling and insertion into an active superconducting solenoid, but slip when compaction loads were applied. Including this feature on an automated reciprocating press will be a challenge.

The most effective use of the high alignment fields that can be provided by superconducting solenoids is in making near-final-shape magnets. Their finite and usually short length in the direction of magnetization makes alignment of the powder grains especially difficult. When subjected to a uniform alignment field, the powder in the die cavity develops a highly nonuniform self-field. Because grains align along the total field lines,

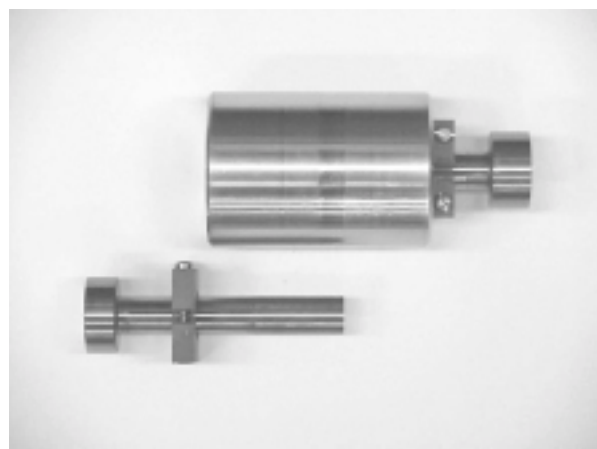


Figure 3. Split rings on punches maintain die-cavity headroom.

unidirectional alignment can be achieved only by increasing the strength of the applied alignment field until the effects of the self-field become negligible. Because the self-field distortion becomes greater for shorter magnets, there will always exist short magnets that the 2-T electromagnets of industry cannot adequately align. Clearly, the higher fields produced by a superconducting solenoid can provide the necessary alignment.

A study of near-final-shape cylindrical magnets was performed for compacts with three different length-to-diameter ratios (L/Ds): L/D = 0.25, 0.50, and 0.73. The results are given in Figure 4. The remnant magnetization, B_r , of the shortest magnets, with a compact L/D = 0.25, improved the most. Quadrupling the alignment field from 2 T increased B_r by 7%. This is equivalent to a 15% increase in the maximum energy product, since BH_{max} is proportional to B_r^2 . The magnets made from compacts thicker than L/D > 0.5 did not appear to suffer self-field effects. Length-to-diameter ratios smaller than those tested are common for near-final-shape magnets, but they could not be accurately made and measured using the small-diameter die ($\frac{5}{8}$ in.) available. Even larger improvements in energy product are expected for L/Ds < 0.25.

The lack of a self-field effect on the alignment of all the compacts was unexpected. Prior to any compact fabrication at Argonne, magnetic code analysis predicted significant effects at up to L/D = 1. Now that the mechanics of powder compaction are better understood, especially the

compaction density at which the grains are mechanically locked into alignment, a more refined analysis is planned that will better predict the alignment fields for short compacts. Also, to fully identify the range in size of near-final-shape magnets, which benefit by alignment in high fields, additional cylindrical magnets will be fabricated with compact L/Ds from 1/8 to 1/2. To make and measure the thinner magnets, a die-punch set was fabricated that has the largest bore ($1\frac{1}{8}$ in.) that can be accommodated in the batch axial-die press facility.

At ORNL, crystallite size, texture (or preferred orientation), and composition of the PM materials pressed at Argonne are being characterized using X-ray diffraction measurements (or neutron diffraction, if required). All these features impact the macroscopic magnetic properties. A goal of this part of the project is to characterize, compare, and correlate engineering and microscopic magnetic properties of magnets aligned in the superconducting solenoid. A select group of the magnets, whose energy products are included in Figure 2, have been characterized for degree of alignment by X-ray diffraction.

The distribution of the inclinations of the easy magnetic axis from the geometric axis is shown in Figure 5 for different alignment fields and conditions. Not unexpectedly, crystal inclination

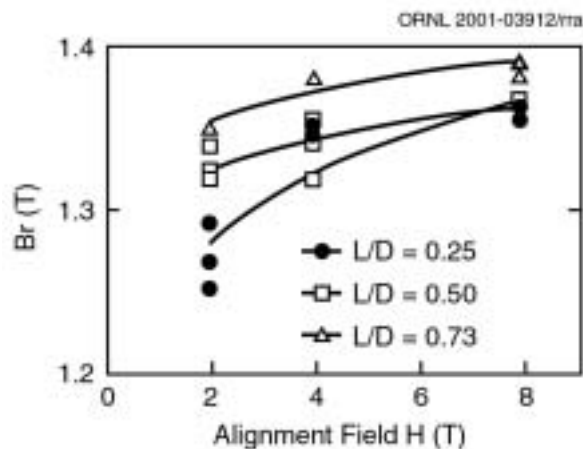


Figure 4. BH_{max} increased by 15% for near-final-shape magnet with L/D = 0.25.

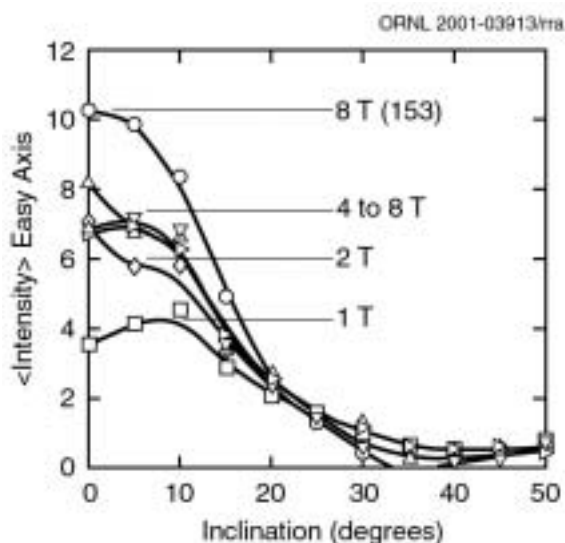


Figure 5. Texture correlates with BH_{max} . Best texture for reciprocating press conditions (153).

was the least for magnet 153, which was pressed in the highest alignment field, 8 T, and was the only one in the group for which the powder-filled die was inserted into the superconducting solenoid with the field on. As also was expected, the greatest inclinations occurred for magnet 131, which was pressed in the lowest alignment field, 1 T. An alignment field of 2 T decreased the inclination, and even smaller but similar inclinations were found for magnets pressed at 4 to 8 T. These trends mirror the trend of the energy products, shown in Figure 2, for the magnets where the alignment field was on only during pressing.

Finally, long, cylindrical compacts ($\frac{7}{8}$ in. in diameter) are being made by cold isostatic pressing, which is known to give the best magnetic properties. (See the compact at the bottom of Figure 6.) Their energy products and textures will define the practical limits on properties achievable with die pressing.



Figure 6. Isostatic-pressed compact, mold, aluminum tube, and rubber bag.

Conclusions

Magnets were routinely made in 2001 using the axial-die press facility that was fabricated and made operational at Argonne in 2000. The maximum energy product of axial-die-pressed magnets was improved to the quality of the more expensive magnets obtained by transverse-die pressing. This achievement alone represents an opportunity for significant cost savings. For relatively long magnets, the percentage of improvement in the maximum energy products was about 12%. For near-final-shape magnets, the improvement was greater, at least 15%.

The main barrier to using a reciprocating feed to automate the alignment and pressing of magnet powder in a superconducting solenoid (i.e., the presence of high magnetic field gradients during sample insertion) was shown not to be an issue. The best magnets were made when batch processing simulated the conditions of the reciprocating feed. In particular, the magnetic field was on when the loose magnet powder in the die cavity was inserted into the bore of the solenoid. Most important, these conditions produced the best magnets. The energy product was within 92% of its theoretical maximum. Apparently, insertion of loose powder into the field gradient of the superconducting solenoid provides a form of magnetic die filling that improves grain alignment. Microscopic measurements of texture support this conclusion. Many in the industry had expected deteriorated alignment.

B. Development of Improved Powder for Bonded Permanent Magnets

Iver E. Anderson, R. William McCallum, and Matthew J. Kramer

Metallurgy and Ceramics Program

Ames Laboratory, Iowa State University

DOE Program Manager: David Hamilton

Contractor: Ames Laboratory, Iowa State University, Ames, Iowa

Prime Contract No.: W-7405-Eng-82

Objectives

- Increase the maximum operating temperature of electric drive motors from 150 to 200°C while maintaining sufficient operating characteristics.
- Reduce the cost of permanent magnet (PM) material in electric drive motors through the use of bonded magnets and injection molding technologies for high-volume net-shape manufacturing.

OAAT R&D Plan: Section 3.5: Task 3; Barriers B, C, D

Approach

- Develop innovative PM alloy design and processing technology for production of improved PM alloy powders for bonded PM magnets with a tolerance for high temperatures.
- Investigate alloy design improvements with melt-spinning methods with the specific goal of developing an improved spherical magnet alloy powder through gas atomization processing.
- Develop an enhanced gas atomization process along with a gas-phase powder surface reaction capability for production and environmental protection of powder for bonded magnets.
- Conduct experimental magnet molding trials on as-atomized and annealed magnet powders to characterize bonded magnet properties in collaboration with Oak Ridge National Laboratory (ORNL). Explore the effect of a novel crystallization/alignment procedure at high magnetic field in collaboration with Argonne National Laboratory (ANL).

Accomplishments

- Initiated selection of baseline PM alloys based on Nd-Fe-B with TiC additions for initial melt-spinning experiments, based on review of phase diagram information for relevant binary and ternary systems.
- Selected alloy constituent forms of melt charge for initial high-pressure gas atomization experiment, using principal baseline alloy composition.
- Initiated design of collaborative experiments with ANL and ORNL.

Future Direction

- Design a unique family of PM alloys to boost coercivity at elevated temperatures and to improve alloy quenchability for maximum yield from gas atomization.
- Develop a modified high-pressure gas atomization process for production of a spherical, rapidly solidified PM alloy powder, optimum for injection molding of bonded magnets.

- Investigate a gas phase reaction coating process for the atomized PM alloy powder to protect PM powders during the injection molding process and bonded magnet use.
- Establish a suitable injection molding process for producing bonded PM samples from the new PM alloy powder and high-temperature polymer.
- Characterize the magnetic properties of bonded magnets as a function of process variables, especially modifications of crystallization conditions and temperature, up to 200°C.

Introduction

To meet the cost and performance objectives of advanced electric drive motors for automotive applications, it is essential to improve the alloy design and processing of PM powders. To enable the widespread introduction of electric drive automobiles, two primary objectives that should be pursued for PM materials are (1) to increase the useful operating temperature for magnets to 200°C and (2) to reduce the active magnet material cost to about 25% of its current level. Currently, magnet material can operate in temperatures from 120 to 150°C, and the finished cost of sintered magnetic material is approximately \$90/kg. As an alternative PM material form, polymer-bonded particulate magnets offer the benefit of greatly simplified manufacturing, but at a more moderate level of stored magnetic energy that is still compatible with innovative PM motor designs. However, to exploit the potential of bonded PM materials for such motors, it is necessary to develop a particulate magnet material with high-temperature properties that can be loaded to a high volume fraction in an advanced polymer binder. Improving materials and processing to allow for increased operating temperature and mass production of net-shape bonded magnets by gas atomization and injection molding will be a significant advance toward high-volume production of advanced electric drive motors at reduced cost.

The accomplishments, expertise, and capabilities of Ames Laboratory appear well suited to meet the significant challenge of these project goals. Scientists from Ames Laboratory received a 1991 R&D 100 Award for research that demonstrated production of rare earth (RE)-Fe-B PMs by gas atomization and injection molding. This innovative work led to the issuance of six significant U.S. patents in the 1990s, including the principal patent on the benefits of using spherical atomized powders for bonded magnets. To support this work and other

studies in advanced powder processing, unique laboratory capabilities for high-pressure gas atomization of high quality metallic powders were developed, as shown in Figure 1. As a part of the



Figure 1. High-pressure gas atomization facility to be employed for research on processing of spherical permanent magnet alloy powders.

required equipment for magnet powder processing studies, Ames Laboratory has facilities for powder sizing and handling, including controlled-atmosphere capabilities, as well as a novel fluidized bed coating system and facilities for injection or compression molding of metal-filled polymers. As a demonstration of the available expertise in PM alloy design, Ames Laboratory investigators also received a 1996 R&D 100 Award for research on developing

an alloy based on RE-Fe-B with TiC additions that exhibits high quenchability and a high energy product. The results of this work also led to two more recent U.S. patents. The alloy design work is facilitated by fully developed laboratory capabilities for well-instrumented, controlled-atmosphere melt-spinning of ribbon samples, as shown in Figure 2, and for magnetic analysis (superconducting quantum interference device, vibrating sample magnetometer), calorimetric analysis (differential scanning calorimeter, differential thermal analysis), and microstructural analysis (scanning electron microscopy, transmission electron microscopy, auger electron spectroscopy, X-ray photoelectron spectroscopy), and oxidation and corrosion measurements.

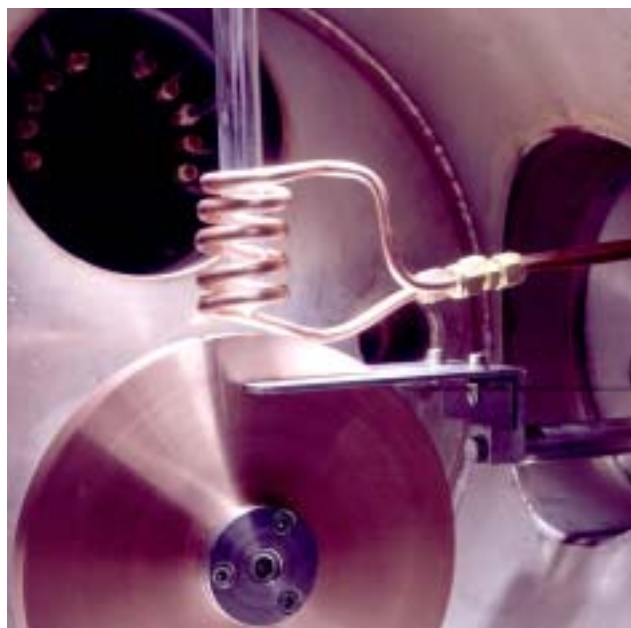


Figure 2. Well-instrumented, controlled-atmosphere melt spinning apparatus for preparation of ribbon samples for permanent magnet alloy design work.

Ames Laboratory scientists also interact with all national laboratories that are active in the DOE-Basic Energy Sciences Center of Excellence for Synthesis and Processing, which has focused on PM materials in the six years since its formation. Continued Ames Lab industrial interactions include Magnequench (Anderson, Indiana) on alloy design and rapid solidification processing, including the recent award of an LTR-cooperative research and development agreement on advanced sensors and

control of the melt-spinning process. Ames Laboratory scientists have also interacted over the last 10 years with Arnold Engineering (Norfolk, Nebraska) on injection molding and bonded magnet processing.

Approach

Innovative PM alloy design and processing technology will be developed for production of improved PM alloy powders for bonded PM magnets with a tolerance for high temperatures. Melt-spinning will be used to select alloy modifications that boost coercivity at elevated temperatures (up to 200°C) and improve alloy quenchability for optimum yield from a gas atomization process. A modified high-pressure gas atomization process will be developed for the improved PM alloys to enhance the yield of spherical, rapidly solidified powder. A gas-phase reaction coating process will be developed for enhanced environmental protection of fine atomized powder without degrading magnetic properties or molding rheology, building on recent studies of fluidized bed fluorination of similar RE alloy powders. A model polymer will be selected and used to test injection molding properties for high-temperature bonded magnets. The effects of a conceptual crystallization/alignment procedure conducted at a high magnetic field (up to 9 Tesla) will be investigated in collaboration with ANL. The magnetic properties of bonded powder samples will be determined as a function of loading fraction, powder size, annealing schedule, coating treatment, and temperature, up to a maximum of 200°C. Some of the bonded magnets also will be provided to ORNL for additional characterization in a collaborative effort.

Results

Currently, an evaluation of baseline PM alloys is under way, based on a review of all available phase diagram information for relevant binary and ternary systems and our understanding of the solidification process. Starting with Nd-Fe-B with TiC additions, alloying routes are being identified that have the potential to increase the high-temperature performance without adversely affecting the quenchability of the base alloy. Alloy constituent forms of the melt charge have been selected for initial high-pressure gas atomization experiments

using the principal baseline alloy composition. Discussions have been started with Thomas Mulcahy of ANL and John Hsu of ORNL on the design of collaborative experiments in high-temperature magnetic alignment and bonded magnet testing, respectively.

Conclusions

Because this project began in June 2001 and the accomplishments to date are preliminary in nature, no significant conclusions can be drawn at this time.

Bibliography

1. R. W. McCallum, K. W. Dennis, B. K. Lograsso, and I. E. Anderson, "Method of Making Bonded or Sintered Permanent Magnets," U.S. Patent 5,240,513, August 31, 1993.
2. R. W. McCallum, K. W. Dennis, B. K. Lograsso, and I. E. Anderson, "Method of Making Permanent Magnets," U.S. Patent 5,242,508, September 7, 1993.
3. I. E. Anderson, B. K. Lograsso, and R. L. Terpstra, "Environmentally Stable Reactive Alloy Powders and Method of Making Same," U.S. Patent 5,372,629, December 13, 1994.
4. R. W. McCallum, K. W. Dennis, B. K. Lograsso, and I. E. Anderson, "Method of Making Bonded or Sintered Permanent Magnets (continuation)," U.S. Patent 5,470,401, November 28, 1995.
5. I. E. Anderson and R. L. Terpstra, "Apparatus for Making Environmentally Stable Reactive Alloy Powders," U.S. Patent 5,589,199, December 31, 1996.
6. I. E. Anderson, B. K. Lograsso, and R. L. Terpstra, "Environmentally Stable Reactive Alloy Powders and Method of Making Same," U.S. Patent 5,811,187, September 22, 1998.
7. R. W. McCallum and D. J. Branagan, "Carbide/Nitride Grain Refined Rare Earth-Iron-Boron Permanent Magnet and Method of Making," U.S. Patent 5,803,992, September 8, 1998.
8. R. W. McCallum and D. J. Branagan, "Carbide/Nitride Grain Refined Rare Earth-Iron-Boron Permanent Magnet and Method of Making," U.S. Patent 5,486,240, January 23, 1996.
9. D. J. Branagan and R. W. McCallum, "The Effects of Ti, C, and TiC on the Crystallization of Amorphous $\text{Nd}_2\text{Fe}_{14}\text{B}$," *J. Alloys and Compds.*, **245** (1996).
10. D. J. Branagan, T. A. Hyde, C. H. Sellers, and R. W. McCallum, "Developing Rare Earth Permanent Magnet Alloys for Gas Atomization," *J. Phys. D: Appl. Phys.*, **29**, 2376 (1996).
11. M. J. Kramer, C. P. Li, K. W. Dennis, R. W. McCallum, C. H. Sellers, D. J. Branagan, L. H. Lewis, and J. Y. Wang, "Effect of TiC Additions to the Microstructure and Magnetic Properties of $\text{Nd}_{9.5}\text{Fe}_{84.5}\text{B}_6$ Melt-spun Ribbons," *J. Appl. Phys.*, **83**(11), pt. 2, 6631 (1998).
12. D. J. Branagan and R. W. McCallum, "Changes in Glass Formation and Glass Forming Ability of $\text{Nd}_2\text{Fe}_{14}\text{B}$ by the Addition of TiC," *J. Alloys and Compds.*, **244** (1–2), 40 (1996).
13. B. K. Lograsso, R. Reaves, I. Anderson, and R. W. McCallum, "Powder Processing of Rare Earth-Iron-Boron Permanent Magnets," *Inst. Phys. Res. and Tech., Rev. Part. Mater.*, **3**, 223 (1995).
14. D. J. Branagan and R. W. McCallum, "Altering Cooling Rate Dependence of Phase Formation during Rapid Solidification in the $\text{Nd}_2\text{Fe}_{14}\text{B}$ System," *J. Magn. Magn. Mater.*, **146** (1–2), 89 (1995).
15. I. E. Anderson, B. K. Lograsso, and R. W. McCallum, "High Pressure Gas Atomization of Rare Earth-Iron Alloy Permanent Magnet Powders," *Int. Conf. Process. Mater. Prop.*, Warrendale, PA, ed. H. Henein, O. Takeo, 1993, p. 645.

Publications/Presentations

R. W. McCallum and I. E. Anderson, "Bonded Magnets—Maturity, Cost, Suppliers," Segmented Electromagnetic Array Workshop at the Oak Ridge National Transportation Research Center, March 19–20, 2001.

C. Carbon Foam for Electronics Cooling

J. W. Klett, April McMillan, Lynn Klett, Nidia Gallego
Carbon and Insulation Materials Technology Group
Oak Ridge National Laboratory

DOE Program Manager: Patrick Davis
ORNL Technical Advisor: David Stinton

Contractor: Oak Ridge National Laboratory, Oak Ridge, Tennessee
Prime Contract No.: DE-AC05-00OR22725

Objectives

- Coordinate with automotive partners to develop carbon foam heat exchanger and heat sink designs to dissipate 30 W/cm² using current cooling fluids, achieving a targeted heat flux/weight ratio of >30% over current standards.
- Additional processing studies will be conducted to increase understanding of the effects of processing conditions on foam microstructure that affect thermal properties, as well as the strength, durability, and toughness of the foam.

OAAT R&D Plan: Section 3.5: Task 4; Barriers B, C, D

Approach

- Study fundamental mechanisms of heat transfer using the carbon foam.
- Develop a testing method to evaluate the foams in addition to designs using the foams.
- Compare results with existing data on heat sinks and current heat exchanger designs.
- Collaborate with original equipment manufacturers (OEMs) on designs and explore options together.
- Begin development of a low-cost fabrication method for the graphite foam.

Accomplishments

- Demonstrated superb heat transfer (35 W/cm²) at temperatures of less than 60°C with a reduction in cooling flow rates of 62% compared with current designs.
- Collaborated with Anteon for design optimization. Studies showed blind holes successfully reduce the pumping power required while maintaining high heat transfer.
- Collaborated with the National Security Agency (NSA) on a novel passive cooling system that utilizes evaporative cooling.
- Performed several extrusion runs yielding foam.

Future Direction

- Continue collaboration with industrial suppliers and OEMs for enhanced design studies.
- Test and evaluate different designs of heat sinks to determine their effect on heat transfer.

- Develop a fluid dynamics mathematical model for predicting heat transfer from the foam to fluid flowing through the foam.
- Continue development of the extrusion process.
- Continue collaboration with NSA on heat pipe/thermosyphon design studies targeting passive cooling of $150\text{W}/\text{cm}^2$.

Introduction

Approximately two-thirds of the world's energy consumption is wasted as heat (e.g., in incandescent light bulbs, internal combustion engines, air conditioning, power plants). This waste will likely get worse as the power levels of computer processors and other electronic devices increase. Computer chips with power levels of up to 1000 W may be commonplace in less than 5 years. High-efficiency heat exchangers are being incorporated into computers and electronics to recover some of the heat losses and increase efficiencies. The primary function of the heat exchanger in these applications is to reduce the temperature of the electronics, improving both life and reliability. The second task of the heat exchanger is to recover the energy for use in other applications, thereby reducing the total energy consumed. Unfortunately, most heat exchangers dissipate captured heat from the electronics as low-quality heat (very low temperatures compared with ambient air). Subsequently, this recovered heat is simply dumped to the ambient air and wasted. However, a unique graphite foam developed at the Oak Ridge National Laboratory (ORNL) and licensed to Poco Graphite, Inc., promises to allow for novel, more-efficient heat exchanger designs that can possibly dump high-quality heat, allowing recovery of energy for other applications. This unique graphite foam (Figure 1) has a density of between 0.2 and $0.6\text{ g}/\text{cm}^3$ and a bulk thermal conductivity of between 40 and $187\text{ W}/\text{m} \cdot \text{K}$. The ligaments of the foam exhibit a thermal conductivity higher than that of artificial diamond and, in combination with a very accessible surface area ($> 4\text{ m}^2/\text{g}$), the overall heat transfer coefficients of foam-based heat exchangers can be up to two orders of magnitude greater than those of conventional heat exchangers. As a result, foam-based heat exchangers could be dramatically smaller and lighter than conventional designs.

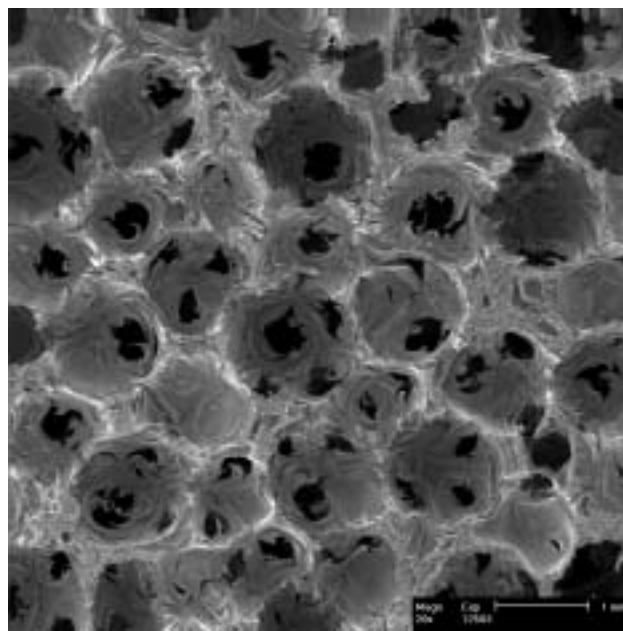


Figure 1. ORNL graphite foam.

Power Electronics Cooling

To characterize the behavior of the foam as a heat sink, a test chamber was built which allows measurement of the power dissipation capacity. As shown in Figure 2, the foam is mounted to an aluminum plate (usually by brazing) and placed in a cavity where the cooling fluid flows. The system is designed with no gap around the foam, forcing the fluid to pass through the pores of the foam. The system is sealed with O-rings, and pressure taps are inserted into the chamber to measure the pressure drop of the foam heat sink. A simulated power inverter is mounted to the aluminum plate and is capable of generating up to 800 W ($32\text{ W}/\text{cm}^2$). As the cooling fluid passes through the system, the temperatures of the heater and inlet and outlet fluid are measured. The overall heat transfer coefficient (U_o) is calculated from Eq. (1), where ΔT_{LM} is the log mean temperature difference between the heater

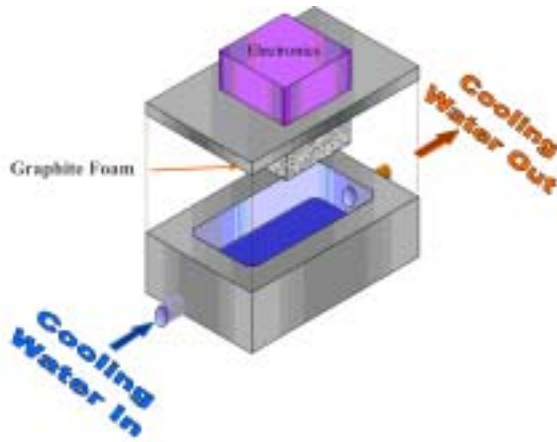


Figure 2. Schematic of test rig to evaluate heat sink geometries.

and the cooling fluid, A is the area (foot print) of foam attached to the aluminum plate, and q is the heat dissipated to the cooling fluid. With this test rig, different base plates, foam geometries, and other heat sink devices such as aluminum foam were compared.

$$U_o = q / (A \cdot \Delta T_{LM}) \quad (1)$$

The graphite foam was compared in head-to-head tests with aluminum foam. Figure 3 shows the temperature of the simulated power inverter as a function of the power density of the electronics. The graphite foam yielded significantly lower temperatures (less than 60°C) than the aluminum foam (up to 155°C). Clearly, the graphite foam performs as a better heat sink. Another significant difference in the materials is seen as a non-linearity in the profile for the aluminum foam. This is a result of the low thermal diffusivity of the aluminum foam

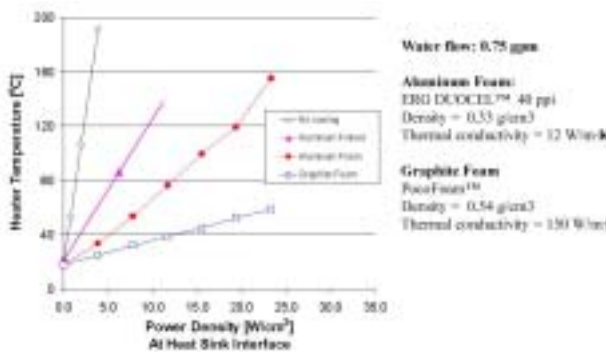


Figure 3. Simulated power electronic temperature versus power density for various heat sinks.

(less than 10 times that of carbon foam). After a change in the power level of the heaters, the aluminum foam heat sink took more than 20 minutes to reach an apparent steady state condition, while the graphite foam heat sink reached a steady state in approximately 2 minutes. The high thermal diffusivity may be more important than the heat transfer coefficient. Because they have a quicker response to transient conditions, the graphite foam heat sinks will not allow power electronics temperatures to peak at as high a level, thereby dramatically enhancing the reliability and life of the devices.

In another test, the same graphite and aluminum foams were bonded with the S-bond™ technique (developed by MRi, Inc.) to different base plates [aluminum, copper, and aluminum silicon carbide (AlSiC)]. Table 1 compares the heater temperatures at a power density of 23 W/cm² for the different foams and base plates. It is clear from these results that the graphite foam out-performs the aluminum foam with all the different base plates. Another important result is that the material chosen for the base plate does not affect the performance of the graphite foam heat sink. In contrast, the aluminum foam performs better with copper and AlSiC base plates than with aluminum base plates (although it does not perform better than graphite foam with those plates).

Table 1. Heater temperatures for various base plates with graphite and aluminum foams

Base plate	Foam type	Electronic temp. @23 W/cm² (°C)
Aluminum	Aluminum	155.2
Copper	Aluminum	136.2
AlSiC	Aluminum	134.2
Aluminum	Graphite	59.8
Copper	Graphite	58.7
AlSiC	Graphite	59.3

To further demonstrate the effectiveness of the graphite foam, air at 15 standard ft³/minute was used as the cooling fluid instead of water. Figure 4 shows the air-cooling data overlayed on the water-cooling data shown in Figure 3. The performance of the air-cooled graphite foam is comparable to that of the aluminum foam with water cooling, indicating that

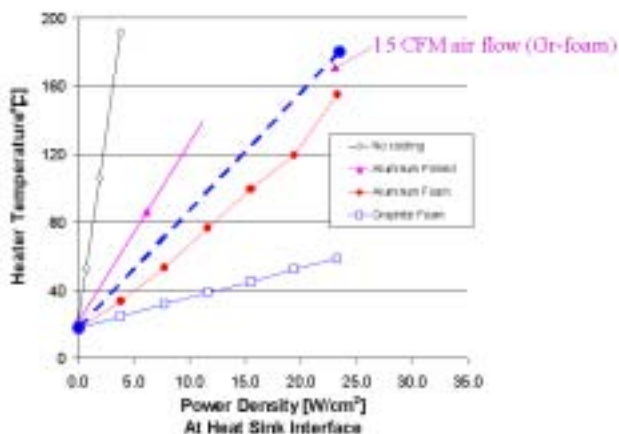


Figure 4. Simulated power electronics temperature versus power density for graphite foam using air cooling compared with water cooling.

perhaps air can be used with proper geometries of the foam in some applications. The use of air cooling would dramatically reduce the complexity of the cooling systems used to cool power electronics by eliminating the recycling of cooling fluids.

It is noted that the pressure drop through the foam is relatively high (~2 psi/in for air at 4 m/s and ~2 psi for water at 0.003 m/s). However, low-pressure-drop systems can be engineered to maintain high heat transfer while reducing pressure drop and pumping power. For instance, HEPA filters are successfully used in many applications despite the pressure drop associated with sub-micron pores. Collaborative research with Anteon Corp. has shown that blind holes and corrugation can significantly reduce pressure drop while maintaining high heat transfer (Garmen and Elwell 2001).

Passive Evaporative Cooling

In a collaborative effort with the NSA, graphite foam has been demonstrated to be an efficient evaporator for thermosyphons and heat pipes. In this design, the electronic chip is flipped upside down and the heat sink is bonded directly to the back of the chip, thereby reducing the thermal resistances typically found in chip applications. The heat sink is submerged under a fluorinated hydrocarbon that evaporates as heat is applied and condenses in another cavity of the device. The fluid is recycled to the evaporator through gravity to complete the cycle. In previous work, copper foam and diamond film

evaporators have been exhaustively evaluated with power densities of up to 28 W/cm^2 at operating temperatures of less than 100°C . After the copper and diamond evaporators were replaced with graphite foam, power densities of up to 100 W/cm^2 were attained. Figure 5 shows the foam brazed to the computer chip, and Figure 6 shows the thermosyphon chamber that has been fitted with graphite foam heat sinks to promote improved cooling on the condenser.

It is anticipated that the foam will be useful in many types of evaporative cooling applications. This totally passive system with high heat dissipation capabilities has great potential for cooling power electronics in automotive applications.

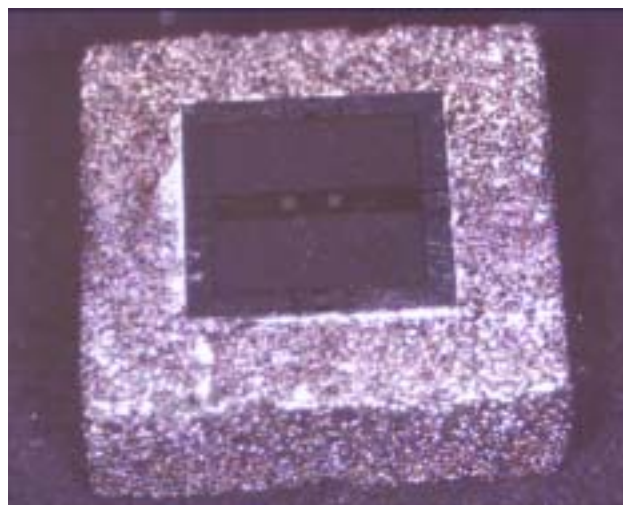


Figure 5. Computer chip brazed directly to graphite foam with MRi S-Bond™ technique.

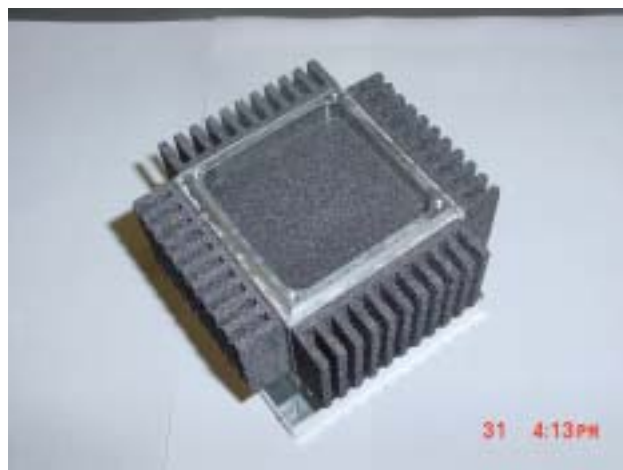


Figure 6. Thermosyphon chamber with graphite foam fins and graphite foam condenser.

Extrusion of Graphite Foam

The objective of this research effort is to reduce the production costs of graphite foam by manufacturing the foam in a continuous mode using an extrusion apparatus. Figure 7 shows a schematic of the extrusion apparatus built for this research. The mesophase pitch is loaded into the feed hopper of the extruder. From the hopper, the mesophase pitch drops onto the screw, which forces it down the extruder barrel. The barrel is heated gradually to the melting temperature of the mesophase pitch. The molten mesophase passes through a koch mixer and enters the metering pump, which controls the flow rate at which the molten mesophase enters the foaming chamber. In the foaming chamber, the temperature is raised gradually to the foaming temperature and further to the coking temperature. The foam is then cooled at the die head and extruded.

Two experimental extrusion runs have been performed using an ARA-24 mesophase pitch from Mitsubishi Gas Chemical Co. On the first run, a maximum temperature of 400°C was reached because of limitations in the equipment. This temperature was enough to start the foaming process; however, it was not high enough to reach the coking stage. Figure 8 (a and b) shows scanning electron microscope (SEM) photographs of samples collected along the foaming chamber. The porosity or bubbles observed in Figure 8a are probably due to the beginning of off-gassing of the mesophase (i.e., foaming); in Figure 8b, a more porous structure is observed.

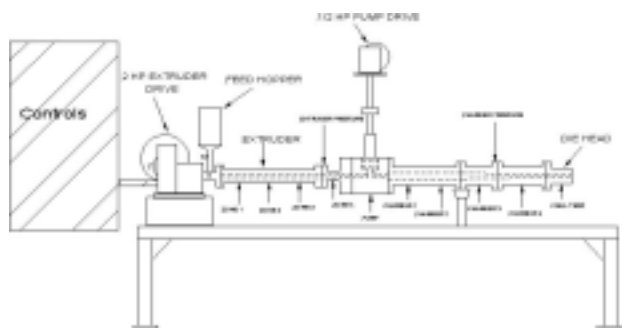
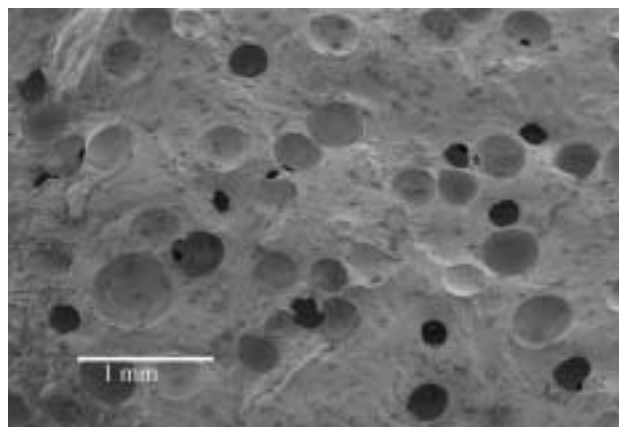
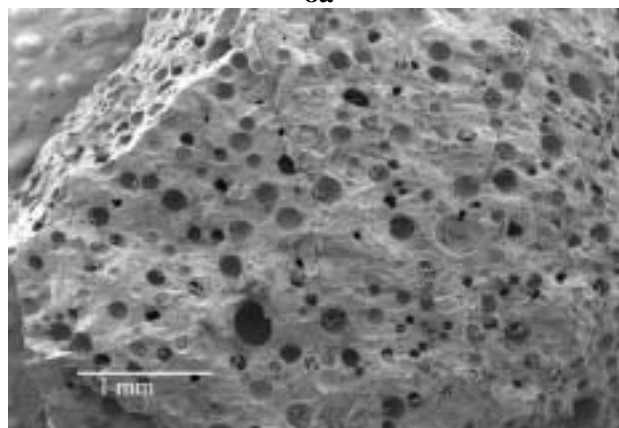


Figure 7. Schematic of extrusion apparatus.



8a



8b

Figure 8. SEM photographs of samples collected from the first extrusion run.

In the second run, a maximum temperature of 500°C was achieved. This temperature allowed the mesophase to reach the foaming and coking temperatures; however, the sharp tapering of the foaming chamber toward the die head was found to be a limiting factor at the moment of extrusion. Samples were collected from inside the foaming chamber and examined under the SEM. Figure 9 shows some SEM photographs of these samples. A porous structure, similar to the one achieved with the batch process, is observed in these samples.

Modifications of the foaming chamber are under way to eliminate the tapering of the chamber and improve the extrusion process.

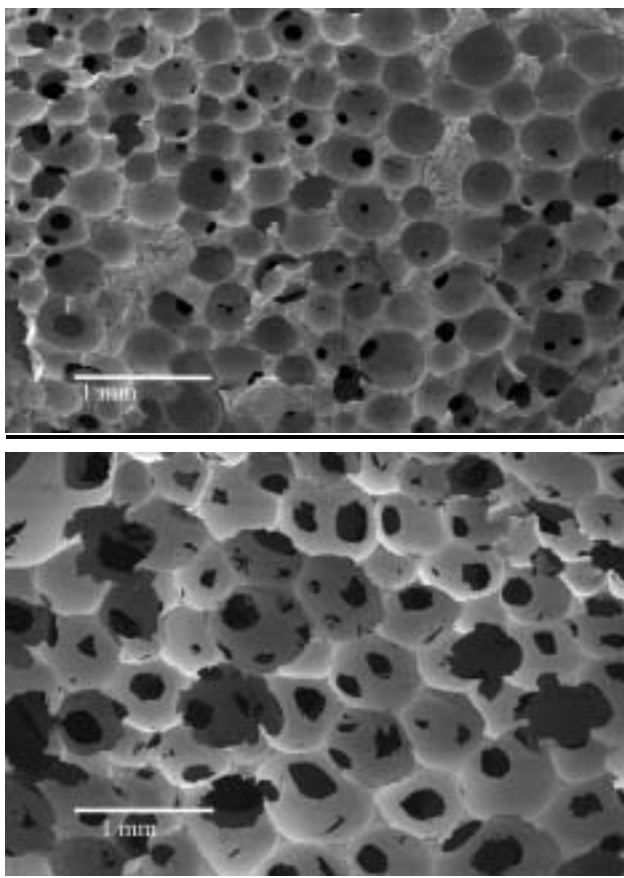


Figure 9. SEM photographs of samples collected from the second extrusion run.

Conclusions

It is evident that graphite foam is an efficient thermal management material. When compared with several types of heat exchangers, foam-based designs significantly out-performed conventional systems. It was demonstrated that the foam-based heat exchangers can be used to reduce the volume of cooling fluid required, or eliminate the water cooling system altogether. Additionally, the foam responds to transient loads significantly faster than do traditional heat sinks. This response time may be crucial for power electronics, as it could dramatically lower temperatures during peak loads. These peak loads drive the cooling system requirements even though they are experienced for a minimal amount of the operational life.

The foams have also been demonstrated to be efficient evaporators in heat pipes and thermosyphons. It is anticipated that future work with the NSA will lead to passive cooling devices

capable of dissipating heat loads of up to 150 W/cm².

Finally, a novel fabrication method has been developed to alleviate the cost issues associated with producing graphite foam. This process is being characterized and de-bugged. Although it has been shown that foam can be produced using the extrusion method, significant work remains to be performed to optimize extrusion as a commercially viable fabrication method.

Publications

R. W. Garman and R. J. Elwell, "Thermal Performance of a Graphite Foam Material with Water Flow for Cooling Power Electronics," PCIM 2001 Conference, Chicago, September 2001.

A. McMillan and J. Klett, "High-Conductivity Carbon Foams and Applications," Second Annual Carbon Foams Workshop, Wright-Patterson Air Force Base, Ohio, November 2-3, 2000.

J. Klett, "High-Thermal-Conductivity Graphite Foams," Conference Workshop, American Carbon Society, Clemson University, Clemson, S.C., October 2000.

K. Kearns, J. Klett, D. Rogers, "Carbon and Graphite Foams," National Space and Missile Materials Symposium, San Diego, February 2000.

J. W. Klett, C.-C. Tee, D. P. Stinton, and N. A. Yu, "Heat Exchangers Based on High-Thermal-Conductivity Graphite Foam," in *Proceedings of the First World Conference on Carbon*, July 9-13, Berlin, Germany, 2000.

J. Klett, A. McMillan, Ron Ott, "Heat Exchangers for Heavy Vehicles," in *Proceedings of the Society of Automotive Engineering Government/Industry Meeting*, Washington, D.C., June 19-21, 2000.

J. Klett, L. Klett, T. Burchell, C. Walls, "Graphitic Foam Thermal Management Materials for Electronic Packaging," in *Proceedings of the Society of Automotive Engineering Future Car Congress*, Crystal City, Washington, D.C., April 2-6, 2000.

J. Klett, B. Conway, "Thermal Management Solutions Utilizing High-Thermal-Conductivity Graphite Foams," in *Proceedings of the 45th International Society for the Advancement of Materials and Process Engineering Symposium and Exhibition*, Long Beach, Calif., May 21-25, 2000.

J. Klett, R. Hardy, E. Romine, C. Walls, T. Burchell, "High-Thermal-Conductivity, Mesophase-Pitch-Derived Carbon Foams: Effect of Precursor on Structure and Properties," *Carbon*, 32(8), 2000.

Patents Issued

"Process for Making Carbon Foam," U.S. Serial Number 6,033,506, Oak Ridge National Laboratory, March 7, 2000.

"Pitch-Based Carbon Foam Heat Sink with Phase Change Material," U.S. Serial Number 6,037,032, Oak Ridge National Laboratory, March 14, 2000.

"Pitch-Based Carbon Foam and Composites," U.S. Serial Number 6,261,485, Oak Ridge National Laboratory, July 17, 2001.

D. dc Bus Capacitors for PNGV Power Electronics

B. A. Tuttle, D. Wheeler, G. Jamison, J. S. Wheeler, and D. Dimos
Sandia National Laboratories

DOE Program Managers: Patrick Davis

David Hamilton (202) 586-2314; fax: (202) 505-844-9781; e-mail: david.hamilton@ee.doe.gov

Contractor: Oak Ridge National Laboratory, Oak Ridge, Tennessee
Prime Contract No.: DE-AC05-00OR22725

Objectives

- Develop a replacement technology for the currently used aluminum electrolytic dc bus capacitors for year 2004 new-generation vehicles.
- Develop a high-temperature polymer dielectric film technology that has dielectric properties technically superior to those of aluminum electrolytic dc bus capacitors and is of comparable or smaller size.
- Scale up cost-competitive polymer film dielectric technology: (1) develop a continuous process for dielectric sheet fabrication and (2) fabricate prototype capacitors.

OAAT R&D Plan: Section 3.5: Task 4; Barriers A, B, C, and D

Approach

- Work with automobile design and component engineers, dielectric powder and polymer film suppliers, and capacitor manufacturers to determine state-of-the-art capabilities and to define market-enabling technical goals.
- Develop a project plan with automobile manufacturers and large and small capacitor companies to fabricate polymer dielectric sheets suitable for the manufacture of PNGV capacitors.
- Synthesize unique conjugated polyaromatic chemical solution precursors that result in dielectric films with low dissipation factors (DFs) and excellent high-temperature dielectric properties.
- Develop polymer film processes and technologies that will lower costs to permit competitive high-volume capacitor manufacturing.
- Interact with Oak Ridge National Laboratory (ORNL) with regard to mechanical characterization of films.

Accomplishments

- Invented chemical synthesis procedures that resulted in polymer films with five times the energy density of commercial polyphenylene sulfide at 110°C. These films exhibited properties ranging from dielectric constants of from $K = 6$ and $DF = 0.009$ to $K = 4$ and $DF = 0.002$. These hydroxylated polyphenylene films (PP+OH) met technical requirements for commercialization.
- Developed and evaluated four different process steps for PP+OH films to lower cost; three of the new processes were successful.
- Developed a new hydroxylated polystyrene (PVP) chemistry that would be cost-competitive in commercial markets and meet technical specifications for commercialization.

- Collaborated with TPL, Inc., to fabricate free-standing dielectric sheets that had breakdown strengths of greater than 4 MV/cm from -40° to 110°C .
- Collaborated with ORNL to characterize mechanical properties of PVP films.

Future Directions

- Perform extensive electric field and temperature characterization to determine that the Sandia National Laboratories (SNL) polyfilm dielectrics will meet the PNGV requirements for breakdown field and DF for temperatures from -40° to 110°C .
- Interface with the appropriate scale-up company to fabricate large rolls of slit dielectric polymer sheet (10-kg lots) suitable for fabrication of multilayer capacitors (2 to 200 μF); TPL, Electronic Concepts, and AVX/TPC are potential collaborators.
- Have General Motors (GM) and SNL evaluate large-value (20 μF to 200 μF) capacitors, fabricated by vendor(s), in simulated electric hybrid vehicle environments.
- Develop more cost-effective synthesis routes for lower-DF polymer film dielectrics that meet 2004 PNGV requirements.

Results

Strategy and Interactions

SNL has actively worked with a number of representatives from the automobile industry to obtain their perspective on what is needed for advanced automobiles. In FY 2001, SNL has continued its emphasis on the development of polymer film dielectrics for two reasons. First, GM has been in favor of soft-breakdown dielectric film technology—a phenomenon that bulk ceramic capacitors do not exhibit. Second, emphasis on polymer dielectrics provides a greater balance of the DOE effort between polyfilm and ceramic technologies, as requested by the Electrical/Electronics Tech Team.

These interactions led us to conclude that the most viable replacement technology for the electrolytic dc bus capacitors is multilayer polymer film capacitors. Reducing the size of the polymer capacitors was most often cited by automobile design engineers and capacitor manufacturers as a needed technology-enabling breakthrough. In addition, it is necessary to improve high-temperature (110°C) performance while keeping the technology cost competitive. For polymer film dielectrics, a goal for commercialization of a dielectric constant of 6 and a DF of less than 0.01 was initially agreed to by AVX/TPC and GM. However, based on the GM criteria for capacitance density of $2.0 \mu\text{F}/\text{cm}^3$, the team agreed that if a polyfilm of $K = 4.5$ could be developed that could meet the temperature

requirements, then that film would be suitable for scale-up activities.

The initial scale-up strategy consisted of the following steps: (1) develop a polymer film technology that meets requirements, (2) synthesize 10-kg to 20-kg batches, (3) develop a continuous process for 3- μm -thick polymer films, and (4) fabricate it into prototype capacitors. This approach had to be modified for two reasons: (1) the cost of dielectric film technology became a high priority in FY 2001, and (2) the synthesis and development of a continuous process had to be broken down into multiple steps to be accomplished. Although an initial polymer film technology (PP+OH) was developed that met all criteria and was exceedingly low-loss, its cost was prohibitive. Although SNL was successful in developing three new processes that reduced the cost of the PP+OH technology by a factor of ten, costs were still not satisfactory for PNGV applications. Thus a second polymer film technology, hydroxylated polystyrene, was developed that exhibited more loss than PP+OH but is 10 to 100 times more cost-effective. This new technology has five times the energy-density-handling capability of the commercial standard of polyphenylene sulfide.

Inverter designs and operating conditions for dc bus capacitors vary from manufacturer to manufacturer. GM has presented 2-to-5-year goals and 10-year goals for dc bus capacitors that other auto manufacturers feel are satisfactory milestones for the PNGV program. Specific goals for 2004

commercialization include (1) -40°C to 110°C operation, (2) capacitance density of greater than $2\text{ }\mu\text{F}/\text{cm}^3$, and (3) 575-V dc operation with 250 A RMS of ripple current capability. In addition, GM has requested fail-safe operation; Ford and Daimler-Chrysler have not voiced as strong an opinion as to the fail-safe criterion. The fail-safe criterion is analogous to soft breakdown of the dielectric, rather than catastrophic electrical discharge and mechanical failure that can be observed in bulk ceramic dielectrics. Soft breakdown occurs as a result of the vaporization of the thinner electrode layers of the polymer dielectric near electrical breakdown sites.

Based on those criteria, an individual dielectric layer thickness of approximately $3\text{ }\mu\text{m}$ for polyfilm capacitors is projected. These thickness values are based on operating field strengths of $2\text{ MV}/\text{cm}$ for the newly developed polyfilm capacitors. Based on these assumptions and on measurement of presently available commercial capacitors, size comparisons and capacitance densities of 500- μF dc bus capacitors for different technologies were obtained (Figure 1). Soft-breakdown behavior and lower cost are assets for polymer film capacitors. The projected polymer film capacitor volume is calculated assuming that 40% of the capacitor space is not active and 200-nm-thick electrodes are used. Note that the volumetric capacitance efficiency for a $K = 4.5$ polyfilm capacitor of $2.4\text{ }\mu\text{F}/\text{cm}^3$ exceeds the 2004 commercialization goal of $2\text{ }\mu\text{F}/\text{cm}^3$.

Polymer Film Dielectric Development

SNL polymer film dielectric development has been based on the request from manufacturers that the new polyfilm dielectrics have voltage and temperature stability equivalent to those of present

polyphenylene sulfide (PPS) technology. Thus a structural family of polymer dielectrics has been designed and synthesized to meet two of the most stringent PNGV requirements: (1) low dielectric loss and (2) extremely good temperature stability. Figure 2 shows a schematic diagram of SNL's conjugated, polyaromatic-based structure and indicates the large number of molecular modifications to this structure that are possible. Our present effort emphasizes molecular engineering of higher-polarizability structures that will enhance dielectric constants yet retain acceptable dielectric loss characteristics. A patent disclosure has been initiated covering the design and synthesis techniques for this polymeric family. Three initial molecular modifications to the base structure were made: (1) propyl bridge substitution, (2) sulfur bridge substitution, and (3) replacement of R-side groups with high-electronegativity fluorine ions to enhance polarizability.

The dielectric properties of a series of films from this structural family resulted in films that were stable with respect to voltage and temperature as shown in Figures 3 and 4. We increased the dielectric constant compared with industry standard PPS from $K = 3$ to $K = 4$ while maintaining similar loss and breakdown field characteristics. However, the dielectric constants were below the desired value of 6.

For FY 2001, we have investigated two different hydroxylated polymer film structural families to enhance K . A schematic diagram of the structure of the hydroxylated polyphenylene polymer is shown in Figure 3. Unlike the previous molecular modifications to the stiff-backbone conjugated polyaromatic structure, hydroxyl modifications

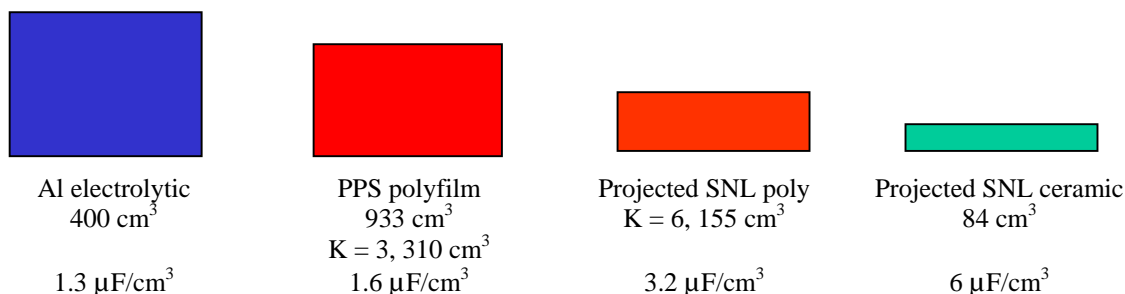


Figure 1. Size diagram of 500- μF dc bus capacitors of different technologies.

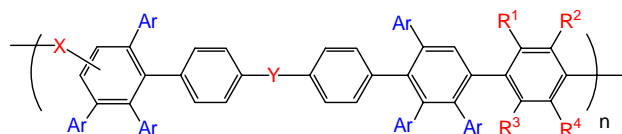


Figure 2. Schematic diagram of SNL conjugated polyaromatic film base structure.

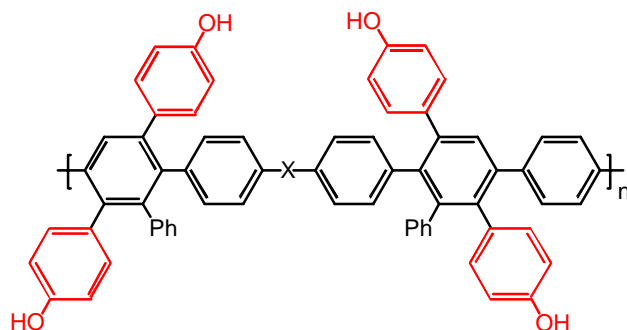


Figure 3. Schematic diagram of hydroxylated polyphenylene structure.

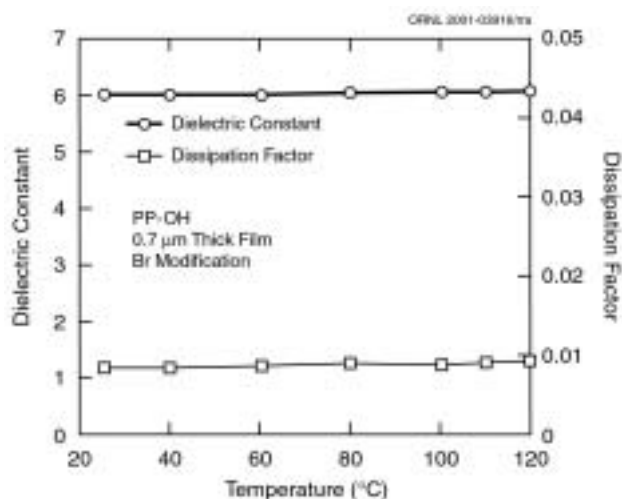


Figure 4. Dielectric constant and dissipation factor vs temperature for a hydroxylated polyphenylene film annealed at 200°C.

resulted in substantial changes to both dielectric constant and DF. Figure 4 shows the dielectric properties of a spin-deposited hydroxylated polyphenylene film (PP+OH) annealed at 200°C. The film has a dielectric constant of 6 and a DF = 0.009 that is stable to 120°C. These properties exceed the technical requirements for scale-up. There is considerable flexibility in modification of the dielectric properties through thermal annealing treatments. In Figure 5, a PP+OH film exhibits extremely low loss—the DF is 0.0025 from 25°C to 110°C. It has a dielectric constant of 4. The stiff

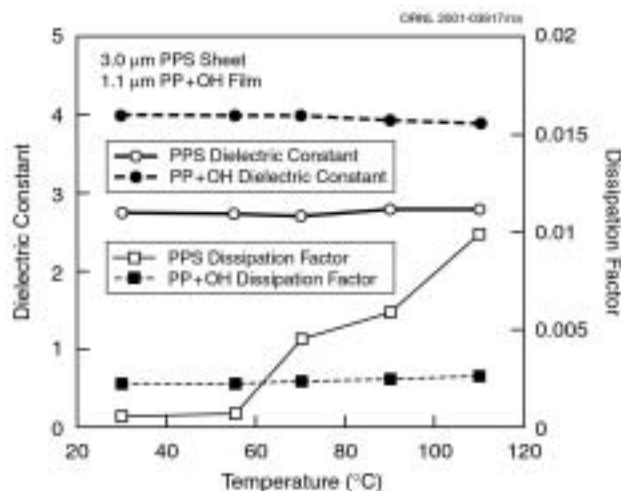


Figure 5. Dielectric constant and dissipation factor versus temperature for a hydroxylated polyphenylene film annealed at 300°C and commercial PPS film.

backbone chemistry of PP+OH results in far superior DF at 110°C compared with commercial PPS (DF = 0.01).

Synthesis routes for hydroxylated polystyrene (PVP) films were designed and implemented because the cost of this technology was 1 to 2 orders of magnitude less than that of the PP+OH film technology developed by SNL. Because of the chemical structure of this compound, it was postulated that these films would have loss characteristics inferior to those for a polypropylene film of similar geometry. Our PP+OH films had a dielectric constant of 6 that was stable from 25°C to 110°C. Although the loss met specifications (DF < 0.01) at 25°C, unacceptable loss (DF = 0.065) was measured at 110°C. A study was initiated to incorporate crosslinker chemistry into our PVP polymers to reduce the flexibility of the polymer chains and thus decrease dielectric loss.

Development and incorporation of a VECTOMER crosslinker chemistry reduced the loss to 0.01 at 110°C, as shown in Figure 6. As expected, the dielectric constant also decreased. However, the dielectric constant of 4.7 is acceptable for PNGV applications and scale-up activities.

A critical issue for PNGV capacitors is the dielectric breakdown strength of the polymer films. The capacitor energy density for our polymer film capacitors that exhibit linear dielectric behavior with field is proportional to the square of the field. For our spin-deposited polymer films deposited on

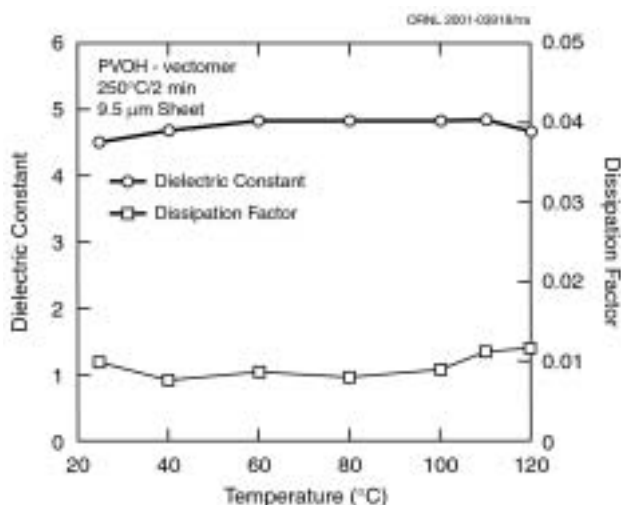


Figure 6. Dielectric constant and dissipation factor of SNL hydroxylated polystyrene film with VECTOMER cross-linker.

aluminum-coated silicon wafers, the breakdown strength had been limited to 2 MV/cm. We had postulated that if smooth interfaces between the dielectric and the electrode film could be achieved—as would be the case for free-standing dielectric sheets—that breakdown strength would be increased. We worked with TPL to fabricate 5 × 5 in. freestanding polymeric sheets of the crosslinked hydroxylated polystyrene films in 3- and 10-μm thicknesses. A recently targeted area of our investigations has been the dielectric breakdown strength of our films versus commercially available films. Figure 7 shows dielectric breakdown strength at 25°C and 110°C for spin-deposited and freestanding sheet films of PVP. In addition, the 3.4-μm PVP film is shown to have almost twice the breakdown strength of a 2.5-μm-thick PPS sheet at 110°C. When the higher dielectric constant of the PVP film is taken into account for PPS ($K = 4.7$ versus $K = 2.8$), a factor-of-five difference in the capacitance energy density ($E_D = 1/2 CV^2$) at 110°C is calculated. We have also performed breakdown studies for temperatures as low as -40°C. Our PVP-crosslinked film has a breakdown strength of 5.3 MV/cm compared with 1.3 MV/cm for polypropylene film of a similar geometry. Thus the dielectric breakdown strength of our film chosen for scale-up is essentially twice the desired operating field of 2 MV/cm from -40°C to 110°C.

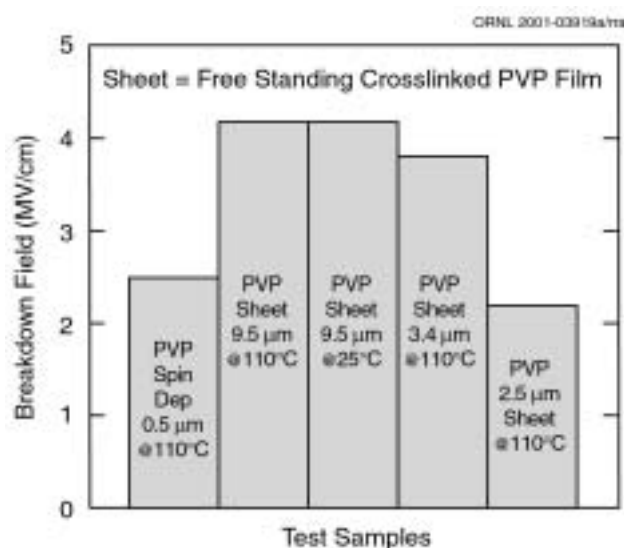


Figure 7. Dielectric strength of SNL crosslinked polymer films and a commercial polymer dielectric.

Summary

Critical economic and technical issues for improvements of dc bus capacitors for new-generation vehicles were determined through discussions with automobile design engineers, chemical synthesis companies, and capacitor manufacturers. Polymer film dielectric development has been emphasized in FY 2001, and we have developed a multi-step project plan for large-scale commercialization of polymer film dc bus capacitors that includes developments of freestanding sheet dielectrics, continuous casting procedures, and fabrication of smaller (1 to 5μF) capacitors. We have developed two new hydroxylated polymer film technologies. Because of cost, we down-selected our hydroxylated polystyrene chemistry for scale-up into polymeric sheets of 3-μm and 10-μm thickness. These dielectric sheets were shown to have five times the energy density of polyphenylene sulfide at 110°C. Extensive testing performed at -40°C showed our new films have greater breakdown strength than polypropylene. Thus the new SNL dielectrics have breakdown fields of greater than 4 MV/cm from -40°C to 110°C. We have submitted both spin-deposited and freestanding sheet polymer films to ORNL for mechanical testing. Future work will be to develop a continuous process for drum

casting of the crosslinked hydroxylated polystyrene films. Once the continuous process has been achieved, then prototype capacitors will be fabricated and evaluated for inverter applications.

Technical Disclosures

D. Wheeler and G. Jamison, "Novel Polymer Film Synthesis Routes of Voltage and Temperature Stable Dielectrics," October 5, 1999.

Presentations

1. G. M. Jamison, D. Wheeler, and B. A. Tuttle, "Novel Polyarylene/Polyimides as High K, Low Loss Dielectrics," Pacificchem 2000 Conference, Honolulu, Hawaii, December 16, 2000.

2. B. A. Tuttle, J. A. Voigt, D. Wheeler, G. Jamison, J. Cesarano, J. E. Smay, T. Scofield, J. Gieske, P. Clem and W. R. Olson, "Dielectric Materials Development at Sandia National Laboratories," University of Illinois Materials Science Department Seminar Series, September 14, 2000. (Invited)

3. B. A. Tuttle, D. Wheeler, G. Jamison and D. Dimos, "High-Temperature Capacitor Review," Electrical/Electronics Technical Team Meeting, Detroit, Michigan, February 22, 2001.

E. Mechanical Reliability of Electronic Ceramics and Electronic Ceramic Devices

M. K. Ferber, L. Riester, C-H Hsueh, and M. Lance

Mechanical Characterization and Analysis Group

Oak Ridge National Laboratory

DOE Program Manager: Patrick Davis

ORNL Technical Advisor: David Stinton

Contractor: Oak Ridge National Laboratory, Oak Ridge, Tennessee

Prime Contract No.: DE-AC05-00OR22725

Objectives

- Predict and assess the mechanical reliability of electronic devices with emphasis on those used for automotive power electronics (e.g., capacitors).
- Correlate the mechanical characterization of polymer film capacitors developed by Sandia National Laboratories (SNL) to the dielectric behavior.

OAAT R&D Plan: Section 3.5: Task 4; Barriers A, D

Approach

- Characterize the reliability of the electronic ceramics using thermomechanical stress modeling and probabilistic design and life-prediction techniques specifically developed for ceramics.
- Develop an analytical model predicting residual stresses in ceramic devices.
- Develop techniques to characterize polymer films developed by SNL and correlate mechanical behavior with dielectric behavior.

Accomplishments

- Used a micro-mechanical test apparatus to directly measure the strength of small multi-layer ceramic capacitors (MLCCs).
- Developed an analytical model for predicting residual stresses in MLCCs and applied it to explain strength differences in several varieties of 1206 MLCCs.
- Received the first series of polymer film samples from SNL and characterized them using a mechanical properties microprobe.

Future Direction

- Develop hardware and test procedures for characterizing polymer films as a function of temperature.
 - Use the mechanical properties microprobe to track changes in polymer structure resulting from in-service use.
-

Introduction

A lack of mechanical reliability of electronic ceramics in MLCCs can often limit the reliability of their electronic function. The application of ceramic life prediction codes (developed for structural ceramic component design in high-temperature gas turbine engines) is used in concert with the mechanical testing analyses of the electronic ceramics because they portray the probabilistic strength and fatigue properties of electronic ceramics in an appropriate (but underutilized) manner. The primary effort in FY 2001 involved the direct measurement of the three-point flexure strength of the MLCCs.

Because of the interest in polymer film capacitors, a collaboration with SNL was initiated to evaluate SNL's materials. Synthetic chemists at SNL are currently fabricating a number of different temperature-stable polymers for the PNGV program. The 2004 goal is to have a polymer film dielectric that can operate continuously at 110°C. Although these films are expected to be similar to polyphenylene sulfide in terms of properties, they are truly unique films that have not been used before by the capacitor industry. Therefore, the mechanical characterization of these new materials would be very beneficial, if not mandatory.

Results

MLCCs for Automotive Power Electronics

In FY 2000, an in-situ measurement technique was used to assess the mechanical strength of MLCCs.¹⁻³ (The capacitor size examined is illustrated in Figure 1.) The basic approach involved the calculation of the Weibull strength distribution from the measurement of potential strength-limiting flaw-size distributions (using image analysis) and the use of the Griffith equation. The dielectric ceramic in all three MLCC sets contained two different and concurrent flaw types that were studied as potential strength-limiters: pores and secondary phase "inclusions" (see Figure 2 for a representative microstructure that shows both).

More recent studies have focused on the direct measurement of the three-point flexure strength using the micro-mechanical test facility shown in Figure 3. The X-Y-Z stages, which are driven by computer-controlled stepper motors, provide for precise positioning of the specimen. During testing,



Figure 1. Multi-layer ceramic capacitors of 0805 (top) and 1206 (bottom).

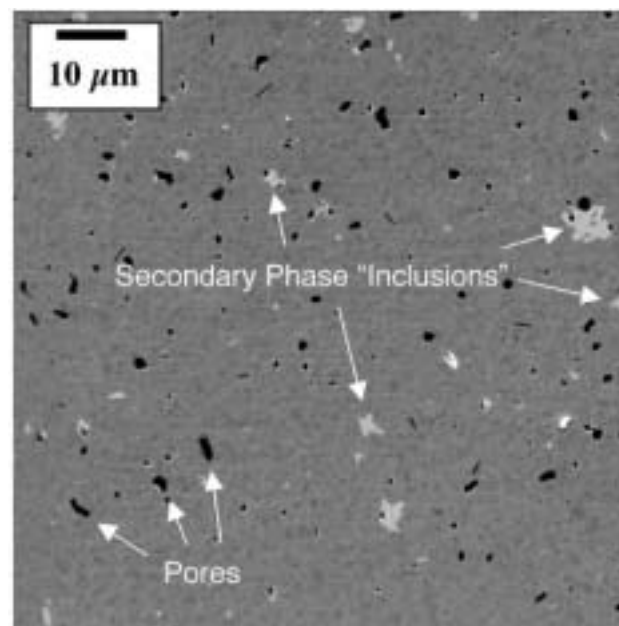


Figure 2. The size distributions of two potential strength-limiting flaw types were measured: pores and secondary phase "inclusions."

the capacitor is first placed on a lower three-point support fixture that is attached to the Z-stage. The load then is applied by raising the Z-stage at a controlled rate so that the specimen contacts the fixed upper load point, which is attached to a load cell. The strength data generated using this facility

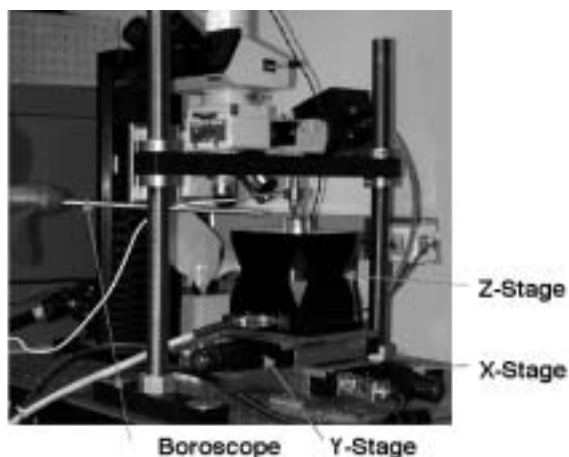


Figure 3. Overview of the X-Y-Z stage assemblage used to position the specimen.

are currently being compared with indirect strength measurements determined by microscopic imaging.

We have tested both the 805 and 1206 capacitors. The corresponding fixtures are shown in Figure 4. The fixture for the 805 MLCCs is

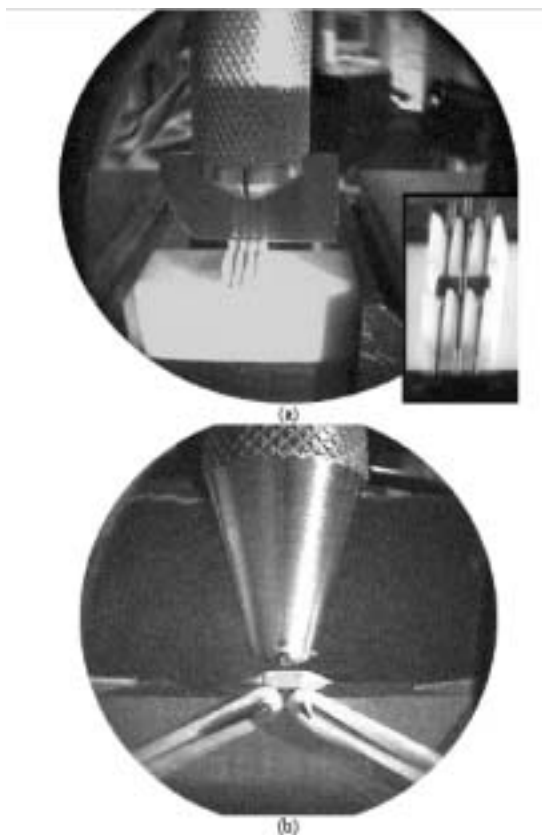


Figure 4. Three-point test fixture used for (a) 805 and (b) 1206 MLCCs.

fabricated from an aluminum oxide block with loading pin-guide grooves machined at the appropriate locations. The inset in Figure 4a illustrates the pin-and-groove arrangement. The fixture for the 1206 MLCCs (Figure 4b) consists of a lower metal support plate with two pins that are located by means of two machined edges. Rubber bands are used to pull the pins snugly against the edges. The upper pin is supported on a small bearing, thereby providing some articulation to facilitate alignment.

Assessment of Polymer Capacitors

Five films (Table 1) provided by SNL have been analyzed to date. These films were deposited on

Table 1. Summary of polymer films evaluated to date

No.	Base designation	Thickness	Anneal	Anneal
		(Å)	T (°C)	Time (m)
1	PVP5	3937	300	2
2	PVP5-2X	28485	180	4
3	PVP5-2X	20064	180	4
4	PVP5	4989	200	2
5	PVP5	5830	160	2
6	PVP5	4976	250	2

100-nm aluminum/400-nm SiO₂/Si wafers. The SiO₂, which is applied by chemical vapor deposition and then thermally annealed, was put on by a commercial manufacturer to passivate the Si. The mechanical properties microprobe³ was used to measure hardness and elastic modulus as a function of depth of penetration. Figure 5 illustrates typical results for the hardness.

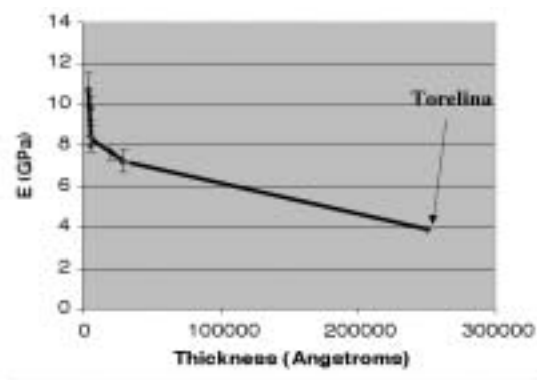


Figure 5. Relationship between hardness and polymer film thickness. The Torelina is a commercial film.

Publications

1. A. A. Wereszczak, L. Riester, J. W. Hill, and S. Cygan, "Mechanical and Thermal Properties of Power Electronic Ceramic Multilayer Capacitors," *Ceramic Transactions, Proceedings of the American Ceramic Society*, 2000.

2. A. A. Wereszczak, K. Breder, L. Riester, T. P. Kirkland, and R. J. Bridge, "In-Situ Mechanical Property Evaluation of Dielectric

Ceramics in Multilayer Capacitors," SAE Paper 00FCC-116, SAE 2000 World Congress, Arlington, Virginia, April 2000.

3. A. A. Wereszczak, K. Breder, L. Riester, T. P. Kirkland, and R. J. Bridge, *Toward the Assessment of Mechanical Robustness of Ceramic Multilayer Capacitors (MLCCs)*, ORNL/TM-1999/202, Oak Ridge National Laboratory. October 1999.

3. FUEL CELLS

A. Carbon Composite Bipolar Plates

T. M. Besmann, J. W. Klett, and J. J. Henry, Jr.

*Surface Processing and Mechanics Group and Carbon and Insulating Materials Group
Oak Ridge National Laboratory*

DOE Program Managers: JoAnn Milliken and Patrick Davis

ORNL Technical Advisor: David Stinton

*Contractor: Oak Ridge National Laboratory, Oak Ridge, Tennessee
Prime Contract No.: DE-AC05-00OR22725*

Objectives

- Develop a slurry-molded carbon fiber material with a carbon chemical-vapor-infiltrated sealed surface as a bipolar plate that meets DOE cost goals of less than \$10/kW.
- Collaborate with potential manufacturers with regard to testing and manufacturing of such components.

OAAT R&D Plan: Section 3.3: Task 13; Barrier B

Approach

- Fabricate fibrous component preforms for the bipolar plate by slurry molding techniques using carbon fibers of appropriate lengths.
- Fabricate hermetic plates using a final seal with chemical-vapor-infiltrated carbon.
- Develop commercial-scale components for evaluation.

Accomplishments

- Demonstrated ability to mold two-sided prototypical 100-cm² active area plate.
- Demonstrated polarization behavior in a cell that was comparable to graphite.
- Measured thermal diffusivity and determined thermal conductivity.
- Provided two-sided specimens to industrial partners for evaluation.
- Licensed technology to Porvair Fuel Cell Technology.

Future Direction

- Develop bipolar plate material/configuration to meet unique requirements of various users.
 - Transfer technology and aid in scale-up with Porvair.
-

Introduction

In FY 2001, the Oak Ridge National Laboratory (ORNL) carbon composite bipolar plate effort has achieved several programmatic goals in molding two-sided preforms, measuring thermal diffusivity, and licensing the technology. Two-sided components 2.5 mm thick with a 100-cm² active area have been produced. Sample components are being tested at Plug Power, Honeywell, Ballard, and International Fuel Cells for their evaluation. Previously, it was demonstrated that projected costs would meet program goals of \$10/kW, that the material properties met program requirements, and that the component had the substantial advantage of weighing almost 50% less than competing materials.

Approach

Fibrous component preforms for the bipolar plate are prepared by slurry molding techniques using 100- μ m carbon fibers (e.g., Fortafil) in water containing phenolic resin. The approach is such that a vacuum molding process produces a low-density preform material. A phenolic binder is used to provide green strength, which also assists in providing geometric stability after an initial cure. A set of brass molds were fabricated with channels that were 0.78 mm (31 mil) deep and wide. The molds are used to impress channels and other features into the preform material. The surface of the preform is sealed using a chemical-vapor-infiltration (CVI) technique in which sufficient carbon is deposited on the near-surface fibers to make the surface hermetic. This is accomplished by placing the preforms in a furnace heated to 1300–1500°C and allowing methane under reduced pressure to flow over the component. The hydrocarbon reacts and deposits carbon on the exposed fibers of the preform; when sufficient deposition has occurred, the surface becomes sealed. Thus the infiltrated carbon provides both an impermeable surface and the electrical conductivity necessary to obtain power efficiently from the cell. Processing times are in the range of 4 hours.

Results

Bipolar plates with flow field patterns and other necessary features molded into both sides were produced using brass molds fabricated to produce plates with 100-cm² of active area of the Los

Alamos National Laboratory (LANL) design (Figure 1). Slurry-molded preforms 2.5 mm thick were produced for fabrication into two-sided bipolar plates. These were placed between the brass molds, and the assembly was placed in a heated press. The mold was uniformly compressed to 10 kPa (14 psi) at 200°C and held briefly to both impress the features and cure the phenolic resin. The molded preforms released readily from the mold (a common release agent is used), and the features were precisely reproduced in the preform. The plates were subsequently sealed using the CVI process.



Figure 1. Completed carbon composite bipolar plate.

A xenon flash diffusivity technique was used to measure thermal diffusivity of the composite at room temperature. A xenon flash lamp provided a heating pulse to the specimen front surface. An infrared detector was used to record the back surface temperature rise after the pulse. Using the analysis described in ASTM Designation E1461 1992, “Standard Test Method for Thermal Diffusivity of Solids by Flash Method,” the thermal diffusivity of the specimen was calculated. Measurements of the through-thickness thermal properties of the plate material were performed using a square sample cut from the plate with a thickness $d = 2.461$ mm. Five measurements were taken, yielding an average thermal diffusivity $\alpha = 0.0290$ cm²/sec, S.D. = 0.0004. The specific heat of graphite was assumed to yield a thermal conductivity of 1.37 W/mK. This is a moderately low value because of the significant porosity in the material.

Polished cross-sections revealed the structure of the carbon composite bipolar plate. Figure 2 shows the flow field in the plate, revealing the sealed surface of the porous material. The relatively poor tolerances on the mold appear to have caused some disruptions in the surface of the plate. However, higher-precision molds used by a fuel cell manufacturer evaluating this technology have demonstrated preparation of high-tolerance components.

The 100-cm²-active-area, two-sided bipolar plate prepared at ORNL was tested in a fuel cell at LANL. Figure 3 indicates the measured resistivity and cell



Figure 2. Optical micrograph of a polished cross-section of a carbon composite bipolar plate.

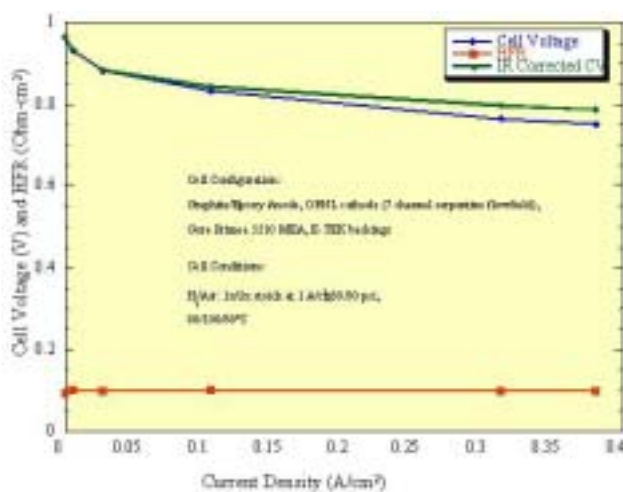


Figure 3. Resistivity and cell voltage from testing at LANL reveals good properties and behavior.

voltage behavior. The plate performed well in a cell; however, LANL reports using high flow rates in order to compensate for leakage from the seals along the edges. It is expected that this problem would be easily remedied by use of an adhesive seal.

Conclusions/Future Work

During this period, the fabrication of molded two-sided bipolar plates and their infiltration with carbon was demonstrated. Thermal properties and cell behavior were measured. Although the through-thickness thermal conductivity was low, the cell behavior was good. The technology has been licensed to Provoir Fuel Cell Technology, and sample plates are being evaluated by several fuel cell manufacturers. DOE targets and the properties of the materials are compared in Table 1.

Table 1. Material property targets and values.

Property	DOE target	POCO Graphite	Carbon composite
Bulk conductivity (S/cm)	>100		200–300
Surface resistivity (Ω/cm)		8	12
Hydrogen permeability (cm ³ /cm ² -sec)	<2 × 10 ⁻⁶	Meets target	Meets target
Corrosion rate (μA/cm ²)	<16	80	6
High-volume production cost (\$/kW)	<10	40	5.50

Future work will concentrate on developing carbon composite bipolar plates with unique properties to meet the requirements of the several fuel cell manufacturers. It will also involve assisting Porvoir with technology transfer and with scale-up in size and production.

Publications/Presentations

T. M. Besmann, J. W. Klett, J. J. Henry, Jr., and E. Lara-Curzio, "Carbon/Carbon Composite Bipolar Plate for Proton Exchange Membrane Fuel Cells," *J. Electrochem. Soc.* **147**(11) 2000.

Patents Issued

"Bipolar Plate/Diffuser for a Proton Exchange Membrane Fuel Cell," U.S. Patent 6,037,073, March 14, 2000.

“Bipolar Plate/Diffuser for a Proton Exchange Membrane Fuel Cell,” U.S. Patent 6,171,720, January 9, 2001.

B. Cost-Effective Surface Modification for Metallic Bipolar Plates

M. P. Brady and L. D. Chitwood

Oak Ridge National Laboratory

DOE Program Managers: JoAnn Milliken and Patrick Davis

ORNL Technical Advisor: David Stinton

Contractor: Oak Ridge National Laboratory, Oak Ridge, Tennessee

Prime Contract No.: DE-AC05-00OR22725

Objective

- Develop a low-cost metallic bipolar plate alloy that will form an electrically conductive and corrosion-resistant TiN surface layer during thermal nitriding to enable use in a polymer electrolyte membrane (PEM) fuel cell environment.

OAAT R&D Plan: Section 3.3: Task 13; Barrier B

Approach

- Conduct a study of the nitridation behavior of a series of inexpensive Ni-Ti and Fe-Ti base alloys that can meet DOE bipolar plate cost goals.
- Identify a combination of Ti level, ternary, and higher-order alloying addition(s), and nitridation reaction conditions that result in the formation of an adherent, dense TiN surface layer.
- Immerse nitrided alloy coupons in a 5% hydrofluoric acid solution, measure weight loss, and conduct cross-section electron microscopy evaluation to screen for the presence of defects in the nitride layer. Characterize nitride layer microstructure and composition by X-ray diffraction and electron probe microanalysis. Use this information in a feedback loop to modify alloy chemistry and nitridation processing conditions to optimize the protectiveness of the nitride surface layer.
- Measure the electrical conductivity of select nitrided alloys by direct current four-point probe.
- Evaluate the corrosion behavior of select nitrided alloys in simulated PEM fuel cell environments [in collaboration with Los Alamos National Laboratory (LANL)].

Accomplishments

- Evaluated the nitridation behavior of a series of developmental Ni-Ti and Fe-Ti base alloys with ternary and quaternary alloying additions. Identified alloy chemistries/nitridation conditions that led to the formation of adherent TiN-base surface layers with good corrosion resistance in short-term, 5% hydrofluoric acid immersion screenings.
- Demonstrated the capability of a new, industrial-scale high-density infrared processing technique to nitride model Fe-Ti and Ti alloys in seconds (compared with hours/days using conventional nitriding techniques).
- Delivered a series of model and developmental alloys to LANL for corrosion testing in simulated PEM fuel cell environments. Established via a model refractory alloy that a nitrided surface can exhibit sufficient corrosion resistance, without significant Nafion membrane contamination, in a PEM fuel cell environment.
- Revealed through testing at LANL that the first generation of developmental nitrided Ni-Ti and Fe-Ti base alloys exhibited inadequate corrosion resistance. Post-exposure analysis suggested that the corrosion

susceptibility was related to poor nitride coverage at alloy grain boundaries. Preliminary evaluation of the first alloy of a second generation of Ni-Ti base alloys designed to eliminate this problem indicated a corrosion current density on the order of $1-2 \times 10^{-6}$ A/cm² at 0.98V vs. saturated calomel electrode in pH3 sulfuric acid at room temperature. This result is close to meeting DOE corrosion resistance goals.

Future Direction

- Optimize composition/nitridation conditions for the second generation of Ni-Ti and Fe-Ti base alloys in order to eliminate corrosion susceptibility resulting from poor nitride coverage at alloy grain boundary sites. A go/no go decision will be made regarding the ability of these nitrided alloys/approach to meet DOE bipolar plate corrosion resistance goals.
- Down-select alloy composition and explore scale-up issues with commercial alloy producers.
- Implement a process optimization study for inexpensive, rapid nitridation using high-density infrared processing.
- Supply nitrided bipolar plates to LANL and fuel cell manufacturers for in-cell performance evaluation.

Introduction and Approach

The bipolar plate is one of the most expensive components in PEM fuel cells. Thin metallic bipolar plates offer the potential for significantly lower cost than the machined graphite bipolar plates currently used and the potential for lower weight and volume and better performance than developmental carbon fiber and graphite bipolar plates currently under consideration. However, inadequate corrosion resistance can lead to high electrical resistance and/or contaminate the PEM. Metal nitrides (e.g., TiN) offer electrical conductivities an order of magnitude greater than that of graphite and are highly corrosion resistant. Unfortunately, conventional coating methods leave “pin-hole” defects in the nitride layers that result in accelerated local corrosion and unacceptable performance.

The goal of this effort is to develop a Ti-containing bipolar plate alloy that will form an electrically conductive and corrosion-resistant TiN surface layer during thermal (gas) nitriding. There are three advantages to this approach. First, because the nitriding is performed at elevated temperatures, pin-hole defects are not expected because thermodynamic and kinetic factors favor complete conversion of the metal surface to nitride. Rather, the key issues are nitride layer cracking, adherence, and morphology (discrete internal precipitates vs. continuous external scales), all of which can be controlled through proper selection of alloy composition and nitridation conditions. Second,

thermal nitridation is an inexpensive, well-established industrial technique. Third, the alloy can be formed into final shape by inexpensive metal forming techniques, such as stamping, prior to thermal nitridation.

Existing commercial alloys were typically designed to form oxide layers for corrosion protection and do not thermally nitride to form a corrosion-resistant surface layer. Therefore, this effort is focused on designing a new family of alloys specifically to form a corrosion-resistant TiN surface. As shown in Figure 1, for a series of model Ti-base alloys studied under this program, alloy composition can significantly influence the corrosion resistance of the resulting nitride surface layer.



Figure 1. Nitrided model Ti-alloy coupons after 20 h immersion in 5% hydrofluoric acid, illustrating that alloy composition can significantly influence the corrosion resistance of the resultant TiN-base surface layer.

Results to date strongly support proof of principle for thermal nitridation to protect a metallic bipolar plate. A model thermally-nitrided refractory alloy, Tribocor 532N (Nb-30Ti-20W wt. %), exhibited a corrosion current density of only 6.1×10^{-7} A/cm² at 0.98 V vs normal hydrogen electrode and stable behavior for 700 h under 1 A/cm² in the LANL corrosion test cell (data of Kirk Weisbrod, pH3 sulfuric acid, 2 ppm F⁻, 80°C) and exhibited essentially no Nafion membrane contamination (~1% active sites affected) after a 300-h immersion screening in pH2 and pH6 sulfuric acid (with air or hydrogen) (data of Christine Zawodzinski, LANL). These results establish that a nitrided surface can perform well in a PEM fuel cell environment. The key challenge is whether such corrosion-resistant nitride zones can be produced from an alloy that is sufficiently inexpensive to meet DOE bipolar plate cost goals (refractory alloys such as Tribocor 532N are too costly for transportation related applications).

Results

Efforts have focused on the development of inexpensive Ni-(5-15)Ti and Fe-(5-15) Ti wt. % base alloys that can meet the DOE cost goals. As shown in Figure 2, composition/processing conditions to form an adherent TiN surface layer on Ni-Ti and Fe-Ti base alloys have been identified. Bulk electrical conductivities were in the range of $1-2 \times 10^4 \Omega^{-1}\text{cm}^{-1}$ after nitriding, which surpasses the DOE electrical conductivity target by two orders of magnitude.

Corrosion testing at LANL in simulated PEM fuel cell environments indicated insufficient corrosion resistance in the first generation of the Ni-Ti and Fe-Ti base alloys. Post-exposure analysis suggested that the susceptibility was related to preferential nitridation at alloy grain boundaries, which was exacerbated by alloy grain growth during the nitridation treatment. A worst-case example of this phenomenon is shown in Figure 3 for nitrided Fe-35Ni-8Ti, a composition that was borderline for external TiN surface layer formation. Although the TiN layers shown in Figure 2 are of much higher quality, there are similar, occasional small local regions of preferential grain boundary nitridation

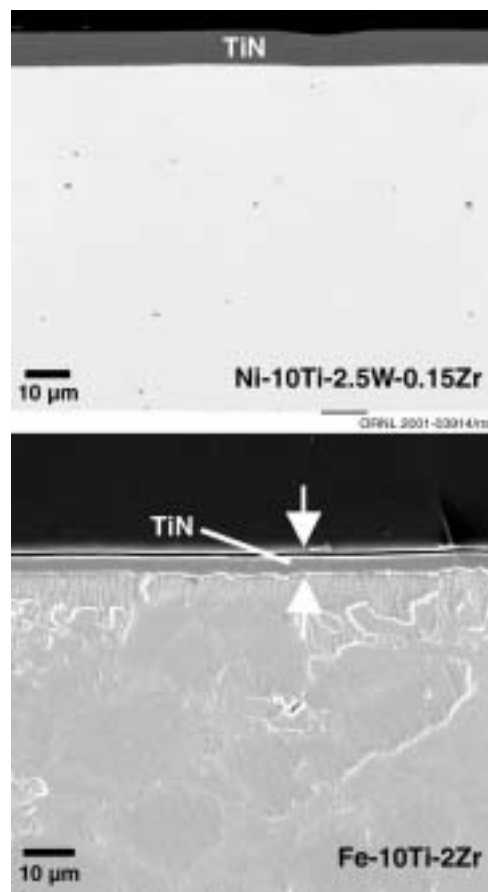


Figure 2. Cross-section electron micrographs of nitrided Ni-Ti and Fe-Ti base alloys (wt. %) showing external TiN surface layer formation.

that degrade the continuity and protectiveness of the TiN surface layer.

A combination of process and alloy optimization is being pursued to eliminate this problem. A heat treatment step prior to nitridation has been added to coarsen the alloy grain structure so that appreciable grain growth during the nitridation treatment does not occur. In addition, a promising alloying addition has recently been identified to modify the nitrogen permeability of the alloy to minimize preferential grain boundary nitridation. Preliminary results have yielded corrosion current densities in the range of $1-2 \times 10^{-6}$ A/cm² at 0.98 V vs. normal hydrogen electrode in pH3 sulfuric acid at room temperature, which are close to the DOE bipolar plate corrosion resistance goal.

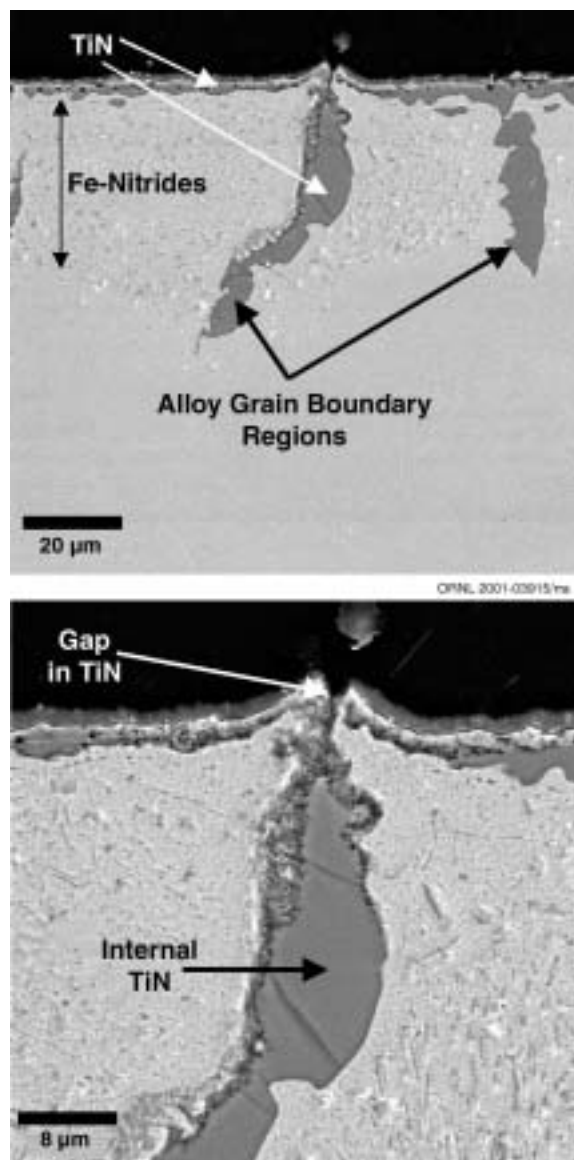


Figure 3. Cross-section electron micrographs of nitrided (Fe-35Ni-8Ti wt. %) highlighting preferential nitridation and gaps at alloy grain boundary sites. (Worst-case example shown to illustrate effect).

Alternative nitriding approaches are also under investigation. High-density infrared processing (<http://www.ms.ornl.gov/sections/mpst/process/craigblue/default.htm>) is of particular interest because of the rapid heating rates ($>400^{\circ}\text{C}/\text{second}$) and applicability to continuous processing (collaboration with C. Blue and V. K. Sikka, Oak

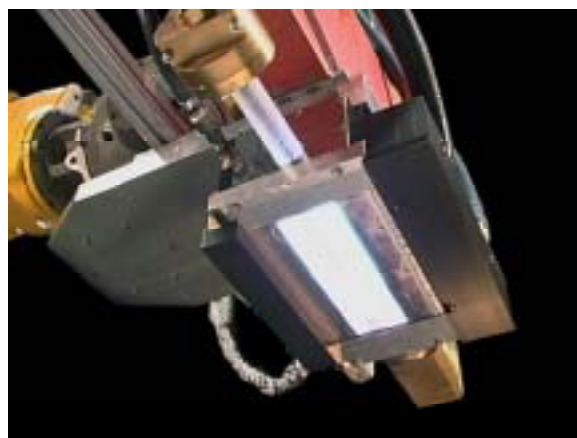


Figure 4. High-density infrared processing lamp.

Ridge National Laboratory) (Figure 4). Preliminary screening showed that model Ti and Fe-Ti base alloys could be nitrided in seconds by rapid infrared heating to just under their melting points in an atmosphere containing nitrogen (conventional nitriding is done at lower temperatures and typically takes hours/days). Although conventional thermal nitriding is commercially available and relatively inexpensive, the use of infrared processing has great potential to further reduce cost and increase throughput volume for the industrial-scale production/nitriding of metallic bipolar plates.

Conclusions/Future Work

Good progress has been made in developing inexpensive Ni-Ti and Fe-Ti base alloys to form a corrosion-resistant nitride surface layer. However, issues remain regarding inadequate nitride coverage and protection at alloy grain boundary sites. Efforts are focused on optimization of alloy composition/nitridation conditions to eliminate this susceptibility. A go/no go decision will be made regarding the ability of these nitrided alloys and this approach to meet DOE bipolar plate corrosion-resistance goals, and an alloy composition will be down-selected. Work will then focus on scale-up issues with commercial alloy producers and on delivery of nitrided bipolar plates to LANL and fuel cell manufacturers for in-cell performance evaluation.

C. Low-Friction Coatings and Materials for Fuel Cell Air Compressors

George R. Fenske (primary contact), Oyelayo Ajayi, John Woodford, and Ali Erdemir
Argonne National Laboratory

DOE Program Manager: Patrick Davis

Contractor: Argonne National Laboratory, Argonne, Illinois
Prime Contract No.: W-31-109-Eng-38

Objectives

- Develop and evaluate the friction and wear performance of low-friction coatings and materials for fuel cell air compressor/expander systems. Specific goals are
 - 50 to 75% reduction in friction coefficient
 - one-order-of-magnitude reduction in wear
- Transfer the developed technology to DOE industrial partners.

OAAT R&D Plan: Section 3.3: Task 13; Barrier D

Approach

- For various air compressor/expander systems being developed, identify the critical compressor components requiring low friction.
- Apply Argonne's near-frictionless carbon (NFC) coatings to the components when appropriate and evaluate their performance.
- Develop and evaluate polymer composite materials containing boric acid solid lubricant.

Accomplishments

- Identified the radial air bearings and thrust bearings of Meruit's turbocompressor as components that require both low friction and low wear rate for satisfactory performance.
- Performed thrust washer wear tests that showed that Argonne's NFC coating reduced friction by about four times and wear rate by two orders of magnitude. Both exceeded the project goals.
- Increased the scuffing resistance of a steel surface by about 10 times with NFC coatings.
- Began durability testing of NFC-coated air-bearing hardware components.
- Completed initial friction and wear testing of nylon-12 polymer with B₂O₃ addition. Significant reduction in wear was observed with the addition of B₂O₃, especially under high relative humidity.
- Achieved a 50% reduction in friction for application in Variex-variable displacement compressor/expander using Hitco C/C composite and anodized aluminum contact pairs.
- Designed and constructed a new high-speed test rig for evaluation materials for Mechanology's toroidal intersecting vane machine (TIVM).

Future Directions:

- Continue durability testing of NFC-coated air-bearing hardware in air-bearing rig.
 - Complete commercial fabrication and tribological evaluation of injection-molded polymer and boric acid composite material.
 - Develop and evaluate appropriate coating and/or material for high-sliding-speed TIVM vanes.
-

Introduction

A critical need in fuel cell systems for vehicles is an efficient, compact, and cost-effective air-management system to pressurize fuel cell systems to about 3 atmospheres. Pressurization of fuel cells will result in higher power density and lower cost. A compact, lightweight, highly efficient compressor/expander is required to pressurize the fuel cell systems. Several compressor/expander systems are currently being developed for DOE. The efficiency, reliability, and durability of compressors depend on effective lubrication or friction and wear reduction in critical components such as bearings and seals. Conventional oil or grease lubrication of compressor components is not desirable because such lubricants can contaminate and poison the fuel cells stack. The objective of this project is to develop and evaluate low-friction coatings and/or materials for critical components of air compressor/expanders being developed by various contractors for DOE vehicle fuel cell systems. The work this year focused on Meruit's turbocompressor air bearings and Mechanology's TIVM.

Approach

For various air compressor/expanders being developed, we will identify the key critical components that require a low friction coefficient and wear resistance. Through its R&D program, the tribology group at Argonne has developed low-friction and low-wear coatings and materials. Most notable is the discovery of an amorphous carbon coating with extremely low friction coefficients (<0.001 in dry nitrogen) and very low wear. Where appropriate, the NFC coating will be applied to the critical component(s). Another approach is the development of polymeric-boric acid composite material. The NFC coatings and polymer composite materials will be evaluated under conditions expected to be typical for the components.

Results

Meruit Air Bearing

Initial tests of a prototype of Meruit's journal and thrust bearing showed the desirable low friction coefficient; however, failure can still be caused by excessive wear or seizure (scuffing). As reported last year, laboratory screening tests showed that NFC coating substantially reduced the friction coefficient and significantly increased wear and scuffing resistance. Consequently, air-bearing hardware components (Figure 1) were coated with NFC for durability evaluation in the air-bearing test rig at FD Contours.



Figure 1. Near-frictionless-carbon-coated air-bearing hardware for durability testing.

The durability test consists of start-and-stop cycling of the air bearing. Under full-speed operation, there is no contact in either the journal or the thrust bearings. Contact and sliding between surfaces occur only during the start and stop of the bearing. Damage that occurs during the start and stop determines the durability of the bearing. The performance of the bearing can also be measured in

terms of time to lift-up and time to coast to a complete stop after contact.

An NFC-coated journal bearing is currently undergoing durability testing. Dimples of known dimensions were inserted into contact areas of the coated bearing shaft. Wear measurements are taken after some predetermined number of start/stop cycles by measuring changes in the dimple dimension. Wear measurements have already been taken after 250, 1000, 2000, and 4000 cycles. A plot of linear wear is shown in Figure 2. The original coating thickness was about 3 μm . Two of the dimples showed accelerated wear between 2000 and 4000 cycles because air bearings were unbalanced during that test. Further testing is in progress.

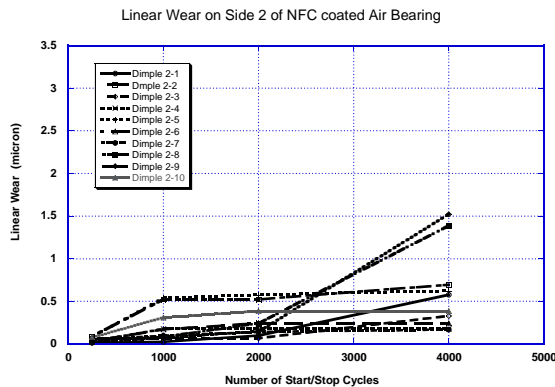


Figure 2. Linear wear in NFC-coated air bearing during durability test.

Mechanology TIVM

Mechanology has completed the design and construction of a prototype TIVM compressor/expander (Figure 3). Analysis shows that an overall system friction coefficient of less than 0.3 is required to meet the DOE program target for efficiency. The primary sources of friction in the TIVM are vane sliding interface, housing compressor seal, and expander bearings. The most critical of these three sources is the vane sliding interface because of its high sliding speed of 60–75 m/s. Consequently, effort during this past year was devoted to evaluating and developing material and/or coatings for the TIVM vane. A new high-speed friction and wear test rig (Figure 4) was constructed. Screening tests evaluating the variation of friction with sliding velocity have been completed for some low-friction materials. Figure 5 shows the



Figure 3. Mechanology's prototype toroidal intersecting vane machine.



Figure 4. High-speed friction and wear testing rig.

friction behavior for steel-on-steel contacts with an average friction coefficient of 0.5. The steel and Delrin contact pair showed a lower friction coefficient, especially at higher speeds (Figure 6); however excessive wear occurred in the Delrin. Evaluation of more materials and coatings is in progress.

Publications

M. F. Alzoubi, O. O. Ajayi, J. Woodford, A. Erdemir, and G. R. Fenske, "Scuffing Performance of Amorphous Carbon during Dry-Sliding Contact," presented at ASME/STLE Joint Tribology Conference, Seattle, October 1–4, 2000.

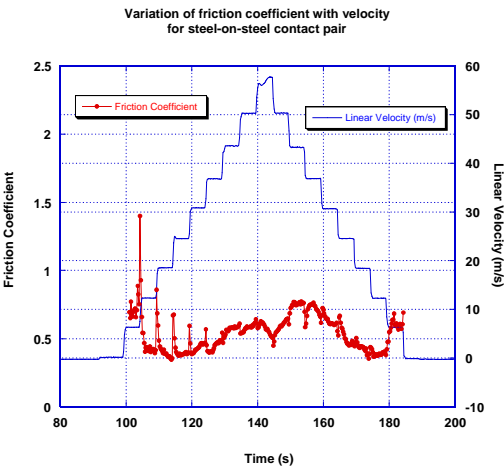


Figure 5. Variation of friction coefficient with sliding velocity for steel-on-steel contact pair.

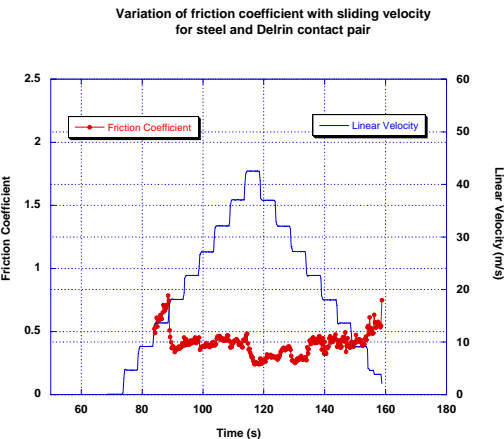


Figure 6. Variation of friction coefficient with sliding velocity for steel-on-Delrin contact pair.

D. Microstructural Characterization of PEM Fuel Cells

*D. A. Blom and L. F. Allard
Materials Analysis User Center
Oak Ridge National Laboratory*

*DOE Program Manager: Patrick Davis
ORNL Technical Advisor: David Stinton*

*Contractor: Oak Ridge National Laboratory, Oak Ridge, Tennessee
Prime Contract No.: DE-AC05-00OR22725*

Objectives

- Use transmission electron microscope (TEM) characterization techniques to optimize the distribution of precious metal catalyst for increased efficiency and reduced catalyst loading.
- Provide insight into the performance loss in polymer electrolyte membrane (PEM) membrane electrode assemblies (MEAs) upon use in a fuel cell system.

OAAT R&D Plan: Section 3.3: Task 13; Barriers A, B

Approach

- Characterize the microstructure and chemical composition of PEM MEAs before and after use to correlate performance to the microstructure at the level of a nanometer (nm) and up.
- Prepare samples for TEM observation that are thin over large areas to facilitate the ability to understand the entire MEA as a unit.
- Maintain the relationships among the constituents of the MEAs in the TEM samples in order to achieve insight into the operation of the real system.

Accomplishments

- Observed 50-nm-thick chemical composition change at the interface between membrane and electrodes (both anode and cathode).
- Quantified the change in platinum catalyst size distribution upon aging.

Future Direction

- Investigate aging characteristics of other MEAs.
 - Study the effect of different aging conditions.
 - Improve the specimen preparation technique to achieve thinner sections that preserve the porosity of the electrodes
-

Introduction

PEM fuel cells hold great promise for use as an environmentally friendly power source for automobiles. One of the key hurdles in making PEMs commercially viable is to reduce the cost by reducing the amount of precious metal catalyst necessary to provide high-power-density operation at a low temperature. For efficient catalysis to occur, gas molecules must be able to interact easily with the surfaces of the catalyst particles. A pathway for diffusion of protons must exist in close proximity to the active sites on the catalyst, and an electrically conductive pathway from the catalyst to the electrodes is required for electron transport. Finally, water (the by-product of the fuel cell reaction) has to be transported away from the catalyst for a continuing reaction to occur. These requirements show the complexity of building an efficient PEM fuel cell and clearly indicate the opportunity for atomic-scale microstructural and chemical characterization to provide feedback on the geometry and distribution of the various components for optimum performance.

Approach

A new specimen preparation technique was developed in FY 2000 to allow PEM fuel cell MEAs to be characterized in a TEM. An MEA consists of a proton-conducting polymer membrane (which is gas-tight) sandwiched between two catalyst layers that are surrounded by two porous electrodes for gas diffusion and electrical conductivity. Specimens for TEM study must be extremely thin, on the order of 100 nm or less in thickness. Preparing thin specimens without disturbing the geometry and distribution of the components of an MEA was the initial challenge of this project. To provide reliable information on the microstructure, the MEA must be disturbed as little as possible so we can be sure that we are characterizing the microstructure as it exists during operation.

Commercial MEAs were purchased for our initial characterization efforts. The microstructures of the various MEA components were analyzed for both an as-manufactured MEA and an MEA that had been aged in a fuel cell test stand. W. L. Gore and Associates, Inc., agreed to provide fuel cell testing and aging of a third-party MEA. Gore ran the MEA continuously for 325 hours at 75°C in fully

humidified ambient-pressure hydrogen and air at a constant voltage of 0.6 V. Under those test conditions, minimal change in cell performance was recorded over the duration of the test. The chemical and structural composition of the interface between the PEM and the electrodes was studied. Additionally, the size distribution of the platinum catalyst particles was measured for both MEA samples.

Results

Figures 1 and 2 illustrate the microstructural change that was observed at the interface between the PEM and the electrodes. The fresh MEA is shown in Figure 1 and the aged MEA in Figure 2. The electrode is on the left side of both images. Platinum catalyst particles are visible as small dark spots in both electrode layers. The fresh interface is abrupt, while the interface in the aged MEA shows an interfacial layer of approximately 50 nm. Figure 3 is a high-angle annular dark field (HA-ADF) image, collected on a Hitachi HD-2000 scanning TEM (STEM), of the fresh MEA. HA-ADF images (also known as Z-contrast images) are unique in that the

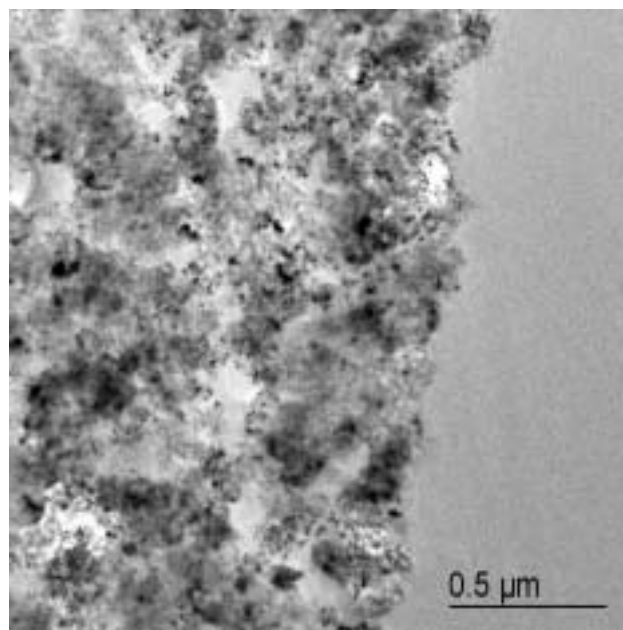


Figure 1. TEM micrograph of the interface between the polymer electrolyte membrane and catalyst for an unused MEA. The small dark particles are platinum.

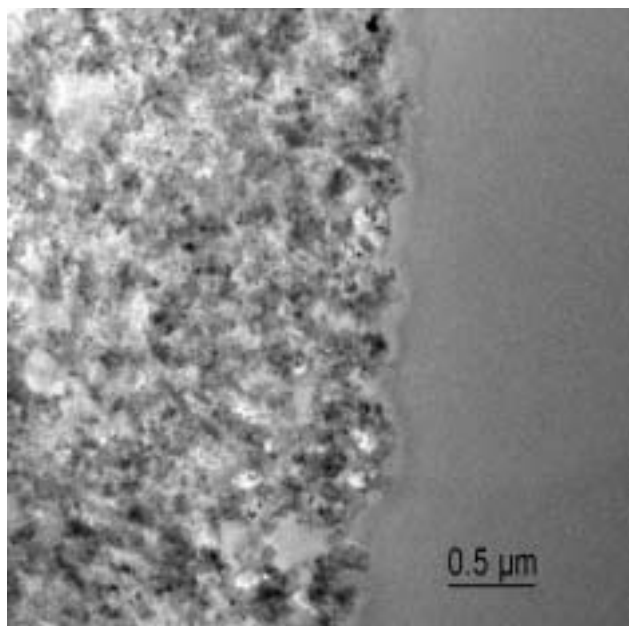


Figure 2. TEM micrograph of the interface between the PEM and anode for an aged MEA. Note the thin interfacial layer that has developed during the aging process.

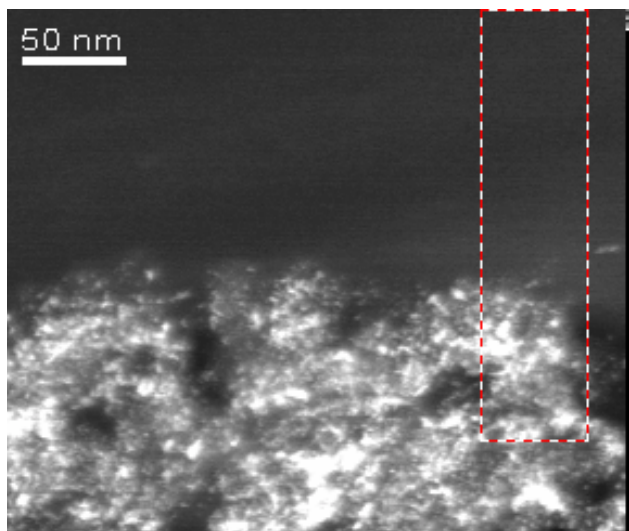


Figure 3. High-angle annular dark field image of the electrode/PEM interface in a fresh MEA. The bright pixels correspond to the platinum catalyst particles. The box on the right hand side of the image outlines the area that is shown in Figure 4.

image contrast is due to the electron scattering ability of the atoms in the sample. Elements with a higher atomic number (Z) scatter more strongly than lower- Z elements. In the case of PEM MEAs, the small platinum catalyst particles scatter electrons

much more strongly than do the other components of the MEA. The small box outlined in Figure 3 illustrates the area from which elemental information was collected. The images in Figure 4 were collected by scanning a focused electron beam across the sample while simultaneously collecting the X-rays emitted from the sample. As high-energy electrons impinge upon a material, some of them lose energy in a variety of ways. One of the interactions leads to the production of X-rays that have an energy characteristic of the element. Figure 4 shows the spatial distribution of Pt, F, and S. These images are known as X-ray maps, and the brightness level is related to the number of X-rays of the appropriate energy that were collected as the electron beam passed over the sample. From Figure 4, it is clear that the interface between the PEM and the electrode is abrupt both chemically and structurally.

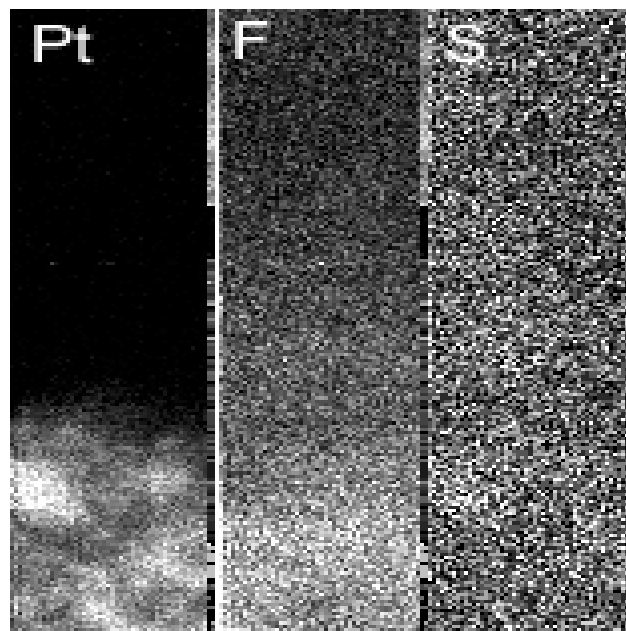


Figure 4. X-ray maps collected from the small area that is outlined in Figure 3.

Figure 5 is a HAADF image of the interface between the PEM and the anode of an aged MEA. The interfacial layer seen previously in Figure 2 is also evident in the Z-contrast image. X-ray maps of this area are shown in Figures 6–8. There is an overlap in energy between the sulfur X-ray line used for the map in Figure 7 and one of the minor X-ray

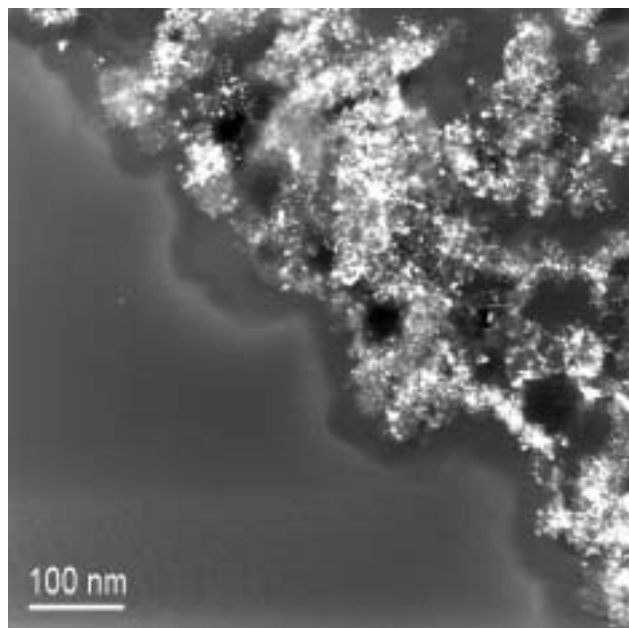


Figure 5. High-angle annular dark field image of the anode/PEM interface in an aged MEA. Note the thin interfacial layer visible.

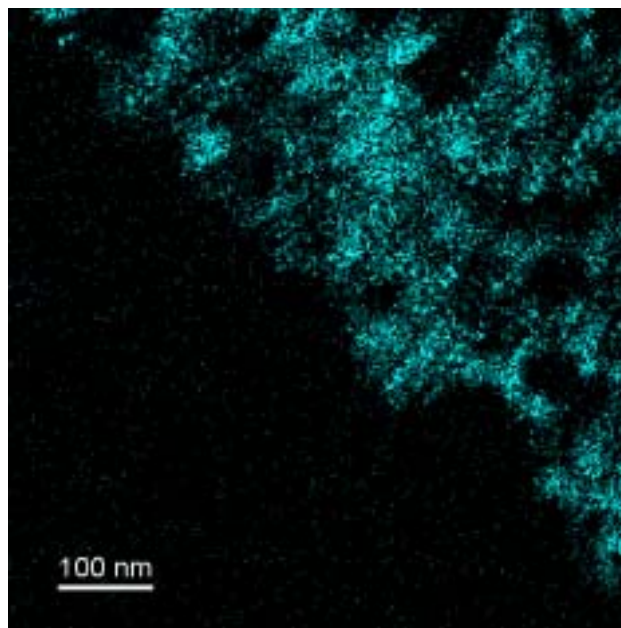


Figure 6. Platinum X-ray map of Figure 5. Bright pixels correspond to the location of platinum atoms in the sample.

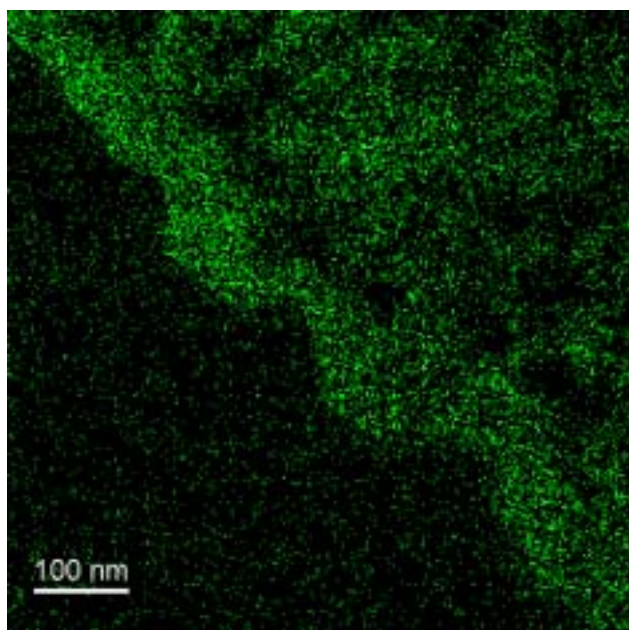


Figure 7. Sulfur X-ray map of Figure 5. Bright pixels correspond to the location of sulfur atoms. Because of overlap in energy of a minor platinum X-ray line and the primary X line, some of the pixels in the electrode are due to the combination of platinum and sulfur content.

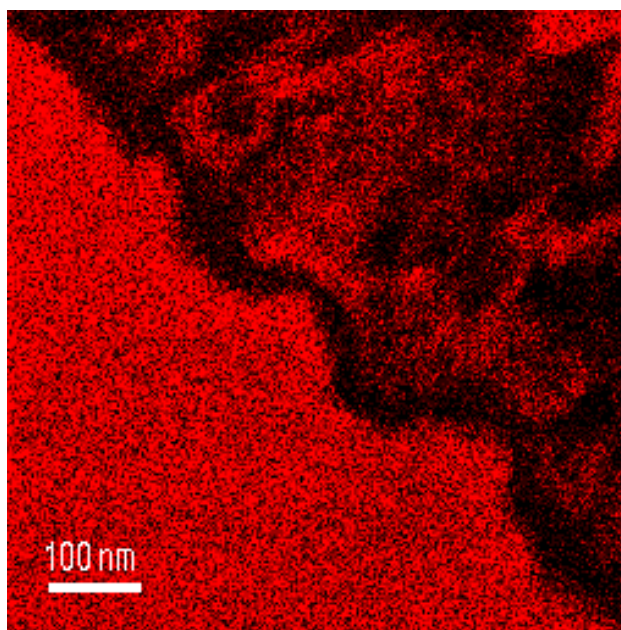


Figure 8. Fluorine X-ray map of Figure 5. Bright pixels correspond to the location of fluorine atoms. Note the depletion in fluorine content in the interfacial layer seen in Figure 5.

lines of platinum. Therefore, the sulfur map contains some signal that is due to platinum. In the anode, where the platinum catalyst is prevalent, the sulfur map is not completely due to sulfur content; but in the PEM and at the interface, the sulfur map accurately shows the distribution of sulfur in the MEA. The interfacial layer is enriched in sulfur and depleted in fluorine relative to the bulk of the membrane. Similar chemical changes have been observed at both the cathode and anode interfaces with the membrane material.

Figure 9 is an example of the HA-ADF images used to quantify the size distribution of the platinum catalyst particles. The bright pixels correspond to the small catalyst particles. Image processing was applied to the as-collected image in order to visually separate the catalyst particles from the rest of the MEA components. Figure 10 shows the as-processed image. The platinum catalyst particles are now more easily separated from the rest of the MEA. Figure 11 is the histogram of platinum catalyst size for the fresh MEA. Particles of less than 1 nm in diameter were most frequent. After aging, the histogram changes to that shown in Figure 12. The size distributions were very broad for both the fresh and the aged MEAs. The median size of catalyst particle for the fresh MEA was 1.8 nm, while the used MEA had a median catalyst particle size of 3.2 nm. The relative frequency of the <1 nm particles has decreased during the aging process, suggesting that particle coarsening has begun.

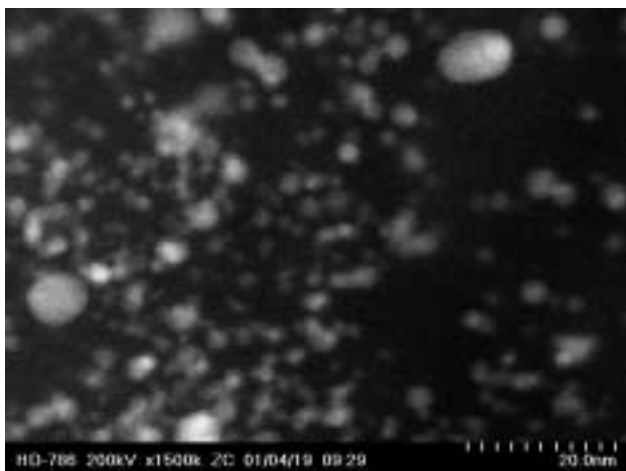


Figure 9. As-collected high-angle annular dark field image used to determine the size distribution of the platinum catalyst particles.

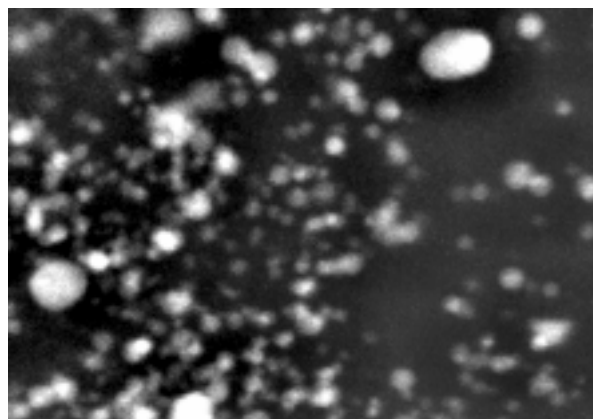


Figure 10. The image in Figure 9 following image processing to enhance the contrast between the platinum catalyst particles and the other MEA components.

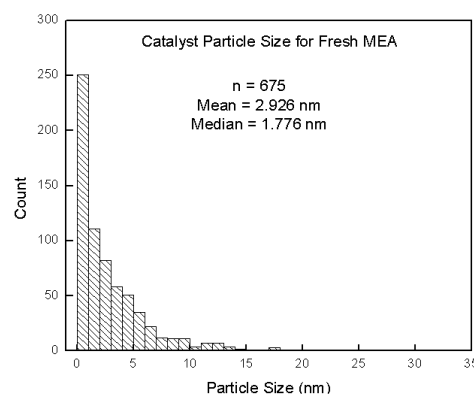


Figure 11. Platinum catalyst size histogram for the fresh MEA. The median particle size is 1.8 nm, and the most common size is 0–1 nm.

Conclusions

A new specimen preparation technique has been developed and demonstrated that produces thin cross-sections of PEM fuel cell MEAs suitable for microstructural and micro-chemical characterization in a TEM. Initial observations of precious metal catalyst content and distribution indicate that the microstructure of the catalyst layer is far from optimized in a commercially available PEM MEA. Cross-sections have been produced that preserve the geometry and distribution of the MEA components and that are thin over wide areas, allowing for the simultaneous study of the microstructure and chemical composition representative of the cathode,

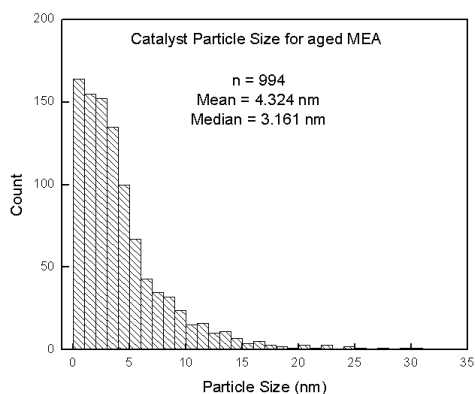


Figure 12. Platinum catalyst size histogram for the aged MEA. The frequency of the smallest particles has decreased, while the median particle size has increased to 3.2 nm.

membrane, and anode of an MEA as it existed during use in a fuel cell. By carefully maintaining the spatial relationships in the real system, it becomes possible to correlate the fuel cell performance and performance changes with TEM micro-characterization. Initial aging/use studies were conducted. Negligible performance degradation was

observed for the given test conditions over 325 hours of continuous use; however, several microstructural changes have been observed to occur as an MEA ages. An interfacial layer approximately 50–100 nm wide, enriched in sulfur and depleted in fluorine relative to the bulk PEM, has been shown to develop at both the cathode and anode interfaces of the PEM. The size distribution of catalyst particles in the fresh MEA was quite broad, with a median particle size of 1.8 nm. After the aging process, the smallest catalyst particles decreased in number, while the particles between 2 and 5 nm were more common. Coarsening of the platinum catalyst occurred during the aging test. Further studies are under way to correlate performance loss with microstructural changes. Further MEA testing will be conducted in order to attempt to understand the correlations among microstructure, atomic level, chemical composition, and MEA performance.

Presentations

D. A. Blom and L. F. Allard, “Microstructural Characterization of Proton Exchange Membrane Fuel Cells,” DOE 2001 Review, Office of Transportation Technology Fuel Cells Program, Oak Ridge National Laboratory, June 6–8, 2001.

E. Nano-Particulate Porous Oxide Electrolyte Membranes as PEMs

M. Isabel Tejedor and Marc A. Anderson
Environmental Chemistry and Technology Program
University of Wisconsin

Mark A. Janney
Metals and Ceramics Division
Oak Ridge National Laboratory

DOE Program Manager: Patrick Davis
ORNL Technical Advisor: David Stinton

Contractor: Oak Ridge National Laboratory, Oak Ridge, Tennessee
Prime Contract No.: DE-AC05-00OR22725

Objectives

- Develop microporous inorganic membranes of TiO_2 with high proton conductivity that are capable of operating at above 100°C with minimal water management problems.
- Develop processes to fabricate porous nickel or graphite paper electrodes that support the membrane.
- Demonstrate fuel cell behavior in porous oxide electrolyte membrane- (POEM-) based membrane electrode assemblies (MEAs).

OAAT R&D Plan: Section 3.3: Task 13; Barriers A, B

Approach

Accomplishments

- Demonstrated proton conductivity in POEMs at temperatures of up to 110°C at relative humidities between 13 and 44%.
- Studied the effects of surface area and surface conditioning on proton conductivity.
- Demonstrated manufacturing repeatability for membrane-coated tape-cast nickel substrates having nearly Knudsen flow.

Future Direction

- Develop a better understanding of the relationships and interactions among the various layers in the MEA and how they control the performance of the overall fuel cell system.
 - Investigate using the nickel substrate as the cathode instead of the anode in the MEA.
 - Further develop graphite fiber paper supports as a potential substitute for nickel substrates.
-

Introduction

Nano-particulate POEMs are being developed as a radical alternative to polymer electrolyte membranes (PEMs) for fuel cells. These new membranes can operate at temperatures of over 100°C, retain water at these elevated temperatures, and provide proton conductivities of the same order of magnitude as the Nafion membranes currently employed. In addition, POEMs should reduce membrane cost by substantially reducing the amount of platinum catalyst required to operate a fuel cell, and minimize CO poisoning of the platinum by operating at elevated temperatures.

POEMs must be supported on a structural substrate because the membranes are thin (≤ 200 nm), porous (~ 40 vol % void space), and brittle (an inherent property of ceramic membranes). The porous substrate provides for both electrical conductivity and gas distribution. Because the membrane is composed of 5–10-nm particles, an intermediary sandwich layer (particle diameter of 50 to 500 nm) is required to provide geometric compatibility.

The POEM MEA is a complex materials system, not just a collection of individual components. The MEA (anode/membrane electrolyte (separator)/cathode) is a composite material. It simultaneously performs a variety of operations. One cannot consider any particular aspect of this materials system in isolation; all functions must operate in concert with one another. The anode has to conduct and at the same time convert hydrogen gas to protons at the membrane surface. The membrane must act to conduct protons, but not electrons, which would cause a short. Finally, the cathode must convert gaseous oxygen to O^{2-} ions, which then combine with the protons that have migrated through the membrane. The cathode reaction is a four-electron-transfer reaction and is quite difficult.

Results and Discussion

Membrane Development

Proton conductivity in hydrophilic, mesoporous, inorganic membranes such as those used in this investigation derives from the movement of H^+ ions (1) by hopping along surface sites on the membrane particle, (2) by migrating through the electrical double layer near the surface of the pores, or (3) by

migrating through the bulk pore fluid (Figure 1). The conductivity of a particular membrane depends on the conditioning of the pore surfaces and on the relative humidity, which determines how much water resides in the pores. In the as-fired condition, the pore surfaces are poorly protonated. Conditioning the membrane material in aqueous solution tends to increase the degree of protonation, depending on the pH of the solution and the presence of additional ions, such as phosphate. The most effective conditioning process examined so far is to treat the membrane at a pH of 1.5. This process effectively protonates all of the surface sites in the pores.

An extensive study was conducted of the effect of surface conditioning of the membrane materials. Figure 2 shows the effect of surface conditioning on the adsorption of water onto the various membrane materials as a function of relative humidity. The samples were conditioned, rinsed repeatedly in deionized water to remove excess ions in solution and bring the pH of the membrane up to its isoelectric point, dried, and then rehydrated during the isotherm testing. Clearly, the membrane treated at pH 1.5 before testing is the most hydrophilic. Even at the low relative humidity of 35%, it adsorbed 40 molecules of H_2O/nm^2 . In general, the

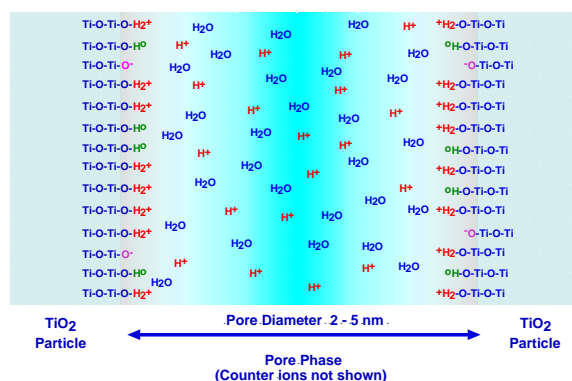


Figure 1. Proton conductivity in hydrophilic, mesoporous, inorganic membranes derives from the movement of H^+ ions by hopping along surface sites on the membrane particles and migrating through the pore fluid. Appropriate surface conditioning increases the degree of protonation of the pore surfaces, which in turn increases the conductivity of the membrane.

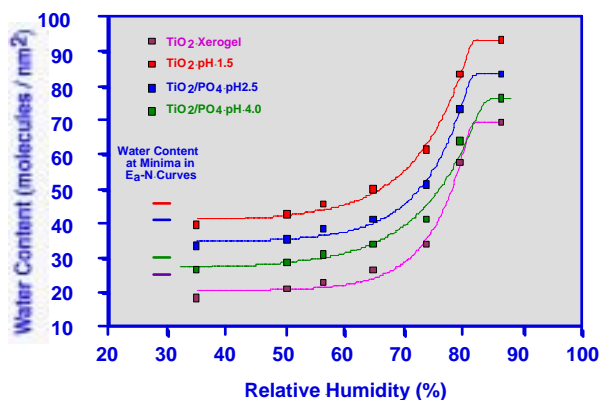


Figure 2. Adsorption of water vapor on TiO_2 membrane materials varied with surface conditioning. Materials pretreated at pH 1.5 prior to testing were the most hydrophilic.

more hydrophilic the membrane, the higher the proton conductivity. This finding is further illustrated in Figure 3, which shows the activation energy for proton conduction, E_a (kJ/mol), as a function of the density of water molecules, N (molecules/nm²), on the pore surface for four different conditioning treatments—as received, treated with phosphate at pH 4, treated with phosphate at pH 2.5, and treated in pH 1.5 water. The minimum in each E_a - N curve shows that there is a change in the mechanism for proton conduction as the amount of water in the membrane increases. Note that the minimum in each of the E_a - N curves

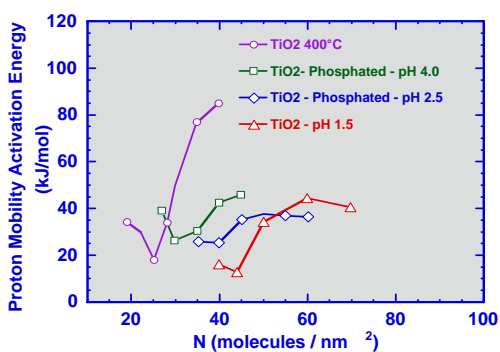


Figure 3. Activation energy for proton conduction, E_a , was a function of surface conditioning treatment and a function of water content, N , of the membrane materials. Note that the minimum in the E_a curves occurs at the knee in the water vapor adsorption isotherms (shown in Figure 2).

corresponds with the knee in each corresponding adsorption isotherm (Figure 2). This demonstrates that the change in mechanism corresponds with the change in adsorption mechanism from surface adsorption to capillary condensation.

Another major achievement was demonstrated this year: proton conductivity in POEMs at temperatures above the boiling point of water. Figure 4 shows that the proton conductivity of a membrane conditioned at pH 1.5 increased linearly with temperature to a point above the boiling point of water, 100°C. The relative humidity of this test was held constant at 44%.

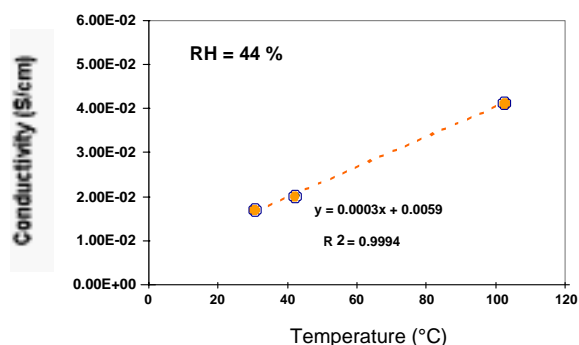


Figure 4. The conductivity of a membrane conditioned at pH 1.5 increased linearly with temperature to a point above the boiling point of water, 100°C.

Support Development

The initial electrode/support is based on a tape-cast, sintered porous nickel foil. The sintered nickel foil has a porosity of about 55 vol % and an average pore size of about 2–5 μm . A sandwich layer having a similar porosity and a pore size of about 0.1 μm is deposited on top of the electrode. The small pore size of the sandwich layer provides an appropriate surface upon which to deposit the nanoparticle membrane. The TiO_2 membrane is then deposited on top of the sandwich layer.

Figure 5 shows permeability data for six different batches of nickel membranes. It is evident from Figure 5 that the permeability characteristics for dry gases of the six different batches are quite repeatable. For pure Knudsen flow, a figure of merit of 2.65 (ratio of the square roots of N_2 and helium molecular weights) is predicted for the ratio of helium to N_2 flow through the samples. The flow through the membrane-coated support approaches

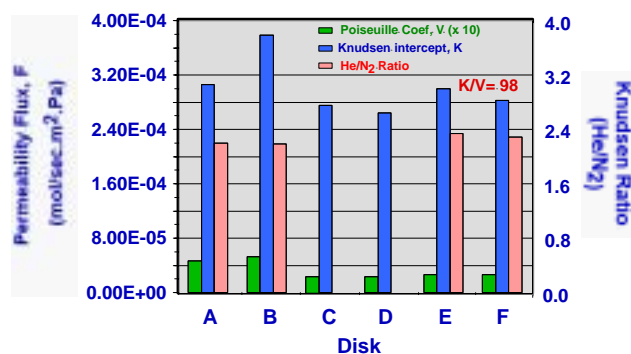


Figure 5. Permeability of nickel supports with sandwich layer was repeatable as shown by the two parameter model, $F = V \cdot P_{avg} + K$.

pure Knudsen flow, with $F = 7.18 \times 10^{-7} P_{avg} + 1.55 \times 10^{-5}$ for helium flow, where F = permeance ($\text{mol/m}^2 \cdot \text{sec} \cdot \text{Pa}$) and P_{avg} = average pressure (Pa) the membrane was tested with humidified gases, the permeance fell nearly to zero. Crossover tests were conducted using humidified N_2 on one side of the membrane and humidified helium on the other. Using humidified gases causes the permeability to drop further because the pores become filled with

water caused by capillary condensation. After 2 hours of running time (effectively steady state), the crossover concentration of helium on the N_2 side was <90 ppm.

Summary

Inorganic, microporous titania membranes were fabricated on porous, electrically conducting nickel substrates with a ceramic sandwich layer. These membranes demonstrated proton conductivity in POEMs at temperatures of up to 110°C at relative humidities of between 13 and 44%. A novel method was developed for applying the ceramic sandwich layer to the nickel substrate; it may be useful in other membrane applications. The current membranes were deposited onto porous nickel substrates that served as the electrodes. An improved graphite fiber-based substrate/electrode having the requisite chemical compatibility with the PEM environment is being developed to replace the porous nickel. PEM fuel cell assembly using multilayer technology manufacturing will be investigated using standard industrial technologies.

F. Metallized Bacterial Cellulose Membranes in Fuel Cells

Hugh O'Neill, Barbara R. Evans, and Jonathan Woodward (Primary Contact)
Chemical Technology Division, Oak Ridge National Laboratory

DOE Program Manager: JoAnn Milliken
ORNL Technical Advisor: David Stinton

Contractor: Oak Ridge National Laboratory, Oak Ridge, Tennessee
Prime Contract No.: DE-AC05-00OR22725

Objectives

- Develop low-cost bacterial cellulose membranes with high proton conductivity that are capable of operating at above 120°C with minimal water management problems.
- Construct and demonstrate the high-temperature operation of a bacterial cellulose membrane electrode assembly (MEA).
- Characterize the properties of the MEA and determine power densities.
- Optimize the power density of the MEA by *in vitro* and *in vivo* membrane modification methods.

OAAT R&D Plan: Section 3.3: Task 13; Barriers A, B

Approach

- Develop an in-house production facility for bacterial cellulose.
- Deposit metals suitable as catalysts in a cellulose matrix.
- Synthesize ion-conducting membranes by
 - a) infusion of electrolytes into the structure followed by dehydration
 - b) chemical modification of the hydroxyl ($-OH$) groups on the fibrils with sulfonate ($-SO_3^{2-}$) groups to enhance H^+ conductivity
 - c) modification of the membrane during synthesis with chemically altered glucose precursors.
- Characterize the native and modified cellulose matrix properties with emphasis on reduced catalyst loading, increased thermal stability, and enhanced ion-conducting properties.
- Test the MEA to demonstrate low hydrogen gas (H_2) crossover, high carbon monoxide (CO) tolerance, high power density, and low cost.

Accomplishments

- Made the initial discovery: the spontaneous deposition of palladium in commercially available bacterial cellulose.
- Made the in-house facility for cellulose production by *Gluconacetobacter hansenii* operational.
- Demonstrated the deposition of palladium, gold, and silver by *G. hansenii* cellulose.
- Determined the thermal stability and H_2 crossover characteristics of native cellulose.
- Modified membrane with sulfonic acid groups.

Future Direction

- Generate proton-conductive membranes with high-temperature stability.
- Develop a catalyst layer.
- Develop current collectors.
- Test an MEA.
- Construct a fuel cell stack for commercial application.

Introduction

In current polymer electrolyte membrane (PEM) fuel cell technology, perfluorosulfonic acid-based membranes (e.g., Nafion) have long been the standard. The most notable drawbacks of this type of membrane are their limited stability at temperatures greater than 100°C, their dependence on H₂O for conduction, and their relatively high cost. Operating temperatures greater than 120°C are considered necessary for catalytic efficiency and protection of the catalyst against CO poisoning.

The present concept proposes a cellulose matrix secreted by bacteria as a suitable material for PEM fuel cell technology development (Figure 1a, b). The catalyst and electrolyte membrane components of the MEA are constructed using bacterial cellulose, underlining the multifunctional nature of this material. In addition, the novel fabrication and processing methods of the components highlight the innovative approach to MEA assembly proposed by this concept. The main impact, at the system level, of a cellulose-based PEM fuel cell is that it will operate at temperatures $\geq 130^{\circ}\text{C}$, circumventing the problems associated with Nafion-based PEM fuel cells.

The initial discovery that led to the idea that this material may be useful for PEM fuel cells was the observation that bacterial cellulose samples incubated in a solution of ammonium hexachloropalladate turned black because of the deposition of palladium (Pd) in the cellulose under ambient conditions (Figure 2a). The precipitated metal formed a homogeneous matrix of finely divided metal particles dispersed evenly throughout the pellicule. When dehydrated, the metallic bacterial cellulose dried to a thin membrane

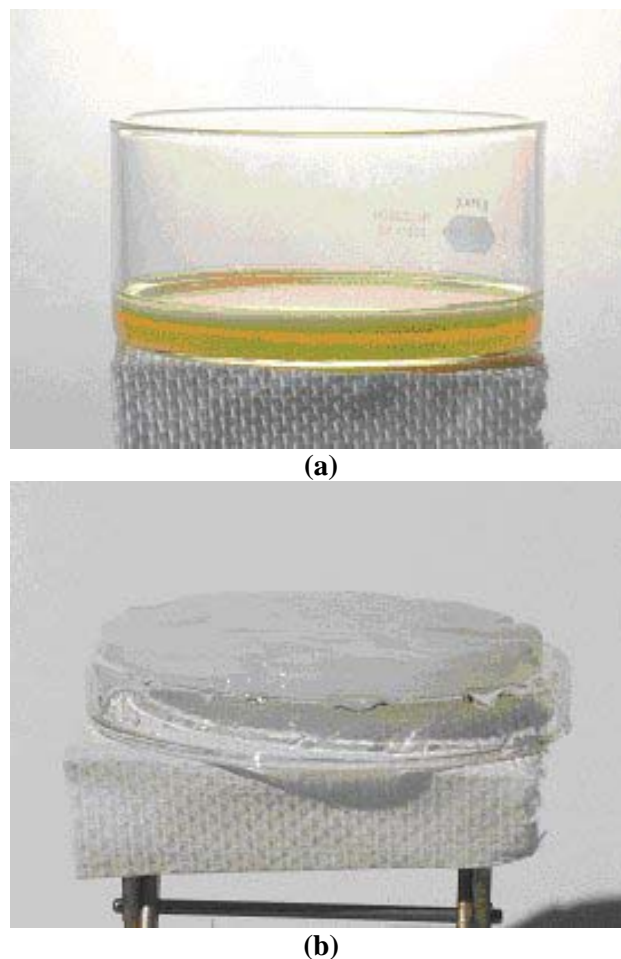
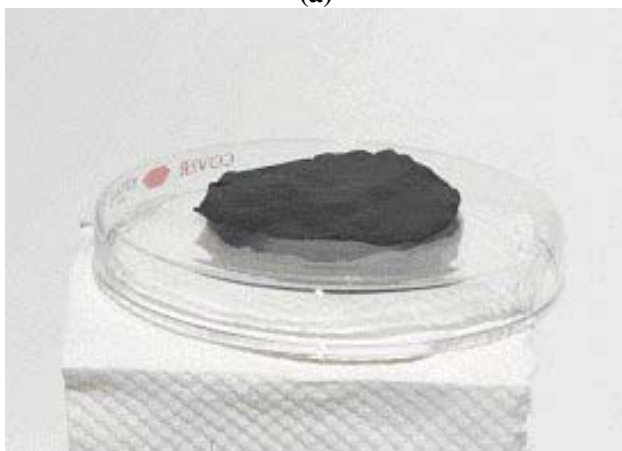


Figure 1. Cultivation and processing of bacterial cellulose. (a) Growth of bacterial cellulose in glucose-rich medium at 25°C. (b) Processed bacterial cellulose after treatment with 1% NaOH and Na-acetate (pH 4.5).



(a)



(b)

Figure 2. Treatment of bacterial cellulose with ammonium hexachloropalladate. (a) Hydrated bacterial cellulose after incubation in ammonium hexachloropalladate. (b) Dried palladated bacterial cellulose.

(Figure 2b) that was electrically conductive and, in the presence of a suitable electron donor, catalyzed the evolution of H_2 in aqueous solution. Therefore, it was plausible that this material could be used for the anodic oxidation of H_2 in fuel cell applications. A hybrid material acting as the current collector and catalyst layer will be synthesized by the incorporation of an electrically conductive material, such as carbon felt or paper, into the cellulose during bacterial growth, followed by deposition of the metal within the resulting matrix. A proton-conductive membrane will be generated by chemical modification of the cellulose to introduce the appropriate reactive groups. The components of the MEA will be assembled using a simple cold-

pressing procedure, resulting in high interfacial compatibility between the layers.

Approach

An in-house production facility for bacterial cellulose has been established. The properties of the bacterial cellulose are identical to those of the commercial product used in the initial experiments. The initial research goals are focused on development of the electrolyte layer of the PEM fuel cell.

Three different approaches for the fabrication of an ion-conducting membrane are under investigation. (1) Over 200 years of chemical modification of cellulose has led to products ranging from textiles to thermoplastics. Similar techniques will be exploited to synthesize a cellulose-based membrane that has a proton-conducting ability that rivals that of Nafion, but operates at higher temperatures ($130^\circ C$). (2) In its hydrated native state, bacterial cellulose holds over 100 times its own weight in H_2O . An electrolyte membrane will be made by dehydrating the material after infusion of electrolytes into the structure. Potential reagents that will be tested are solid acids such as $CsHSO_4$. (3) The membrane will be modified *in vivo* by introduction of chemically reactive groups (SO_3^{2-}) into the cellulose structure by addition of glucose analogs to the medium during cultivation.

Development of the catalyst layer is also under way. The mechanism of palladium deposition is being investigated. This investigation will provide insight into methods to deposit other metals, such as platinum. Future research will focus on the development of current collectors and assembly and testing of the MEA.

Results

As a proof-of-principle experiment, an MEA was constructed by sequentially drying a layer of bacterial cellulose that was infused with 1M potassium chloride between two layers of palladated bacterial cellulose (Figure 3). Platinum (Pt) wires were used as current collectors. Suitable controls were carried out to demonstrate that the Pt was not responsible for the anodic oxidation of H_2 . An output of $84.3 \mu W/cm^2$ ($192 \mu A$ and $0.48V$) was demonstrated using H_2 generated from a simple

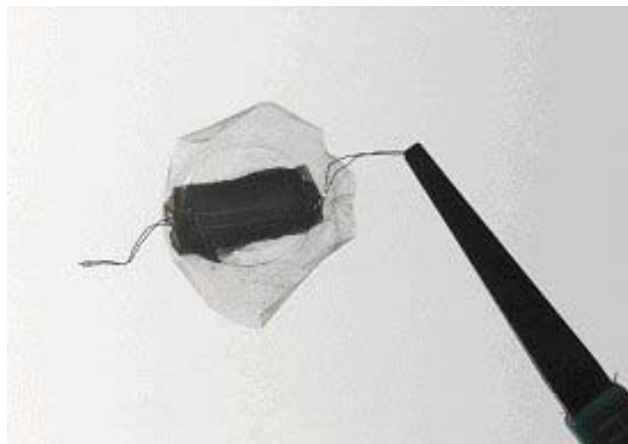


Figure 3. Membrane electrode assembly.

acid-displacement reaction. These results are preliminary and serve only to prove the hypothesis that an MEA made with bacterial cellulose exhibits fuel cell behavior (Figure 4). The experiment was carried out at room temperature and ambient pressure. Optimization of the reaction in terms of temperature, pressure, and humidity would certainly increase the performance.

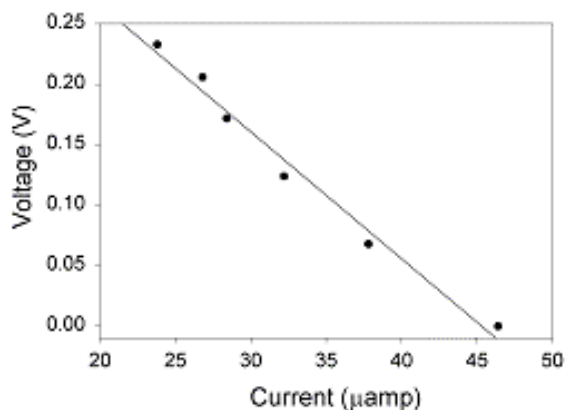


Figure 4. Voltage vs. current curve for membrane electrode assembly. The resistance was increased in 2-kW increments from 1 to 11 kW. The experiment was carried out at 26°C and 1 atm using a 4% H₂ stream at 40 ml/min.

Bacterial cellulose has the desired physical and chemical properties for PEM fuel cell technology. The hydrated bacterial cellulose dries to a thin membrane 34μm in thickness as measured by scanning electron microscopy. The dried membrane

does not rehydrate; no swelling of the dried membrane was evident after boiling for 30 min in H₂O. The thermal properties of the dried material were compared with those of Nafion 117®. Thermogravimetric analysis profiles of the bacterial cellulose and Nafion 117 are shown in Figure 5. The

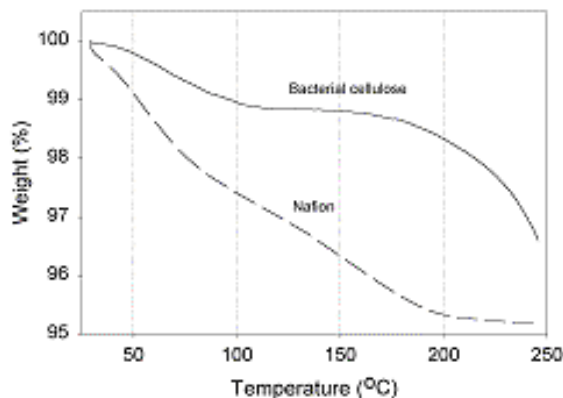


Figure 5. Comparison of the thermogravimetric analysis profiles of bacterial cellulose and Nafion 117.

profile for dry bacterial cellulose indicated that it loses H₂O at up to approximately 100°C, above which there is no weight loss to 130°C. In the dry state, decomposition occurs at above 130°C. However, under humid conditions, it is likely that the thermal stability would be increased. In contrast, the profile for dry Nafion 117 showed that it continually loses weight over the temperature range measured. This demonstrates the favorable temperature stability characteristics of bacterial cellulose compared with Nafion 117. In addition, comparison of the H₂ crossover characteristics of bacterial cellulose and Nafion 117 indicate that bacterial cellulose is 1.75-fold less permeable to H₂ compared with Nafion 117 (Figure 6). It is mechanically stable with regard to tearing and can be folded repeatedly without damage. It is chemically stable under acid and alkaline conditions.

Preliminary data have been obtained for the chemical modification of bacterial cellulose with sulfonate groups. The ion-exchange capacity of the membrane is approximately 1.1-1.2 mequiv/g cellulose. However, the structural integrity of the membrane was adversely affected. Further studies are under way in this area.

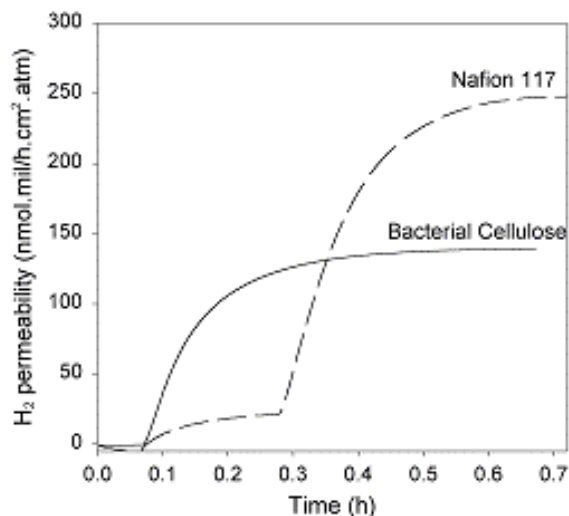


Figure 6. Comparison of the crossover characteristics of bacterial cellulose and Nafion 117. The experiment was carried out in 4% H₂/96% argon at 46 psi and 25°C.

Summary

Bacterial cellulose membranes possess many of the favorable characteristics for PEM fuel cell

technology that Nafion lacks. The operation of a bacterial-cellulose-based MEA was demonstrated, albeit at low efficiency. Efforts are directed toward increasing efficiency by development of the electrolyte layer, catalyst layer, and current collectors. In the context of the program, the synthesis of a bacterial cellulose membrane with ion-conducting ability is the most important goal for the overall success of the project.

Publications/Presentations

H. O'Neill, B. R. Evans, and J. Woodward, "Metallized Bacterial Cellulose Membranes in Fuel Cells," presented at 2001 National Laboratory R&D Meeting, DOE Fuel Cells for Transportation Program, Oak Ridge, Tennessee, June 2001.

Invention Disclosure

B. R. Evans, H. O'Neill, V. P. Malyvanh, and J. Woodward, "Metallization of Bacterial Cellulose for Electrical and Electronic Device Manufacture," ID 0869, S-96, 631, 2001.

G. Carbon Foam for Radiators for Fuel Cells

A. D. McMillan and J. W. Klett

Ceramic Processing Group

Oak Ridge National Laboratory

DOE Program Manager: Patrick Davis

ORNL Technical Advisor: David Stinton

Contractor: Oak Ridge National Laboratory, Oak Ridge, Tennessee

Prime Contract No.: DE-AC05-00OR22725

Objectives

- Develop compact, lightweight, more-efficient radiators for fuel-cell-powered vehicles utilizing Oak Ridge National Laboratory's (ORNL's) unique high-conductivity carbon foam.
- Ascertain certain materials-related issues (e.g., vibration, erosion, corrosion, plugging, thermal shock) for fuel cell cooling systems and begin characterizing the graphite foam for use in these applications.
- Work with Modine to develop prototype fuel-cell radiators.

OAAT R&D Plan: Section 3.3; Task 13, Barrier C

Approach

- Study fundamental mechanisms of heat transfer using the carbon foam.
- Develop a testing method to evaluate the foams and designs using the foams.
- Work with industrial partners to develop complete understanding of fuel cell-related issues.

Accomplishments

- Built and demonstrated a test rig suitable for heat transfer measurement.
- Demonstrated significant improvement in heat transfer coefficients over current systems using bench-scale radiator testing.
- Developed a new braze eliminating the previous thermal impedance at the interface.

Future Direction

- Develop and evaluate engineering designs with improved heat transfer and lower pressure drop.
 - Fabricate radiators for evaluation of materials-related issues such as corrosion, erosion, and vibration.
-

Introduction

Dissipation of heat from fuel cells is more difficult than for internal combustion (IC) engines because fuel cells operate at lower temperatures. The smaller driving force to disperse the heat results in a design problem, that is, excess size and weight of the radiator. Unless more-efficient and compact thermal management systems can be developed, radiators on fuel-cell-powered vehicles will need to be significantly larger and heavier than those on conventional vehicles. The development of a high-thermal-conductivity graphite foam¹⁻³ will lead to novel solutions for thermal management problems. With a thermal conductivity equivalent to that of aluminum 6061 and 1/5 the weight, this material is an enabling technology for thermal management problems ranging from heat sinks, to radiators and satellite panels, to aircraft heat exchangers. In addition, the open porosity yields extremely high ratios of surface area to volume, greater than $2 \text{ m}^2/\text{cm}^3$. This high surface area, combined with the extremely high thermal conductivity of the ligaments, will lead to novel designs that may incorporate porous media heat exchangers and phase change materials. For example, using the foam as a heat exchanger and air for cooling, heat transfer coefficients over two orders of magnitude greater than those of current metallic finned designs have been measured. This result is particularly important with regard to fuel-cell-powered vehicles, as the heat generated by the stack is difficult to dissipate because of the low operating temperatures.

Approach

Novel carbon foam radiators were fabricated and tested in FY 2000 that demonstrated heat transfer coefficients several orders of magnitude higher than those of conventional radiators (Figure 1). Radiator manufacturers, however, were concerned about the durability of the carbon foam and whether heat transfer coefficients would decrease with time. Therefore, bench-scale radiators have been fabricated to examine the effects of heat transfer as a function of aging. Tubes of four different materials (copper, stainless steel, and thick- and thin-walled aluminum) were press-fitted into four solid blocks of graphite foam approximately $4 \times 5 \times 1.5$ in. (Figure 2). These blocks were then placed on a brass plate in an

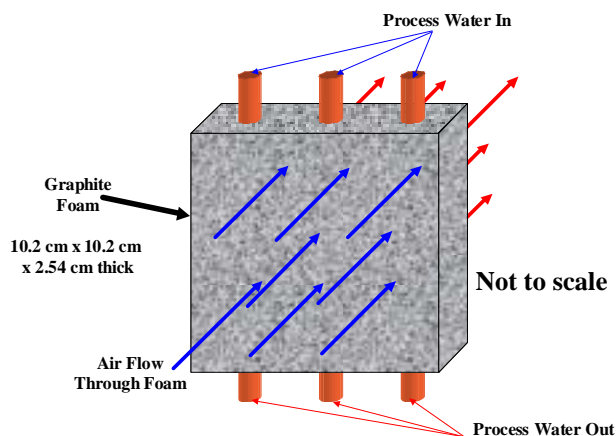


Figure 1. Schematic representation of heat exchanger with cooling air forced through pores of foam. Overall heat transfer coefficient measured at $11,000 \text{ W/m}^2\cdot\text{K}$.



Figure 2. Layout of foam blocks in infrared furnace.

infrared flatbed furnace. The furnace is controlled with a Yokogawa UP550 controller via thermocouple inserted in one block, and data are collected once per second using Labview; the unit runs continuously, cycling a 100°C span. While heat is provided from the infrared lamps, cooling is provided by flowing water through copper coils spot-welded to the underside of the brass plate.

In order to measure the heat transfer coefficient, a test rig was built (Figure 3). Hot water ($\sim 180^\circ\text{C}$) flows from the water bath through the tubes, and air flows through the block of foam. The temperatures of the inlet and outlet fluid are measured, as well as the temperatures of the inlet and outlet air; water and air flows are also measured. The overall heat transfer

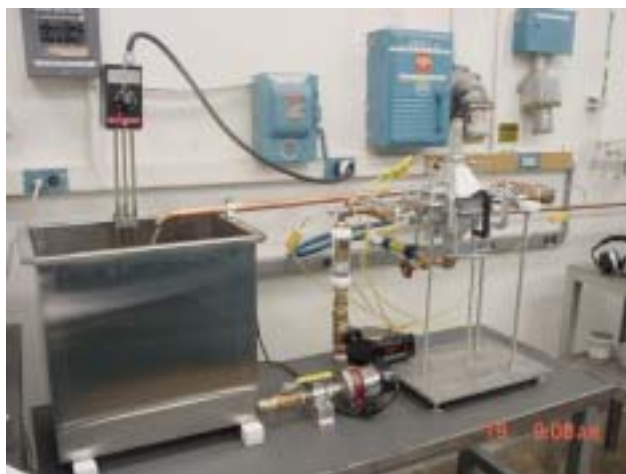


Figure 3. Heat exchanger test rig.

coefficient (U_o) is calculated from Eq. (1), where q is the heat dissipated to the cooling fluid, A is the area (foot print) of the foam, and ΔT_{LM} is the log mean temperature difference.

$$U_o = q / (A \cdot \Delta T_{LM}) \quad (1)$$

Results

Heat exchanger tests

The initial heat transfer coefficient was calculated to be between 3700 and 5400 W/m²·K. Most air/water heat exchangers, like automobile radiators, exhibit an overall heat transfer coefficient of about 20–30 W/m²·K. After 46,000 cycles, no significant change in heat transfer coefficient was observed (Table 1). Although this test demonstrates a

Table 1. Heat transfer coefficients at 5 gal/minute water flow and 110 standard ft³/min air flow

Tube material	Initial heat transfer coefficient (W/m ² ·K)	After 46,000 cycles (W/m ² ·K)
Copper	5367	4379
Stainless steel	3739	3323
Al thin-walled	5128	4074
Al thick-walled	4764	3721

remarkable increase in heat transfer coefficient and provides the tool to dramatically reduce the size of heat exchangers, the pressure drop through the foam was quite high (~2–3 psi/in.). This drop is not unreasonable for land-based systems where

developing a pressure head is feasible. However, in an automobile, where weight and power are a significant concern, this large pressure drop presents a potential problem for an efficient design.

In previous tests, the graphite foam was machined into various geometries in an effort to reduce the pressure drop associated with the solid foam. A 30% improvement in heat transfer is achieved when carbon foam is used in a conventional finned radiator design, while pressure drop is equivalent to that in the aluminum core. The heat dissipation of the foam core was 0.21 W/°C, while the aluminum core dissipated 0.15 W/°C. More efficient heat dissipation permits a reduced air flow, allowing alternatives for placement of the radiator on a vehicle.

Electrical resistivity, thermal conductivity, and compressive strength was measured as a function of aging to determine any degradation of material properties (Figures 4a, 4b). Since measurements indicate no appreciable change over 46,000 cycles, measuring heat flow and heat transfer coefficients as a function of thermal cycling will give a measure of the coefficient of thermal expansion mismatch at the interface. This will be of particular import in testing full-scale mock-ups.

Braze development

In a collaborative effort with Materials Research, Inc., a proprietary conductive braze was developed for joining the graphite foam to a metallic substrate. This braze has allowed for an increase in the heat transfer, as thermal impedance is greatly reduced or eliminated. Prior use of epoxies limited transfer at the interface of the two materials, and other commercial braze materials did not wet the foam. This new technique may enable more complex designs, including stacking layers.

Conclusions

Because of its remarkable thermal properties (an isotropic bulk thermal conductivity as high as 150 W/m·K and a specific conductivity up to six times greater than that of copper) the foam described in this report is potentially an enabling material for many technologies. These unique thermal properties, combined with the continuous graphitic open-celled network throughout the foam, should lead to novel and interesting methods of thermal management.

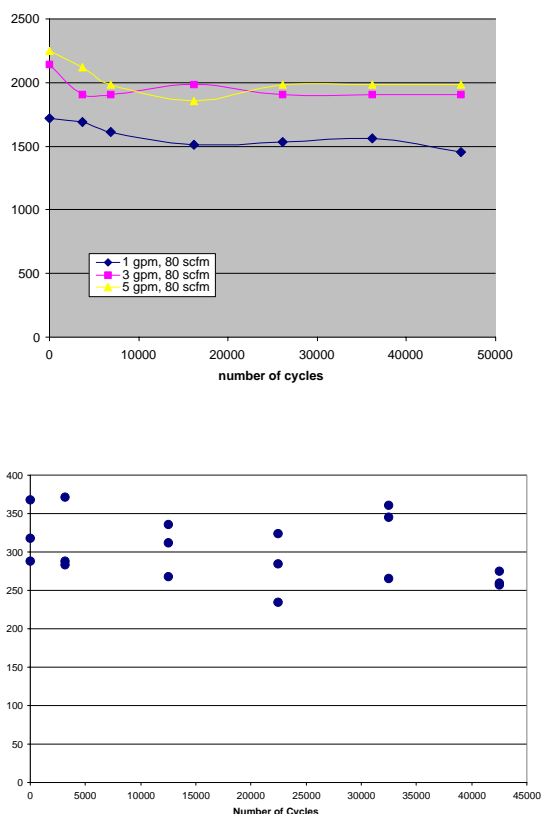


Figure 4. (a) Heat loss of graphite foam with press-fit copper tubes after 46,000 cycles. (b) Compression test results after 46,000 cycles.

Although the data and results presented here illustrate the potential of this material to be an enabling technology, further work is needed. A design for an automobile radiator dramatically smaller than current systems has been developed; ongoing work will determine the effects of tube geometry and examine the brazed interface as a function of thermal cycling. Additional studies on vibration, erosion, corrosion, and plugging are beginning. With a more complete understanding of materials properties, the full potential of this material may be realized. A design for a foam-core radiator will, most likely, be quite different from the current concept of a radiator. The data presented

here indicate that the foam will be most useful and efficient when the full potential of its unique structure is used in out-of-the-box designs and not when it is used simply as a replacement for existing thermal management materials.

Publications

J. Klett, L. Klett, T. Burchell, C. Walls, "Graphitic Foam Thermal Management Materials for Electronic Packaging," in *Proceedings of the Society of Automotive Engineering Future Car Congress*, Crystal City, Washington, D.C., April 2–6, 2000.

J. Klett, B. Conway, "Thermal Management Solutions Utilizing High-Thermal-Conductivity Graphite Foams," in *Proceedings of the 45th International Society for the Advancement of Materials and Process Engineering Symposium and Exhibition*, Long Beach, Calif., May 21–25, 2000.

J. Klett, R. Hardy, E. Romine, C. Walls, T. Burchell, "High-Thermal-Conductivity, Mesophase-Pitch-Derived Carbon Foams: Effect of Precursor on Structure and Properties," *Carbon*, 32(8), 2000.

References

J. Klett, R. Hardy, E. Romine, C. Walls, T. Burchell, "High-Thermal-Conductivity, Mesophase-Pitch-Derived Carbon Foams: Effect of Precursor on Structure and Properties," *Carbon*, 32(8), 2000.

J. Klett, "High Thermal Conductivity Mesophase Pitch-Derived Graphitic Foams," *Composites in Manufacturing*, 14(4), 1999.

J. Klett, C. Walls, T. Burchell, "High Thermal Conductivity Mesophase Pitch-Derived Carbon Foams: Effect of Precursor on Structure and Properties," p. 132 in *Proceedings of the 24th Biennial Conference on Carbon*, Charleston, S.C., July 11–16, 1999.

4. ADVANCED COMBUSTION

A. Microwave-Regenerated Diesel Exhaust Particulate Filter Durability Testing

Dick Nixdorf

Industrial Ceramic Solutions, LLC

DOE Program Managers: Patrick Davis and Kathi Epping

ORNL Technical Advisor: David Stinton

Contractor: Industrial Ceramic Solutions, Oak Ridge, Tennessee

Prime Contract No.: 4000000723

Subcontractor: Microwave Materials Technologies, Inc., Knoxville, Tennessee

Transportation Research Center, East Liberty, Ohio

Objectives

- Develop and demonstrate a low-cost yet very durable microwave-regenerated particulate filter system that captures and destroys more than 95% of the particulates produced by a diesel engine.
- Improve the uniformity and heating efficiency of the microwave field.
- Conduct on-road vehicle durability testing of the microwave filter system.

OAAT R&D Plan: Section 3.2: Task 1C; Barrier B

Approach

- Utilize computer finite-element modeling to improve the design of the microwave source.
- Perform a matrix of ceramic papermaking and binder addition tests to improve the strength and permeability of the ceramic fiber media.
- Validate the materials and microwave improvements in a 1.9-L stationary diesel engine test cell.
- Install and road-test the improved microwave filter system on a 1.9-L and a 7.3-L diesel vehicle.

Accomplishments

- Improved microwave field uniformity in the filter cartridge from heating 10% of the filter to heating 60% of the filter cartridge volume.
- Improved ceramic fiber filter media burst strength from 1 to 6 lb/in.², a 500% improvement in mechanical durability.
- Demonstrated a diesel particulate matter destruction efficiency of greater than 95% on the stationary 1.9-L test cell over the operating range of the engine.
- Installed the microwave filter on a Ford F-250 7.3-L diesel pickup, with full exhaust backpressure and temperature data acquisition, for a 6000-mile road test.
- Fabricated the microwave filter system and began installing it on a 1.9-L diesel Volkswagen Jetta for a 7000-mile controlled test track evaluation, with periodic Federal Test Protocol (FTP) cycle emission testing.

Future Direction

- Integrate the microwave filter particulate matter control unit with NO_x, hydrocarbon, and CO emission devices to develop a total system approach to meet Environmental Protection Agency Tier II requirements.
- Continue on-road durability testing to improve the filter system, precisely defining the operating cost and FTP cycle emissions performance.
- Enlist exhaust system, engine, and vehicle manufacturers in a product development effort to transfer the microwave filter system to future PNGV commercial applications.

Introduction

Current diesel engine particulate filter technologies depend on a catalyst to assist in the regeneration of the filter. Catalyst technology requires an exhaust temperature of approximately 350°C to be effective. Small diesel engines rarely achieve this exhaust temperature, requiring extended operation at over 70 mph. The microwave-regenerated particulate filter can achieve the required particulate removal efficiencies and regenerate at low exhaust temperatures. It is a potential answer to the low-temperature urban driving cycle where the catalyst technologies are ineffective. It may also be a solution to the cold-start issue that is responsible for a significant quantity of both diesel and gasoline engine emissions. Other methods of heating the filter, such as electrical and fuel burners, have been tried since the early 1980s with limited success. The unique microwave filter technology is due to the discovery and use of a special silicon carbide fiber that efficiently converts microwave energy to heat energy. These fibers can achieve temperatures of 1200°C in 9 seconds in a standard household microwave oven. A process has been developed to incorporate this phenomenon into a filter cartridge and microwave regeneration system for use in diesel engine exhaust streams, as shown in Figure 1. This technology has been demonstrated on stationary diesel engines in test cells at the Ford Motor Company, Oak Ridge National Laboratory, and the University of Tennessee. The PNGV partners directed the FY 2001 efforts toward durability testing of the microwave filter system. On-road diesel vehicle testing has been selected as the most effective approach to verification of durability.

Approach

FY 2000 filter problems were principally caused by non-uniform microwave heating of the filter cartridge. Finite-element computer programs were

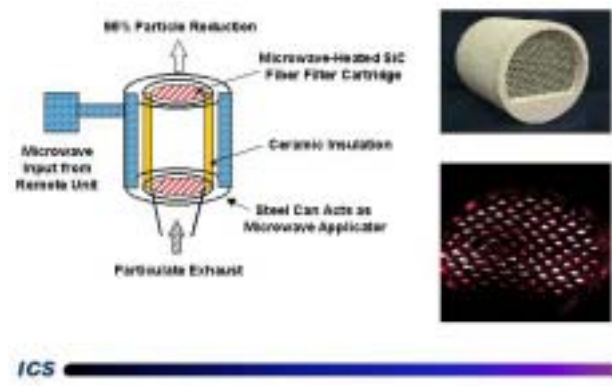


Figure 1. Microwave-regenerated diesel exhaust filter system.

used to model the microwave heating of the silicon carbide filter cartridge. The results of the computer modeling were applied to refine the filter cartridge and microwave component configurations. A microwave engineering effort was conducted to reduce the size of the microwave source components. Calculations of the mechanical stresses on the filter cartridge by the diesel exhaust showed that the current 1.0 psi burst strength of the ceramic fiber filter media needed to be increased to at least 3.0 psi to survive the full-load operating conditions of a diesel engine. A 3-month materials science matrix experiment program was conducted to increase the mechanical strength of the ceramic fiber filter media. This program addressed such variables as ceramic papermaking, binder addition techniques and furnace processing. The microwave and materials improvements were incorporated into an experimental prototype. This prototype system was tested on a 1.9-L stationary diesel engine test cell at Oak Ridge National Laboratory. With satisfactory results from these tests, the on-road diesel vehicle microwave filter systems were designed. Two vehicles were selected for on-road testing of the microwave filter system. Instrumentation was

designed, fabricated and tested to continuously monitor the backpressure resulting from carbon particulate accumulation on the filter, the exhaust flow, and the temperature of the exhaust during vehicle operation. The instrumented filter exhaust systems were installed on a Ford F-250 7.3-L diesel pickup (Figures 2 and 3) and a Volkswagen Jetta 1.9-L diesel car provided by DOE (Figures 4 and 5). The Ford truck is being tested under routine highway driving conditions for approximately 6000 miles. The filter will be removed and microwave-regenerated in the laboratory to understand the effects of microwave heating on the particulate loaded cartridge. The Volkswagen Jetta is being equipped with an on-board microwave regeneration system. This vehicle will be driven for 7000 miles under controlled test-track conditions by the Transportation Research Center near Columbus, Ohio. It will be subjected to FTP-cycle chassis dynamometer emissions testing at periodic intervals. The data from both on-road tests will be used to



ICS

Figure 2. Ford F-250 7.3-L on-road test vehicle.



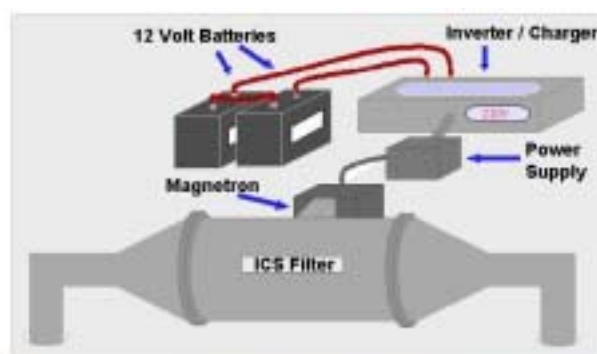
ICS

Figure 3. Test apparatus on the exhaust of the Ford truck.



ICS

Figure 4. Volkswagen Jetta on-road controlled test-track vehicle.



ICS

Figure 5. Schematic diagram of the Volkswagen microwave filter system.

improve the performance of the microwave-regenerated particulate filter, verify system durability, and precisely quantify the fuel penalty resulting from filter operation.

Results

The microwave field finite-element program analysis improved the heating efficiency of the filter cartridge from 10% of the filter volume in FY 2000 to over 60% in FY 2001. The mechanical strength of the ceramic fiber media, at the conclusion of the 3-month experimental matrix optimization program, increased from 1.0 psi to 6.0 psi. Calculations have shown that 3.0 psi would be adequate for a typical diesel exhaust stream. Analysis of the materials matrix data shows that further improvement to 10 psi is attainable. The diesel engine manufacturers have insisted that 95% particulate matter destruction is necessary to comply with the EPA Tier II requirements. Data on the FY 2001 microwave filter

system improvements from the diesel 1.9-L engine test cell demonstrated an average particulate removal efficiency of 97%, over a spectrum of normal engine operating conditions (Figure 6). Preliminary road testing of the filter on the Ford 7.3-L truck proved that the filter could survive the full loading of 1000 ft³/minute of exhaust flow without mechanical failure. The complete results of the on-road testing will be available in September 2001.

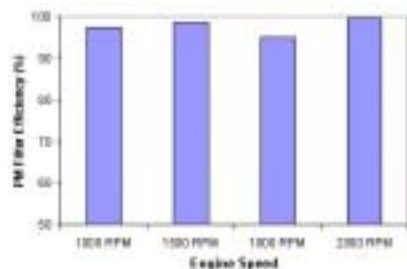


Figure 6. FY 2001 particulate removal efficiency data.

Conclusions

The microwave-regenerated filter was introduced to the DOE PNGV program in FY 1999. The technology has met or surpassed its milestone goals each year. The automotive industry must now be convinced that it is a potential solution to future

particulate emissions standards. Their principal remaining question is the durability of the microwave filter system in on-road testing. The conclusion of the FY 2001 on-road diesel vehicle demonstrations will provide the answer to that concern. Positive results will lead to product development partnerships with exhaust system suppliers, engine builders, or vehicle manufacturers. These strategic partnerships can move this technology to integration into a total commercial diesel exhaust emissions control system.

Publications/Presentations

J. Green, R. Nixdorf, J. Story, and R. Wagner, "Microwave-Regenerated Diesel Exhaust Particulate Filter," SAE Paper 2001-01-0903, Society of Automotive Engineers, Warrendale, Penn.

R. Nixdorf, "Microwave-Regenerated Diesel Particulate Filter," presented at the Society of Automotive Engineers World Congress, Detroit, Mich., March 5–8, 2001.

R. Nixdorf, "Microwave-Cleaned Ceramic Filter Using Silicon Carbide Fibers," presented at the American Filtration Society National Technical Conference, Tampa, Fla., May 1–4, 2001.

J. Wainwright, R. Nixdorf, "Microwave-Regenerated Diesel Particulate Filter," presented at The University of Wisconsin Exhaust Aftertreatment Symposium, Madison, Wis., June 12–13, 2001.

B. Rapid Surface Modifications of Aluminum Automotive Components for Weight Reduction

C. A. Blue, R. D. Ott, P. J. Blau, P. G. Engleman, and D. C. Harper
Oak Ridge National Laboratory

DOE Program Manager: Patrick Davis and Kathi Epping
ORNL Technical Advisor: D. P. Stinton

Contractor: Oak Ridge National Laboratory, Oak Ridge, Tennessee
Prime Contract No.: DE-AC05-00OR22725

Objectives

- Develop a new durability-enhancing coating for aluminum automotive applications—such as engine block cylinder bores, compressor housings, fuel pumps, and sealing surfaces—using innovative rapid, high-density infrared surface modification processes.
- Optimize coatings using characterization techniques such as metallurgical analysis, hardness testing, and tribology and ultimately test in real-world environments.
- Develop a selective area heat treatment process to soften selected areas of 6063 aluminum in automotive body construction parts to serve as built-in crumple zones.

OAAT R&D Plan: Section 3.2: Task 5; Barriers A, B, C

Approach

- Treat the cylinder internal bores and other surfaces with coatings to enhance wear resistance and reduce friction in order to eliminate the need for heavy cast-iron cylinder liners for engines and/or allow the use of machinable aluminum alloys such as 319 and 390 in high-wear areas.
- Investigate two separate plasma-assisted coating application techniques, one using a 300,000-W radiant lamp source to directly fuse a pre-sprayed material onto a surface, and the second using a weld-overlay technique to fuse material into the surface.
- Perform pin-on-disk wear testing, following ASTM standards, to quantify the wear resistance of the 390 aluminum alloy overlays and coating fused by the high-density radiant source. Compare those results with those from bulk 390 aluminum alloy and gray cast iron to quantify the quality of the coatings.

Accomplishments

- Identified a pump thrust body presently cast out of 390 aluminum as a component that, because of wear issues, would benefit from a new wear-resistant coating.
- Completed the development of a plasma-assisted deposition process capable of depositing wear-resistant 390 aluminum onto easily machinable 319 aluminum.
- Identified an additional aluminum surface modification application with Ford— economical placement of crash triggers in aluminum structures, using selective area heat treatment via arc lamp processing .

Future Direction

- Optimize the plasma infrared fusing of wear coatings on aluminum for automotive applications with automotive manufacturers' involvement.
 - Perform additional dry and lubricated wear testing of wear-resistant coatings produced by plasma-infrared fusing.
 - Evaluate and test softening of aluminum automotive body parts, such as built-in crash triggers, by selective area heat treatment.
-

Introduction

A new durability-enhancing coating and surface modification technique using an innovative, rapid, high-density surface modification process has been developed for aluminum automotive applications such as engine block cylinder bores, compressor housings, fuel pumps, sealing surfaces and surface modifications. Treating the cylinder internal bores and other surfaces to enhance wear resistance and reduce friction is intended to eliminate the need for heavy cast-iron cylinder liners for engines and/or allow for use of machinable aluminum alloys such as 319 and apply hard 390 coatings in high-wear areas. In the case of surface modifications, there is interest in the technology in two other areas: preferential softening of 6063 aluminum in the automotive body construction to create preferential crumple zones, and grain refinement of aluminum engine block areas through rapid re-melting to improve fatigue properties.

Fused Cermet Coatings/Overlay Coatings

Two separate approaches are currently being investigated to obtain a wear-resistant coating on 319 aluminum; they also apply to A359. Both have had substantial success. A high-intensity infrared lamp has been used to fuse tungsten carbide (WC)/Ni, WC/Cu, Cr₂C₃/Ni, and Cr₂C₃/Cu coatings directly onto aluminum. In this process, a powder precursor is sprayed at room temperature on aluminum and fused with a 300,000-W plasma arc lamp. The second approach is an overlay process that utilizes simple welding-type equipment. The overlay process melts a precursor with high silicon content directly into the 319-based material to form a 3- to 5-mm-thick layer with the properties of 390 aluminum.

The metallurgical analysis of the 390 overlays reveals that the process produces blocky silicon in a

eutectic matrix that is very similar to bulk 390 aluminum. Wear testing of these coatings revealed that it has wear resistance equivalent to that of bulk 390 aluminum. This process has been patented, and potential application parts are being identified.

The work involving spraying WC/Ni, Cr₂C₃/Ni at room temperature and fusing it onto steel substrates has been completed. Typical processing parameters for this work included power densities of 13.8 to 17 MW/m² with a constant translation speed of 10 mm/sec. Specimens fused at 15.4 and 17 MW/m² had fully dense microstructures with no degradation of the second-phase particles. Plasma-sprayed Ni-20Cr, a common hard facing material, was also fused for wear testing comparisons. This specimen was fused at a power density of 12.0 MW/m² and a scan rate of 5 mm/sec. All fusing work was accomplished under Ar-4%H. Experimentation continues on the direct fusing of these wear-type coatings on aluminum, but the matrix alloys accompanying the carbides are being reevaluated because of wetting issues and because of the potential part to be coated. It is anticipated that Ford will have technical input in this area.

Wear Testing

Wear tests were performed on WC, Cr₂C₃, and plasma-sprayed and fused Ni-20Cr specimens, utilizing a 52100 steel ball as the counter-wear part on the Cameron/Plint reciprocating wear instrument. All the coatings exhibited no measurable wear, even with increasing time and normal load. The only item showing wear was the 52100 steel ball. The next-hardest counter-wear part (ball) that was utilized

was a WC ball. The following test parameters were used: stroke length = 8 mm, frequency = 15 Hz, test velocity = $(8\text{ mm} \times 2) \times (15/\text{sec}) = 240\text{ mm/sec}$, and diameter of ball = 9.52 mm.

For all tests, there was no measurable wear scar on the WC ball. Several different tests were performed with normal loads of 30 and 35 N and distances of 60 to 400 m (500 to 1667 seconds). The wear volumes were normalized with respect to the product of the normal load and the distance, giving the wear rate in $\text{mm}^3/(\text{N}\cdot\text{m})$. The surface roughness, scratch hardness, coefficient of friction, and wear rate for these fused coatings are shown in Figure 1. The Cr_2C_3 coatings had the highest scratch hardness, although it was not significantly higher than that of the other coatings. The plasma-sprayed coating had the most surface roughness. The WC heavy coating had the lowest wear rate, followed by

the WC light (20 microns), Cr_2C_3 , and then plasma-sprayed coatings. The values for the coefficients of friction (COF) were all taken at the beginning of the tests; the WC coatings showed lower values, as would be expected since the counter-wear part was also WC.

From this wear testing, it appears there will not be an universal wear test procedure for these two coatings because of their difference in wear resistance. Suitable parameters must be chosen based on each coating, and the wear resistance of each coating must be compared with that of the base metal.

A candidate part for coating has been identified by Ford, and an invited presentation was made at Ford on May 30, 2001. The part, shown in Figure 2, is a pump thrust body that is presently cast out of

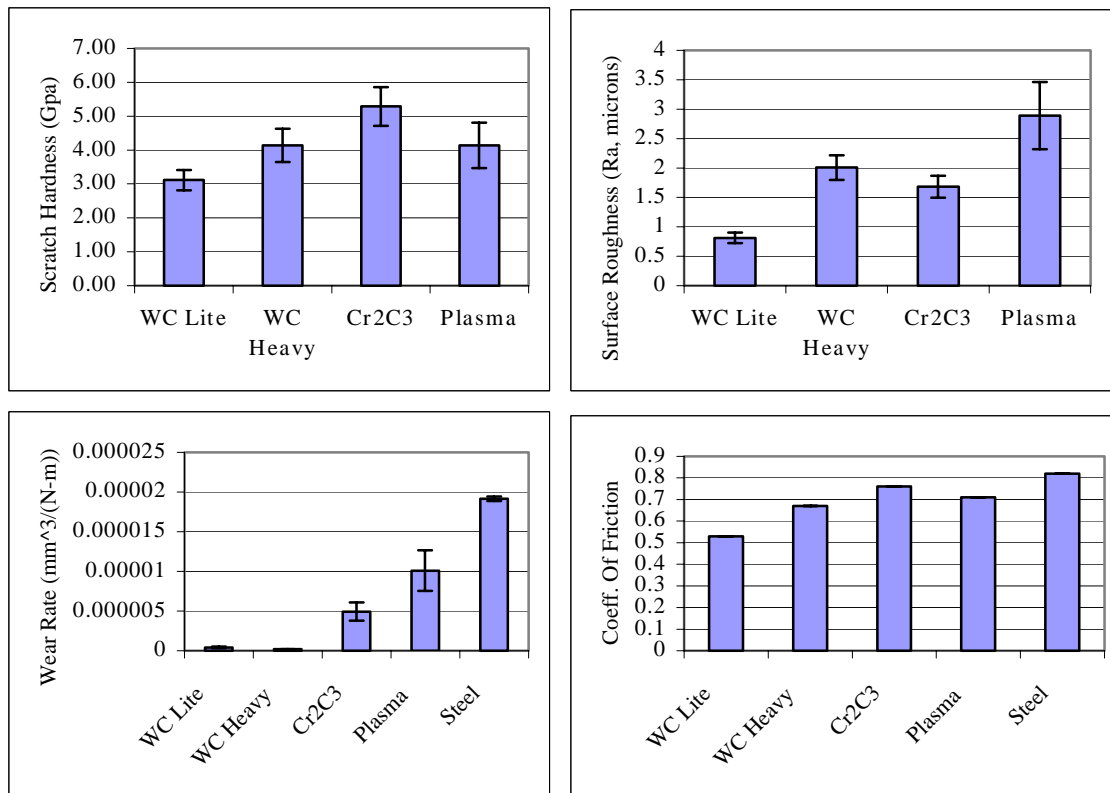


Figure 1. The surface roughness, scratch hardness, coefficient of friction, and wear rate for plasma infrared fused coatings compared with steel.



Figure 2. Aluminum pump thrust body presently cast out of 390 aluminum because of the level of wear resistance needed.

390 aluminum because of the need for wear resistance. The part has ten tapped holes and nine areas to be surfaced; coating them with 390 aluminum is expensive. It would be much less costly to cast this part out of 319 aluminum, a material with lower silicon content, because of the ease of machining and tapping. The presentation outlined the overlay and coating techniques developed in this project in an effort to outline the approach for development of these techniques for the targeted part.

Selective Aluminum Heat Treating

Using aluminum in construction of the automotive body is a promising and practical approach for saving weight and improving fuel consumption. Utilizing aluminum extrusions has the

benefit of lower cost compared with stamped aluminum because of a much lower tooling cost. However, aluminum extrusions do not have built-in crumple zones as stamped sheet does if it is used for the front frame rail structure. Crumple zones could be placed in aluminum structures economically by using selective area heat treatment, via arc lamp processing, to soften selected areas of the structures, eliminating the need to introduce crumple zones mechanically. Samples have been received from Ford for initial trials. After selective heat treating at ORNL, they will be tested in a test rig at Ford.

Summary

Two separate aluminum coating processes have been developed. Metallography, hardness testing, and wear testing have quantified the quality of the coating. A candidate part for coating has been identified by Ford, and an invited presentation was made at Ford. Selective area heat treating of aluminum automotive body construction parts was identified as an additional near-term application of arc lamp processing, which could lead to a 40–50% weight savings over the steel body structure. Testing methods have been developed and employed for evaluating WC- and Cr_2C_3 -reinforced Ni-P cermet coatings.

Publications

P. Engleman, C. Blue, R. Ott, N. Dahotre, and D. Harper, "High-Density Infrared Processing of a WC/Ni-P Cermet Coating," submitted to *Surface Engineering*.

C. Material Support for Nonthermal Plasma Diesel Engine Exhaust Emission Control

Stephen D. Nunn
Ceramic Processing Group
Oak Ridge National Laboratory

DOE Program Manager: Patrick Davis
ORNL Technical Advisor: David Stinton

Contractor: Oak Ridge National Laboratory, Oak Ridge, Tennessee
Prime Contract No.: DE-AC05-00OR22725

Objectives

- Identify appropriate ceramic materials, develop processing methods, and fabricate complex-shaped ceramic components that will be used in Pacific Northwest National Laboratory (PNNL)-designed nonthermal plasma (NTP) reactors for the treatment of diesel exhaust gases.
- Fabricate and ship components to PNNL for testing and evaluation in prototype NTP reactors.
- Develop a component design and establish a fabrication procedure that can be transitioned to a commercial supplier.

OAAT R&D Plan: Section 3.2: Task 1B; Barriers A, B

Approach

- Evaluate commercially viable forming methods to fabricate complex-shaped ceramic components that meet PNNL design specifications.
- Modify processing as needed to accommodate material and design changes.
- Evaluate bonding and sealing materials for preparing assemblies of the ceramic components.
- Investigate metallization materials and processes to apply electrodes to the ceramic components.

Accomplishments

- Fabricated newly designed ceramic components from a tape-cast ceramic raw material.
- Reduced the ceramic component weight by 62% for the same active surface area.
- Reduced the ceramic component processing temperature from 1600 to 850°C, which lowers the fabrication cost and permits the use of readily available silver inks for the electrodes.
- Supplied ceramic components to PNNL for testing and evaluation.

Future Direction

- Fabricate additional ceramic components for testing at PNNL in prototype NTP reactors.
- Identify a glass or glass-ceramic sealing material that will bond to the metal and ceramic materials in the NTP reactor assembly and form a gas-tight seal.

- In collaboration with PNNL, prepare an NTP reactor assembly and test the device in a diesel engine exhaust gas stream.

Introduction

NTP reactors have shown great potential as an effective means of eliminating unwanted exhaust gas emissions from diesel engines. In particular, the NTP reactor is very effective in reducing oxides of nitrogen (NO_x). Researchers at PNNL are developing new, proprietary design configurations for NTP reactors that build on past experimental work. To improve the effectiveness, these designs include ceramic dielectric components having complex configurations. Oak Ridge National Laboratory (ORNL) has extensive experience in the fabrication of complex ceramic shapes, primarily based on prior work related to developing ceramic components for gas turbine engines. The ORNL expertise is being utilized to support PNNL in its development of the new NTP reactor designs.

Approach

Collaborative discussions between ORNL and PNNL are used to establish new ceramic component designs for improved NTP reactors. Meeting NTP reactor design objectives is balanced with the limitations of ceramic manufacturability to arrive at a new component configuration. The ceramic processing facilities and expertise at ORNL are then used to establish fabrication capabilities and to produce components for testing at PNNL. This is an iterative process as both parties gain more knowledge about fabricating the components and about their performance in NTP reactor tests. The ultimate goal is to identify a design that performs well and that can be produced readily by a commercially viable process.

Results

In the early stages of this project, complex-shaped ceramic components were fabricated by the gelcasting process. The gelcasting method was used because of the flexibility it provides for forming ceramic components with complicated shapes. An example of the gelcast parts that were produced is shown in Figure 1. The ceramic plates were assembled in a stack with a gap between the plates. The plates had internal electrodes, which were



Figure 1. Gelcast ceramic components in a three-layer stack. Electrodes are placed in the holes, which run the length of the thin region of the plates. The plates are alternately charged positive and negative to form an electric field in the gap between each pair of plates. Each individual ceramic plate is 6.35×11.43 cm (2.5 in. \times 4.5 in.).

connected to a voltage supply. Alternate plates were connected to either the positive or negative side of the voltage supply to produce an electric field between each pair of plates, and a plasma discharge was generated in the gap. These parts performed well in tests to generate a plasma discharge, but it was decided that the fabrication process was too complicated to be feasible for commercial production.

A new fabrication method is now being used. The process uses commercially available tape-cast ceramic materials, which are used to produce multilayer electronic substrates for hybrid microcircuits. In the green state (unfired), the ceramic tape is flexible and can be shaped and laminated, allowing the formation of complex shapes. The configuration of the NTP ceramic components was modified to be compatible with the new fabrication method. Using the new design and tape-cast material, the weight of the ceramic components was reduced by 62% for the same amount of active surface area. In addition, the ceramic firing temperature was reduced from 1600 to 850°C, a cost saving in the manufacturing process. Another advantage of the new processing

method is that, at the lower firing temperature, silver ink can be used for the electrodes in the component. This development has greatly simplified the task of metallizing the parts.

Several of the new components were fabricated with embedded electrodes and sent to PNNL for testing. Figure 2 shows the components being tested in the laboratory at PNNL. In the assembly, three of the ceramic components are stacked in the test fixture and the parts are connected to a voltage supply to generate a plasma discharge. (In the photograph of this test, the plasma can be seen as a glow between the pairs of plates.) The tests demonstrated that these components produce a uniform plasma discharge and that there is no problem with dielectric breakdown of the ceramic under operating conditions.

In an NTP reactor assembly, the ceramic components will be fixed in place in a metal housing and ceramic spacers will be used to maintain the separation between the individual plates. To form the assembly, a bonding and sealing material will be needed to fix the ceramic components in position

and to form a gas-tight seal to contain the exhaust gases. The bonding and sealing material must be an electrical insulator. ORNL is beginning to evaluate potential sealing materials. Both glass and glass-ceramic materials are being considered for this application, and tests are now under way to identify candidate materials.

Conclusions

A new fabrication procedure was developed at ORNL to produce ceramic components for use in PNNL's NTP reactors. The new process uses commercially available tape-cast ceramic material. A new component design was developed that is compatible with the new fabrication process. The new components weigh 62% less for the same active surface area and are sintered at 850°C instead of 1600°C. Silver ink is used to form the electrodes on the ceramic parts. Components have been tested successfully in the laboratory at PNNL, where it was shown that a uniform plasma could be generated with no dielectric breakdown.

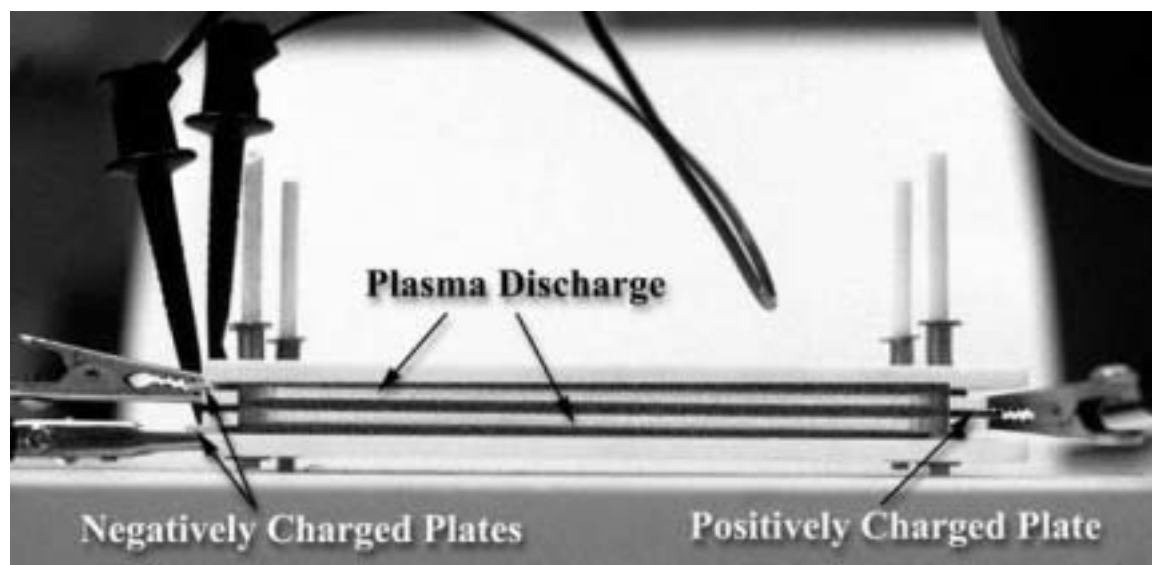


Figure 2. Test assembly used to evaluate the performance of the ceramic components in generating a plasma discharge. The plasma forms in the gap between the oppositely charged ceramic plates.

APPENDIX A: ACRONYMS AND ABBREVIATIONS

ANL	Argonne National Laboratory
ASTM	American Society for Testing and Materials
CIDI	compression-ignition direct-injection
CO	carbon monoxide
CVI	chemical vapor infiltration
DOE	U.S. Department of Energy
EDX	energy-dispersive X-ray spectroscopy
F	fluorine
FTP	Federal Test Protocol
GM	General Motors
HA-ADF	high angle annular dark-field
H ⁺	hydrogen ion
H ₂	hydrogen gas
HEPA	high-efficiency particulate air (filter)
ICS	Industrial Ceramic Solutions
LANL	Los Alamos National Laboratory
MEA	membrane electrode assembly
MLCC	multi-layer ceramic composite
NEP	National Energy Policy
NFC	near-frictionless carbon
nm	nanometer, 10 ⁻⁹ meters
NO _x	oxides of nitrogen
NSA	National Security Agency
NTP	nonthermal plasma
OAAT	Office of Advanced Automotive Technologies
OEM	original equipment manufacturer
ORNL	Oak Ridge National Laboratory
OTT	Office of Transportation Technologies
PEM	polymer electrolyte membrane
PEMFC	polymer electrolyte membrane fuel cell
Pd	palladium
PM	permanent magnet
PNGV	Partnership for a New Generation of Vehicles
PNNL	Pacific Northwest National Laboratory

POEM	porous oxide electrolyte membrane
PPS	polyphenylene sulfide
Pt	platinum
R&D	research and development
S	sulfur
SEM	scanning electron microscope
SNL	Sandia National Laboratories
SO ₃ ²⁻	sulfonate group
STEM	scanning transmission electron microscope
T	Tesla
TEM	transmission electron microscope
TiN	titanium nitride
TIVM	toroidal intersecting vane machine
WC	tungsten carbide
Z	characterized by a high atomic number

This document highlights work sponsored by agencies of the U.S. Government. Neither the U.S. Government nor any agency thereof, nor any of their employees, makes any warranty, express or implied, or assumes any legal liability or responsibility for the accuracy, completeness, or usefulness of any information, apparatus, product, or process disclosed, or represents that its use would not infringe privately owned rights. Reference herein to any specific commercial product, process, or service by trade name, trademark, manufacturer, or otherwise does not necessarily constitute or imply its endorsement, recommendation, or favoring by the U.S. Government or any agency thereof. The views and opinions of authors expressed herein do not necessarily state or reflect those of the U.S. Government or any agency thereof.



Printed on recycled paper

Office of Transportation Technologies Series of 2001 Annual Progress Reports

- Office of Advanced Automotive Technologies FY 2001 Program Highlights
- Vehicle Propulsion and Ancillary Subsystems
- Automotive Lightweighting Materials
- Automotive Propulsion Materials
- Fuels for Advanced CIDI Engines and Fuel Cells
- Spark Ignition, Direct Injection Engine R&D
- Combustion and Emission Control for Advanced CIDI Engines
- Fuel Cells for Transportation
- Advanced Technology Development (High-Power Battery)
- Batteries for Advanced Transportation Technologies (High-Energy Battery)
- Vehicle Power Electronics and Electric Machines
- Vehicle High-Power Energy Storage
- Electric Vehicle Batteries R&D



www.carttech.doe.gov

DOE/EERE/OTT/OAAT - 2001/004